Doctoral theses at NTNU, 2019:15

K. M. Iromi Udumbara Ranaweera

Energy Storage for Control of Distributed Photovoltaic Power Systems

NTNU
Norwegian University of Science and Technology

Doctoral thesis

K. M. Iromi Udumbara Ranaweera

ISBN 978-82-326-3641-9 (printed ver.)
ISBN 978-82-326-3640-2 (electronic ver.)
ISSN 1503-8181

NTNU
Norwegian University of Science and Technology
Thesis for the Degree of
Philosophiae Doctor
Faculty of Information Technology and Electrical Engineering
Department of Electric Power Engineering

Doctoral theses at NTNU, 2019:15

NTNU
Norwegian University of Science and Technology

K. M. Iromi Udumbara Ranaweera

Energy Storage for Control of Distributed Photovoltaic Power Systems

Thesis for the Degree of Philosophiae Doctor

Trondheim, January 2019

Norwegian University of Science and Technology
Faculty of Information Technology and Electrical Engineering
Department of Electric Power Engineering

NTNU
Norwegian University of
Science and Technology

NTNU
Norwegian University of Science and Technology

Thesis for the Degree of Philosophiae Doctor

Faculty of Information Technology and Electrical Engineering
Department of Electric Power Engineering

ISBN 978-82-326-3641-9 (printed ver.)
ISBN 978-82-326-3640-2 (electronic ver.)
ISSN 1503-8181

Doctoral theses at NTNU, 2019:15

Printed by NTNU Grafisk senter

To My Parents...

Acknowledgements

First of all, I would like to thank my supervisor, Professor Ole-Morten Midtgård for providing me with the opportunity to carry out this interesting research at NTNU. I sincerely acknowledge his support, guidance, advices and the encouragement he has given me. He was not only my supervisor but also a good friend to me, which made my whole PhD experience rewarding and enjoyable.

My sincere thanks also goes to Dr. Ole Jakob Sørdalen, the previous director of research at Eltek AS, who provided me with the opportunity to have several short stays at Eltek's R&D departments in Kristiansand and Drammen. These visits helped me to gain industrial exposure and to broaden my knowledge about the latest converter technologies used for renewable energy and storage applications. I am grateful to Kjetil Boysen, Arkadiusz Kulka, and Øystein Olsen from Eltek for sharing their knowledge with me. I would also like to thank Hossien Hafezi and Professor Faranda Roberto Sebastiano from Politecnico di Milano for providing me with PV production data sets.

I am grateful to my colleagues at the Department of Electric Power Engineering for their warm friendship and for being helpful whenever needed. My thanks also goes to the administrative staff at the department for helping me with various practical matters.

Last but not least, I would like to thank my parents for their blessings and the endless support they have given me. Also, I want to thank my beloved husband Sisara for his continued support, encouragement, and patience during the past years. Without their support, I would not have been able to make this thesis a success.

Abstract

The residential energy storage market is growing at a rapid pace in many countries. Increasing the consumption of locally produced energy and the use of energy storage as a backup source have been the main reasons for residential customers to be encouraged to install battery-based energy storage systems. The storage capacity connected to the grid increases with the accumulated use of home storage systems. Increased storage capacity has several benefits for the grid operator. A grid with significant storage allows for increased capacity of power generated from renewable sources. That is due to the fact that storage contributes to maintain stable operation of the grid against variations of power generation from these intermittent sources. Storage systems connected to the distribution grid can help the Distribution System Operators (DSOs) to manage power flow and to alleviate power quality issues. However, these potential benefits can only be realized with properly designed control strategies.

Therefore, the objective of this thesis is to suggest, develop and verify effective control strategies for customer-owned Battery Energy Storage (BES) systems, which are co-located with photovoltaic (PV) systems. In this work, these systems are assumed to be connected to low voltage grids with high level of PV penetration, to reflect future trends and developments that are already taking place. Distribution grids are usually unbalanced to a certain extent. Therefore, the proposed control strategies are designed for three-phase unbalanced grids while the compatibility is ensured for balanced grids as well. In the proposed methodologies, the primary control objective is to fulfil the requirements of the BES owners. The BES systems should however also support the local grid to alleviate over-voltage problems, which is a common issue experienced by distribution grids with high PV penetration levels. But the use of customer-owned BES units for such purposes should not adversely affect the BES owners' local objectives. In this thesis, two methods to control the operation of customer-owned BES systems in a grid-supportive manner are proposed, which do not adversely affect local objectives.

The first method is a local control strategy, in which the control set points are

determined by a local controller based on locally extracted information. A receding horizon control approach is adopted to determine the BES set points. In this approach, an optimization problem is solved repeatedly over a moving time horizon to determine the set points. The objective function of the optimization problem can be locally decided according to the requirement of the BES owner. The Home Energy Management System (HEMS) implements the local objectives. Details of HEMS systems are provided in the thesis and parts of their operation are experimentally tested and verified. The critical period is when the PV production is potentially highest in the middle of the day. The high PV production results in excessive reverse power flow in the grid, which can cause over-voltage problems. Constraining the charging operation of the BES systems to this critical period is a requirement set by the DSO to lower the reverse power flow. The optimization problem is formulated such that the BES systems maintain charging operation over the entire critical period without reaching the maximum state of charge until the critical period is over. Consequently, the reverse power flow in this period will be reduced and the over-voltage issues will be alleviated.

The second method proposed to control the BES set points, is based on a distributed control approach. In this approach, the local controllers of the BES systems determine the set points in the same way as in the first method, whereas a central controller may modify these set points if required. The set points computed from the local optimization process are modified if they fail to maintain the voltages within the statutory limits. These modifications are done during real-time operation. The central controller coordinates the charging set points among the three phases. In this work, we assume that the BES units are connected to the grid using three-phase converters and the per-phase set points of the converters are independently controlled. The active power capabilities of the BES systems can be maximally utilized for voltage support through coordination of the charging operation among the three-phases in an unbalanced grid. This will reduce the unnecessary use of reactive power for voltage support and enhance the performance of the overall grid section.

Both control strategies mentioned above are accompanied by reactive power control as well. Reactive power support from the converters is utilized only when the cumulative storage capacity available in the grid is not sufficient to mitigate the over-voltage problem completely. For the local control strategy, the proposed reactive power support solution is based on a gradual increment of reactive power support from PV inverters. The PV inverters respond to a broadcast signal received from a monitoring device located at a strategic node in the network. For the over-voltage case, the PV inverters decrease their power factors gradually until the problem is solved. For the distributed control strategy, the central controller determines the optimal power factor set points of the converters that can maintain the voltage profile of the grid within acceptable limits.

Simulation studies were carried out to evaluate the performance of the proposed control strategies. The two control strategies were implemented in an IEEE low voltage test feeder and the voltage profiles of two critical nodes were observed. Both

control strategies managed to improve the voltage profile of the network effectively. The distributed control strategy was able to maintain the voltage profile within acceptable limits with reduced reactive power support when compared to the local control strategy. A study was also conducted to evaluate the effect of the DSO's involvement in the control of customer-owned BES systems, on the local objectives of the customers. A rule-based control strategy was used as the base scenario for this comparison. In this rule-based control strategy, the rules were carefully defined to maximize the economic benefits for the customers. From this study, it was discovered that the proposed control strategies do not adversely affect the local objectives. The difference between the cost savings, the self-consumption rates, and the self-sufficiency rates calculated over the period of a month were negligible with or without the involvement of the DSO. Therefore, the local objectives are not adversely affected by the proposed grid-supportive operation of the customer-owned BES systems.

The main contributions of this work have been the two suggested control strategies, the accompanying reactive power support solutions, and their validation for three-phase unbalanced grids. In addition, it was demonstrated that customer-owned BES systems can be used by DSOs to alleviate over-voltage problems in distribution grids without compromising the local objectives of the owners. Grid codes and market models can therefore be designed with this in mind.

Contents

List of Figures

List of Tables

Abbreviations

BES	Battery Energy Storage
DER	Distributed Energy Resources
DG	Distributed Generation
DoD	Depth of Discharge
DSO	Distribution System Operator
FIT	Feed-in Tariff
HEMS	Home Energy Managements System
ICT	Information and Communication Technology
LV	Low Voltage
MPP	Maximum Power Point
MPPT	Maximum Power Point Tracking
PCC	Point of Common Coupling
PV	Photovoltaic
RHC	Receding Horizon Control
RTP	Real Time Pricing
SCR	Self-Consumption Rate
SoC	State of Charge
SSR	Self-Sufficiency Rate
TOU	Time of Use
VUR	Voltage Unbalance Rate

Chapter 1

Introduction

This chapter provides background information about solar PV systems and energy storage and the rationale for the chosen research objectives. The chapter also states the main contributions of this thesis followed by a list of publications. Finally, it outlines the content of the thesis.

1.1 Background

Energy storage is experiencing rapid global growth. It is a promising solution for the optimal utilization of energy produced by intermittent renewable sources such as wind and solar in a dispatchable manner. Storage can be adopted at any levels of the grid, i.e. at generation and transmission levels as utility-scale projects, and at the distribution level as distributed sources. Distributed storage can be owned and operated by commercial, industrial, and residential customers or by the distribution system operator (DSO) itself. Depending on where the storage is located, it is capable of providing a number of services for the DSO, the customer, or for both. Applications of utility-scale storage include: transmission support, transmission and congestion relief, transmission and distribution upgrade deferral, provision of reserve and flexibility capacity, load following, frequency regulation, area regulation, ramp rate control, renewables energy time shift, and renewables capacity firming. The services distributed storage can provide include: maximizing consumption of self-generated electricity for the customer, peak demand management for the customer, time-of-use energy cost management for the customer, and voltage management and peak demand reduction for the DSO [5–7].

The utility-scale storage is the fastest growing segment of the market as multiple grid services can be realized for significantly low per unit cost. The cumulative grid-connected energy storage capacity worldwide increased from 1.4 GWh in 2015 to 2.3 GWh by 2016. A notable growth in the distributed storage market can

also be observed recently, and it is expected to grow rapidly in the coming years, according to the studies done by market research groups at IHS Technology [8], Technavio [9], and Navigant Research [10]. Battery technologies have been the most attractive storage solution at the customer level. The cost of battery technologies has decreased dramatically over the past several years and further cost reduction is expected over the time. For example, the cost of a lithium-ion battery pack decreased by 77% from 2010 to 2016, according to the media. This fall in battery cost has accelerated storage integration at the residential level, particularity paired with solar photovoltaic (PV) systems. In many countries, at the early stage of PV development, several incentive schemes and attractive feed-in-tariff schemes existed for residential PV systems [11]. The cost of PV systems has dropped dramatically so that roof-top PV has become an economical option even without incentives in many countries, for example Germany. However, at the same time feed-in-tariffs have also decreased while the retail electricity rate has increased. For example, in Germany the average price (including module cost, inverter cost and balance of system (BOS) cost) of a roof-top PV system dropped from 5000 €/kWp in 2006 to 1270 €/kWp in 2015. Feed-in-tariffs have fallen an average of 8.9% per year while retail electricity rates increased an average of 4.5% per year [12]. As a result, concern on maximizing the consumption of self-generated energy has increased among PV system owners. Changes in retail electricity tariff structures, such as introducing time-of-use tariffs and demand charges have further motivated customers to consider energy storage systems.

The global PV market has grown exponentially over the past decade. The total installed PV capacity globally surpassed 400 GW by the end of 2017 compared to 5 GW of capacity in 2005 [1]. A significant portion of this capacity is connected to low voltage networks. According to *Global Market Outlook for Solar Power 2016-2020* published by the European Photovoltaic Industry Association, one third of the PV capacity installed in 2015 was rooftop solar systems [14]. Further drops in the costs of PV systems will expand the potential PV system customer base. Distribution grids, which were originally designed for unidirectional power flow, have already experienced bidirectional power flow due to the integration of distributed generators. Further increases in PV penetration levels in residential areas will cause severe reverse power flow issues during high PV production hours. This is because, in this period power production from PV systems is relatively high while the residential load is significantly low. Reverse power flow creates voltage rise issues in distribution grids [15–19]. Rural distribution grids are mostly affected by this problem because of long supply lines, which have long electrical distances from the transformer to the supply points. Besides over-voltage issues, several other problems associated with high PV penetration levels in distribution grids have been identified. The other most common issues are transformer over-loading, voltage unbalance, increased difficulty of voltage control, and variations in power factor of a feeder or a distribution system [20–29]. The severity of these impacts varies with the penetration level, the location of the PV systems, and the electrical characteristics of the distribution systems. To enable high PV penetration levels in distribution grids, the above challenges will need to be overcome. The adoption

of energy storage technologies at the distribution level is one possible solution for many of these challenges.

Increasing interest in storage units among residential customers and the potential of these distributed storage units to provide multiple services to the customer and the DSO have motivated this study to focus on developing effective control strategies for residential storage units.

1.2 Objectives

Storage is useful for the customer and the DSO in many ways. The key services residential storage units are capable of providing for the customer include: increasing the consumption of self-generated energy, peak demand management, and time of use cost management. The value of the storage will be greatly enhanced if it is controlled to meet as many needs as possible. Increasing the number of residential storage units will also have a strong positive impact on the grid if they are operated in a grid-supportive manner. The services that the DSO can obtain from these storage units include peak demand reduction and power quality management. However, it is important to identify the most critical applications and develop control methods accordingly, so that the customer can obtain optimal use of his storage unit while providing necessary services to the DSO.

One major challenge that has been identified in distribution grids with high levels of PV penetration is maintaining the voltage quality within statutory limits. Particularly, over-voltage issues caused by reverse power flow have become a major problem. Curtailment of power feed-in at point of common coupling (PCC), and reactive power support by PV inverters are currently being used to solve over-voltage issues in distribution grids with significant PV penetration [15, 30–34]. Residential storage is another means of mitigating the over-voltage issues in distribution grids. Power flow in the reverse direction can be lowered by storing the power generated by the PV systems in residential storage units, thus reducing the risk of potential over-voltage problems. Proper use of residential storage units will greatly reduce the amount of power curtailed and required reactive power support from PV inverters. Reactive power support from PV inverters is associated with increased network losses and the requirement for an increased amount of VAr resources. The effectiveness of reactive power support depends on the R/X ratio of the local grid impedance. The lower the R/X ratio, the higher the effect of reactive power on the voltage magnitude. However, low voltage (LV) distribution grids are often accompanied by high R/X ratios, making reactive power support less effective for voltage regulation. Therefore, active participation of residential storage units will not only lower the risk of over-voltage, but also improve the performance of the network when compared to reactive power support solutions.

The main purpose of installing a battery energy storage (BES) unit in a residential household may not be supporting the grid, but to maximize the customer's local

objective. Therefore, grid-supportive functions should be introduced without adversely affecting those local objectives. Alternatively, the storage grid connection policies and electricity tariff structures can be changed to shape the operation of the customer-owned BES units so that they are supportive for the grid. The main objective of this PhD work has been to investigate such opportunities and develop grid-supportive control strategies that can fulfil the storage owner's local objectives while supporting the grid to alleviate over-voltage issues.

1.3 Contributions

The contributions of this thesis can be summarized as follows:

- A local control strategy for customer-owned battery energy storage units was developed. The proposed control strategy is aimed to fulfil the requirements of the storage owner while supporting the grid in the alleviation of over-voltage issues in low voltage distribution grids with high PV penetration. This control strategy is mainly based on locally extracted information, therefore, knowledge about the rest of the network is not needed.

- A distributed control strategy for customer-owned battery energy storage units was developed. This control strategy is also designed to fulfil the requirements of the storage owner while supporting the grid in alleviating over-voltage issues. The control scheme consists of a central controller and local controllers for each residential energy system. The central controller attempts to optimize the overall operation of the LV distribution network while the local controllers attempts to optimize the local objectives.

- Two reactive power support solutions were developed to work in coordination with the active power support from the BES units for over-voltage mitigation. Reactive power support from the converters is the secondary solution used when the active power support is not sufficient to maintain the voltage profile within statutory limits.

- Both control strategies were developed and validated for three phase unbalanced grids.

- A performance comparison of two proposed control strategies with respect to rule-based control strategy was done. Required reactive power support for maintaining the voltage profile within the statutory limits was significantly reduced with the two proposed control strategies.

1.4 List of Publications

Journal papers

- I. Ranaweera, O. M. Midtgård, M. Korpås, "Distributed control scheme for residential battery energy storage units coupled with PV systems," Renewable Energy, Volume 113, Pages 1099-1110, 2017.
- I. Ranaweera, O. M. Midtgård, "Optimization of operational cost for a grid-supporting PV system with battery storage," Renewable Energy, Volume 88, Pages 262-272, 2016.

Conference papers

- I. Ranaweera, O. M. Midtgård, M. Korpås, H. Farahmand, "Control strategies for residential battery energy storage systems coupled with PV systems," 2017 IEEE International Conference on Environment and Electrical Engineering and 2017 IEEE Industrial and Commercial Power Systems Europe (EEEIC/I&CPS Europe), Milan, 2017.
- I. Ranaweera, O. M. Midtgård, "Techno-economic optimum control of grid-connected residential battery energy storage units," 6th Solar Integration Workshop International Workshop on Integrating of Solar Power into Power Systems, Vienna, 2016.
- I. Ranaweera, O. M. Midtgård, "Centralized control of energy storages for voltage support in low-voltage distribution grids," 2016 IEEE 16th International Conference on Environment and Electrical Engineering (EEEIC), Florance, 2016.
- I. Ranaweera, O. M. Midtgård, "Energy management system for a photovoltaic system with battery storage participating in grid voltage quality improvement," 5th Solar Integration Workshop International Workshop on Integrating of Solar Power into Power Systems, Brussels, 2015.
- I. Ranaweera, S. A. Sanchez, O. M. Midtgård, "Residential photovoltaic and battery energy system with grid support functionalities," 2015 IEEE 6th International Symposium on Power Electronics for Distributed Generation Systems (PEDG), Aachen, 2015.
- I. Ranaweera, O. M. Midtgård, G. H. Yordanov, "Short-term intermittency of solar irradiance in southern Norway," 29th European Photovoltaic Solar Energy Conference and Exhibition (EUPVSEC), Amsterdam, 2014.

Conference and journal papers, which I have contributed as a co-author:

- Chee Lim Nge, I. Ranaweera, O. M. Midtgård, Lars Norum, "A real-time energy management system for smart grid integrated photovoltaic generation with battery storage", Renewable Energy, Volume 130, Pages 774-785, 2018.
- S. Zaferanlouei, I. Ranaweera, M. Korpås, H. Farahmand, "Optimal scheduling of plug-in electric vehicles in distribution systems including PV, wind and hydro-power generation," 6th Solar Integration Workshop International Workshop on Integrating of Solar Power into Power Systems, Vienna, 2016.
- M. L. Kolhe, I. Ranaweera, A. G. B. S. Gunawardana, "Techno-economic sizing of off-grid hybrid renewable energy system for rural electrification in Sri Lanka," Sustainable Energy Technologies and Assessments. Volume 11. Pages 53-64, 2015.
- H. Vika, O. M. Midtgård, I. Ranaweera, G. H. Yordanov, "Modelling of photovoltaic modules with battery energy storage in Simulink/Matlab with in-SituMeasurement comparisons," 4th International Workshop on Integration of Solar into Power Systems, Berlin, 2014.

1.5 Outline of the Thesis

This thesis is organized as follows:

Chapter 2 explains the challenges of high PV integration in distribution grids and discuss various energy storage applications. Also, it presents a short summary about the types of storage technologies and a review of control strategies for distributed battery energy storage systems.

Chapter 3 gives details about modelling of a grid connected residential energy system comprising a load, a PV system, and a battery energy storage system. Also, it presents a receding horizon control-based local control strategy for the BES unit. The proposed control strategy supports the grid for the alleviation of over-voltage issues. It further proposes a secondary voltage support solution based on reactive power control of distributed generators.

Chapter 4 proposes a distributed control strategy for the active power control of customer-owned BES units. It also presents a secondary solution for over-voltage issues, which is based on the centralized control of the reactive power set points of the distributed generators.

Chapter 5 presents an evaluation of the impacts of two proposed grid-supportive operational strategies on the storage owner's local objectives and the benefits for the distribution system operator.

Finally, Chapter 6 presents a summary and the conclusions of this thesis, along with suggestions for future work.

Chapter 2

Energy Storage for Distribution Grids With High Photovoltaic Penetration

This chapter begins with an overview of the global photovoltaic market and a discussion about the key challenges relating to the increased penetration of PV systems in distribution grids. The chapter describes useful applications of energy storage for enabling high PV integration. It also gives a short summary of different energy storage technologies with an emphasis on battery energy storage technology. Lastly, it outlines different control architectures that can be adopted for controlling distributed battery energy storage systems.

2.1 The Global Photovoltaic Market

The evolution of the global PV installed capacity over the period 2000-2017 is shown in Fig. 2.1. As shown in the figure, it has grown exponentially over the past years. By the end of 2017, total PV capacity had reached 402.5 GW, which represented around 2.14% of global electricity demand [1]. According to market analysts, 2017 was a record-breaking year for the PV market, as global PV installation reached almost the 100 GW threshold in 2017. That was the largest amount of solar PV that was installed in a year until that point. In 2017, China dominated the PV market with 53 GW of newly installed capacity out of 98 GW global installation. By the end of 2017 China was leading the PV market with 131 GW of total PV installed capacity, followed by the United States (51 GW), Japan (49 GW), and

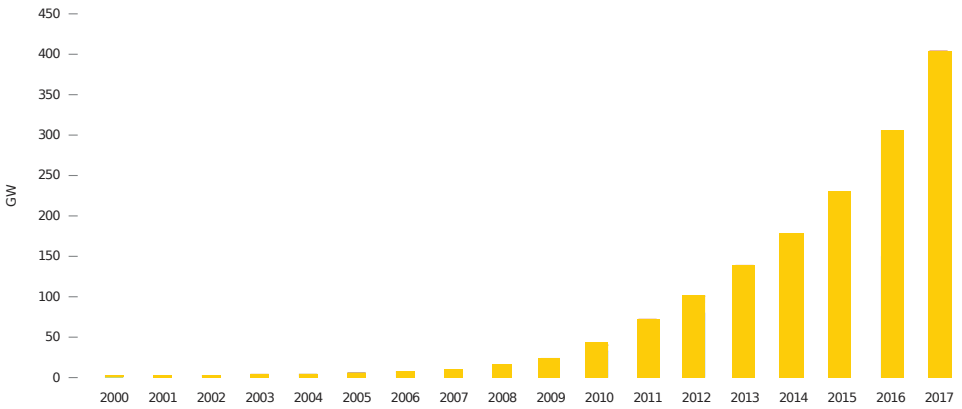

Figure 2.1: Evolution of cumulative global solar PV installation [2].

Germany (42 GW). In 2017, the total PV installed capacity exceeded 1 GW level in 29 countries. Fig. 2.2 illustrates the total installed PV shares by country by the end of 2017. By the end of 2017, Asia Pacific had become the largest solar-powered region while Europe was second. In Europe, solar PV represented 4% of the total electricity demand in 2017. Country wise, Honduras featured the highest PV contribution to its national electricity demand, which was around 13.26%. Germany was in the second place with around 7.47%, followed by Greece 7.34%, Italy 7.11% and Japan 5.93% [1, 2].

2.2 High PV Integration Challenges in Distribution Grids

The lower cost of utility scale solar means it is the fastest growing market segment in many countries. Utility scale solar has now become cheaper than new combined cycle gas turbines, coal, and nuclear power plants [2]. The distributed solar market is also showing rapid growth though it is not as fast as utility scale solar. The cost of roof-top PV systems is becoming lower while utility electricity prices are increasing. Moreover, for distributed solar PV systems, various kinds of attractive business models are available in terms of incentives, feed-in-tariffs, net metering, and tax credits. Consequently, an increasing number of customers are becoming interested in having roof-top PV systems for supplying their local electricity needs. These PV systems are connected to the low voltage grid. The power generation from PV systems is non-dispatchable due to the intermittent nature of the solar resource. Therefore, power generation may not always coincide with load. Consequently, excess generation is exported to the utility grid. The power flow in the grid is then not uni-directional. Integration of these distributed generators (DG) has converted traditional uni-directional power grids to bi-directional grids [15].

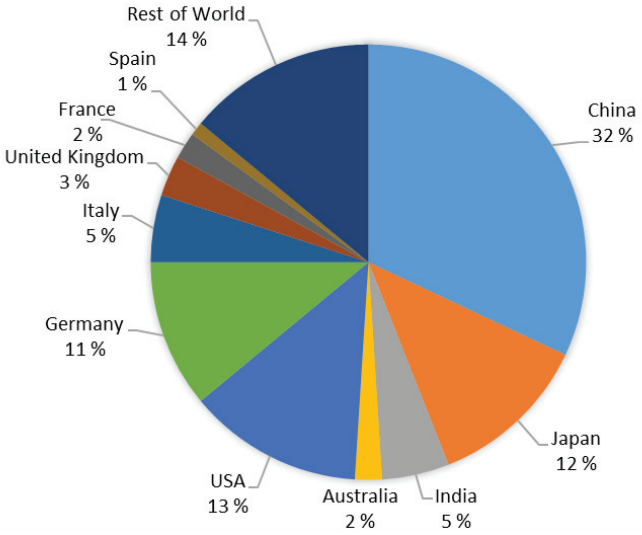

Figure 2.2: Global solar PV markets: Total installed shares by end of 2017 [2].

Traditional LV networks are able to accommodate a certain amount of solar PV systems depending on the characteristic of the network. As the amount of PV increases further, the LV networks will experience several problems. This is particularly the case where the cumulative PV generation level exceeds the local load in the distribution system. The problems that have been experienced and identified with high PV penetration includes: over-voltage, voltage unbalance, voltage fluctuations, reverse power flow, frequent operation of voltage regulation devices, and reactive power fluctuations [16–21, 21–29, 35–37]. Over-voltages, reverse power flow, and voltage fluctuations are the most common problems of high PV penetration.

2.2.1 Over-voltage

Depending on the impedance of the conductors and the distribution of loads, the service voltage varies from node to node. The service voltage normally drops along the line with the increase of electrical distance from the distribution transformer. This is true when there are no DGs feeding power into the network. However, due to power feed-in from DGs, the power flow direction may reverse in some of the line segments. The directions of power flow in the line segments are determined by the amount of net load in each of the nodes. Instead of voltage drop, the voltage level will rise in the line segments experiencing reverse power flow. This can cause over-voltage issues when the amount of power feed-in from the DGs is significant. The amount of power feed-in that a certain traditional LV network is able to manage without causing over-voltage issues is dependent on several factors. The resistance of the conductors, distance to the service point from the transformer, distribution

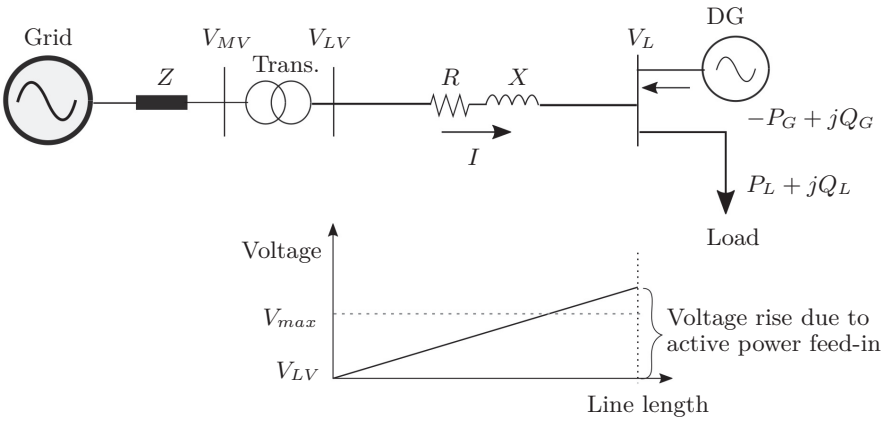

(a) Voltage profile.

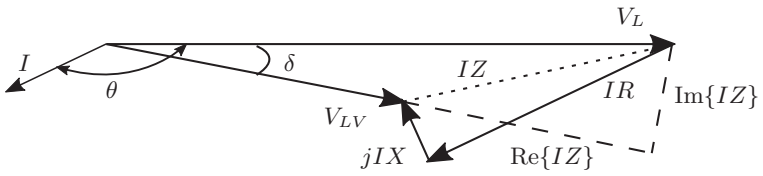

(b) Phaser Diagram.

Figure 2.3: Impact of DGs on the voltage profile of a LV feeder.

of DGs in the network, and the amount of power being fed to the grid from DGs are the primary factors.

Fig. 2.3 illustrates the effect of DGs on the voltage profile of a line using a simple example with one line segment. In the figure, V_{LV} is the secondary side voltage of the distribution transformer, V_L is the service voltage, and R and X are the resistance and the reactance of the line segment.

Applying Kirchhoff's voltage law to the circuit in Fig. 2.3a gives:

$$V_{LV} = V_L + I\,(R + jX) \tag{2.1}$$

Fig. 2.3b shows the corresponding phasor diagram where V_L is considered as the reference voltage. The adopted sign convention is: the active power drawn from the network is considered positive while active power injected into the network is negative. The reactive power consumed from the network is considered positive while reactive power injected into the network is negative.

The voltage drop/rise along the line is given by

$$\Delta V = |V_{LV}| - |V_L| \tag{2.2}$$

The angle between the source voltage and the service voltage (δ) is usually very small in a distribution system [38]. Therefore, the voltage amplitude difference between the source and the load voltage is approximately equal to

$$\Delta V \approx \mathrm{Re}\{IZ\} \tag{2.3}$$

The line current is given by

$$I = \frac{P_r - jQ_r}{V_L^*} \tag{2.4}$$

where

$$\begin{aligned} P_r &= P_L - P_G \\ Q_r &= Q_L + Q_G \end{aligned} \tag{2.5}$$

and

$$IZ = \frac{P_r - jQ_r}{V_L^*}(R + jX) \tag{2.6}$$

$$\begin{aligned} \Delta V &\approx \mathrm{Re}\{IZ\} \\ \Delta V &\approx \frac{1}{|V_L|}(RP_r + XQ_r) \end{aligned} \tag{2.7}$$

According to Eq.(2.7) the voltage drop/rise for a given line is approximately linearly proportional to P_r and Q_r.

Electrical equipment and appliances are designed to operate within a certain range of steady-state voltage. Operating at steady-state voltages outside this range can degrade the performance of the equipment or may damage it. Therefore, The DSO is obliged to maintain the service voltage within certain limits, which is usually standardized by a state regulatory commission. These standards may slightly vary from country to country. According to the European standard-EN50160 [39], the service voltage should be maintained within $\pm 10\%$ from the nominal voltage.

Changing the transformer tap setting to reduce the supply voltage is one solution to the over-voltage problem. However, this may create under-voltage issues during times of high demand. The distribution transformers usually consists of manual tap changers. Therefore, frequent changes of the tap settings to solve both under- and over-voltage issues is not a feasible solution for networks that experience both under- and over-voltage issues. Other solutions include increasing the conductor size of the lines, adding more transformers so that fewer customers are served by an individual transformer, application of voltage regulating equipment in the distribution sub-stations, and balancing of the loads on the primary feeders [40]. Some of these solutions are, however, costly. The inverter-based solutions for the over-voltage issue include power curtailment and reactive power support [15, 30–34]. The DG owners are not able to obtain full benefits from their systems

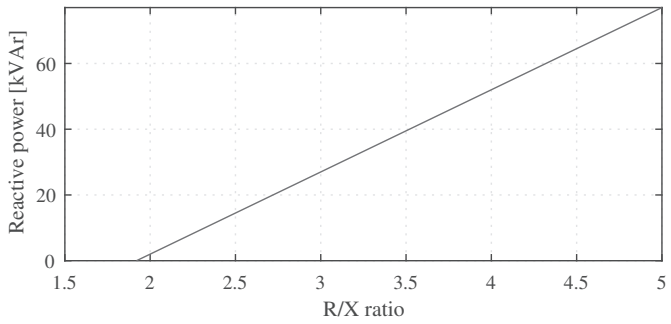

Figure 2.4: Required reactive power compensation for maintaining supply voltage at 240 V when $V_{LV} = 230V$, $P_r = -25kW$ and $X = 0.05\ \Omega$ for different R/X ratios.

when inverters are supposed to curtail power for maintaining the voltage quality of the network. The reactive power support solutions include fixed operating power factor, active power dependant power factor, and voltage dependant reactive power provision [32–34]. Improved methods have been proposed in the literature. The proposed methods aim to minimize the active power curtailment [41–44], and minimize the reactive power support required and associated losses [42–47]. Local control [46, 48–50] as well as decentralized [43], centralized [41, 42] and consensus control [51] concepts have been applied to achieve the above objectives.

According to Eq.(2.7), ΔV is negative $\left(|V_L| > |V_{LV}|\right)$ when P_r is negative (i.e. power is injected to the grid). ΔV can be reduced by absorbing the reactive power from the circuit ($Q_r > 0$). The amount of reactive power required for maintaining ΔV at a certain value is dependent on the R/X ratio of the network. Fig. 2.4 illustrates an example for the variation of the required reactive power compensation for networks with different R/X ratios. In this example, the required reactive power compensation is calculated for maintaining the service voltage at 240 V when $V_{LV} = 230$ V and $P_r = -25$ kW for a line with $X = 0.05\ \Omega$. As can be observed from the figure, the required reactive power compensation for voltage regulation is increasing as the R/X ratio of the network increases. Voltage regulation with reactive power is an effective solution for networks with low R/X ratios, for example transmission networks and MV networks. The R/X ratios of those networks are low (usually < 1), therefore the required reactive power support is also less. The R/X ratio of LV networks is usually high, hence the reactive power requirement for voltage regulation is also high. This can cause high reactive power flow in distribution grids. Therefore, reactive power support is not an effective solution for LV distribution grids.

2.2.2 Reverse power flow

The power flow direction through distribution transformers and MV/LV transformers can reverse during times of light load and high PV generation. This is

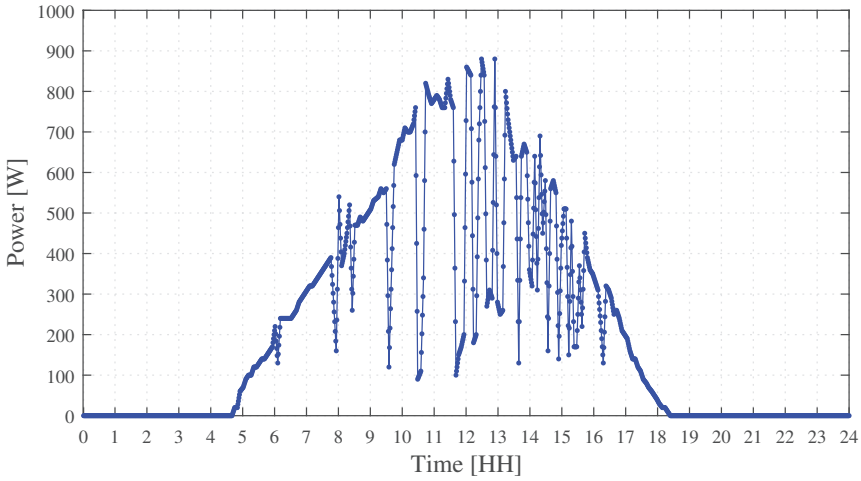

Figure 2.5: Power production from a 1 kWp PV system on a cloudy day at 1 minute resolution. This plot is produced from the measurements recorded from the test station located at University of Agder in Kristiansand, Norway [3].

because the local PV generation exceeds the local demand at these times. This causes a voltage rise instead of a voltage drop along the lines. When the number of PV systems feeding-in power to the network is significant, over-voltage issues can occur. Moreover, reverse power flow can create problems for the voltage regulators. Traditional voltage regulators are unidirectional, therefore they may not be able to operate correctly during reverse power flow. Reverse power flow can also affect the protection systems [35].

2.2.3 Voltage fluctuations

The presence of clouds in the sky causes significant changes in the solar irradiance incident on the earth's surface. Movement of the clouds and their evolution cause changes in irradiance over the time [52]. The rates of these changes are determined by factors such as, the speed of the clouds, the size of the cloud, the sun's position in the sky, and the cloud's altitude. PV panels respond relatively quickly to varying solar irradiance, hence a PV plant's power output fluctuates corresponding to the irradiance [53]. For example, Fig. 2.5 illustrates 1 minute power output measurements from a 1 kWp PV system on a cloudy day in May [3]. As can be seen from the figure, a sudden drop in the PV system's power output can be observed over short time intervals. This can cause voltage fluctuations in customer service voltage. These voltage fluctuations can cause flicker and may result in malfunction of electrical appliances.

2.3 Energy Storage for Enabling High Levels of PV Integration

As the share of generation based on renewable energy sources increases, maintaining the stability of the grid will be challenging. In addition to the demand fluctuations, the generation will also fluctuate as power production from renewable energy sources is intermittent and non-dispatchable. Therefore, energy storage will become an essential element in future electric power grids that accommodates significant amounts of generation based on renewable sources [54–57]. Storage can provide more flexibility to the grid and help to maintain stable operation against the variability of renewable energy sources. Energy storage acts as a back-up for renewable generation and therefore can smooth out generation fluctuations. Further, storage helps to improve the voltage quality in distribution grids with high PV penetration [58]. The presence of storage also helps to maximize the utilization of energy generated from renewable energy sources. Surplus energy can be stored and used later when production from renewable sources is lower or the generation cost of other generators is higher. At low levels of the grid, storage can help to manage distribution networks by improving power quality, efficiency and controllability. There are several applications of energy storage at the end-user level too. Basically, energy storage can be put at any level of the electrical system (generation, transmission, distribution and end-user) and depending on the location and the owner, its functions and applications may vary [6].

2.3.1 Applications of energy storage

Energy storage has the potential to provide a wide range of functions and services to grid operators and end-users. A reduction in generation costs is expected with the use of energy storage systems because storage can be used to store low-cost energy (mostly surplus energy from renewable sources) during off-peak periods. The stored energy then can be used during peak periods. This reduces the need to operate costly generators to cover the peak demand, therefore the generation cost can be reduced. Energy storage can aid renewable sources to smooth out the output fluctuations. Consequently, the complexity of maintaining the balance between demand and supply is reduced. Energy storage systems at the distribution level can control the power flow and mitigate congestion. Moreover, storage helps to improve the quality of supply, such as voltage quality. End-users can increase the self-consumption rates of locally produced electricity with the use of storage systems. With the use of a home energy management system, the operation of the storage systems can be scheduled to maximize cost benefits. Likewise, there are several applications of energy storage for different parties. More details about each application can be found in the sections below.

2.3.1.1 Applications of energy storage for grid operators

The applications of energy storage for grid operators are detailed below.

Renewables capacity firming

One of the important applications of energy storage in the future power grid is capacity firming, which refers to maintaining the output power of renewable sources at a fairly stable level with the aid of storage. The power output of PV power plants can drop suddenly when clouds pass over the plant. The output of wind power plants varies due to changes in the wind speed. These power fluctuations can cause rapid voltage changes and power swings. Therefore, these fluctuations need to be compensated by other dispatchable power sources. The response time of these sources should be as fast as the output fluctuations of PV and wind power plants. The more the share of renewables, the more the need for such dispatchable generators. As most storage technologies have a sufficiently fast response time, energy storage can effectively smooth power fluctuations and control the ramping rates of renewables [59, 60].

Peak shaving

Peak shaving is a method of reducing the load during the period of maximum demand on the power utility. Energy storage provides fast and emission-free operation, therefore it is a better source for supplying peak demand. The energy cost during peak hours is usually high because of the expensive generators that are operating to meet the peak demand. Use of energy storage systems reduces the need for operating these expensive generators. Therefore, utilities can reduce generation costs during peak hours. Energy storage helps to maintain a flatter load profile with a smaller peak, therefore helping grid operators to defer the investments in new costly power plants and grid upgrades [6, 59, 60].

Load levelling

Load levelling refers to storing power during periods of light load on the system and delivering it back to the system during periods of high demand. As the name indicates, it levels out the effective load on the system. Similar to the application of peak shaving, generation costs can be reduced due to a reduction in the load on the less economical peak generation units, while investments in new peak generation plants can be deferred [6, 59–62].

Micro grids

Energy storage is an essential element in micro grids that are usually fully or partly powered by renewable energy sources, such as solar, wind, and biomass. Energy storage maximizes the utilization of locally produced green energy. In islanded mode, the energy storage system maintains the stable operation of the micro grid by maintaining the voltage and frequency at acceptable levels. Energy storage can help with islanding and black start despite of whether other sources are active. Instead of energy storage systems, diesel generators are used in some micro grids. However, diesel generators are not environmentally friendly. In addition to maintaining stable operation, energy storage systems are able to provide several other services to the micro grid, including smoothing intermittent renewable-based generation, peak shaving, load shifting, and providing VAr support [63].

Grid power quality control

Energy storage systems are able to provide a wide range of ancillary services to the grid for improving power quality. Frequency regulation is one of them. Recently, there has been a significant growth in the frequency regulation market because as the share of renewable resources increases, so does the requirement for fast acting frequency regulating reserves. Energy storage has a faster response time compared to other frequency regulating sources. Therefore, it is a good candidate for frequency regulation. Another ancillary service includes improvement of voltage quality in distribution grids. Energy storage devices that are integrated into the grid through power electronic converters are capable of operating in all four quadrants. Therefore, storage is able to compensate for both voltage drop and voltage rise as well as voltage sags and swells. Harmonic compensation is an another ancillary service. Energy storage can act as an active filter for current harmonics in the grid. Likewise, energy storage can provide different ancillary services at different levels of the grid. These ancillary services can be combined with other services such as peak shaving and load levelling [6, 59–62].

Reserve capacity

One of the reliability criteria for the operation of power systems is to maintain sufficient reserve capacity that can be brought online during unexpected outage of a generator(s). The general rule is that the reserve capacity must be at least as large as the capacity of the largest generator in the system. Usually, the generators maintain about 20% reserve capacity that can be brought online whenever there is a failure of a generator(s) [59, 64]. Therefore, as these generators do not operate at their rated capacities, their efficiency is low. In addition, another set of generators are kept running idle, and only connected to the system when required. Most types of energy storage systems have a faster response time, therefore they are well suited to use as a reserve that can be immediately called upon during outage

of a generator. Having such reserve capacity allows other generators to work at their optimum power output and also avoids the need to have stand-by generators running idle [59, 60, 62].

2.3.1.2 Applications of energy storage for end-users

The applications of energy storage for end-users are explained below.

Peak shaving

End-users, particularly commercial and industrial customers, are able to reduce their electricity costs by reducing peak demand with the use of energy storage devices. The electricity bill of these types of customers consists of a demand charge in addition to the energy charge. This demand charge can be as high as the energy charge. It is calculated based on the maximum power usage during a billing period. The power drawn from the utility can be limited to a desired threshold by supplying the power that exceeds the threshold from the energy storage. Consequently, the demand charge can be reduced, hence significant savings can be realized [6, 59].

Time-of-use energy cost management

Customers who are subjected to time-of-use energy tariffs can benefit from the time shifting operation of the energy storage system. The peak load of residential customers normally occurs in the evening, when the production from the PV system is almost zero. Energy prices during this peak load period are usually high. Energy storage can be used to store the excess production from the PV system during peak insolation hours. The storage can also be charged from the grid during the low price period. Then the stored energy can be used to supply the local load or sold to the grid at a later time when the price is high. Storage systems coupled with PV systems could provide significant economic benefits for the residential and commercial customers who are subjected to time-of-use energy tariffs [6, 59, 60, 62, 63].

Back-up power

Energy storage systems provide back-up power for the customer during a power outage. To provide this service, the battery converters should be able to work in both grid-connected and offline mode. When the grid is energized, the battery converter should be synchronized with the grid and in the offline mode, the converter should form a localized grid for the residence. In addition, an islanding mechanism that can isolate the system automatically during an outage should be included in the battery converter. During an outage, the residence must be completely isolated

from the utility grid in order to prevent back-feeding of power into the distribution grid [6, 60].

2.3.2 Energy storage technologies

Electric energy can be converted and stored in many different forms. For example: mechanical, electrochemical, chemical, electrical, and thermal forms. A classification of different energy storage technologies, based on the form of energy stored, is given below.

- Mechanical
  Pumped hydro, Compressed air, Flywheel
- Electro-chemical
  Flow batteries (vanadium redox, zinc bromine, Poly sulphide), Conventional batteries (Lithium-ion, lead-acid, sodium sulfur, nickel cadmium, nickel metal hydride)
- Electrical
  Super capacitors, Super conducting magnetic coils
- Thermal
  Sensible heat storage (water, molten salt), latent heat storage (ice, sodium hydroxide), thermo-chemical storage
- Chemical
  Hydrogen

Among the different storage technologies mentioned above, the technologies that have been currently deployed are pumped hydro, compressed air energy storage, flywheels, batteries, super capacitors, and sensible and latent heat storage. Super conducting magnetic coils and hydrogen are still in the demonstration stage while other technologies like thermo-chemical are still in early stages of development.

Pupmed hydro storage

Pumped hydro plants consists of two reservoirs at two different elevations. During off-peak hours, water is pumped from the lower reservoir to the upper reservoir. The water is released from the upper reservoir to generate electricity when needed. The round-trip efficiencies of pumped hydro plants are in the range of 70% to 85%. Pumped hydro plants are capable of storing huge amounts of energy and are able to charge/discharge at high power. They have a relatively fast response time and a long life span of approximately 50 to 60 years. Over 95% of the total global storage capacity is the pumped hydro [61, 63, 65].

Compressed air energy storage

Compressed air energy storage plants compress air using electricity during off-peak hours. This compressed air is then stored in underground or above-ground structures like caverns, aquifers, abandoned mines, pipes or vessels. When needed, the stored air is mixed with natural gas and this mixture is injected directly into the combustion chamber of a conventional gas turbine system. The efficiency of this system is relatively low, at less than 50% [60, 61, 63, 65].

Flywheels

Flywheels convert electrical energy to kinetic energy and vice versa. A flywheel is simply a rotating mass which is accelerated (charged) by a electric motor. During discharging, the motor acts as a generator. Flywheels have relatively high power density, fast response time and long life spans. They are currently being used for frequency regulation [60–63, 65].

Super capacitors

Capacitors store electric energy as an electrostatic charge. Super capacitors have very high capacitance compared to a conventional capacitor. They have extremely high power capability and have a virtually unlimited cycle life. Super capacitors can be fully charged and fully discharged in seconds. The specific energy densities of super capacitors are relatively low and the self-discharge rates are high. Therefore, they are not able to store energy over longer periods [60–63, 65].

Super conducting magnetic energy storage

Super conducting magnetic storage stores energy in a magnetic field surrounding a coil carrying a direct current. The coil is made of a super conductor having very low resistance. At very low temperatures, around -163°C (110 K), some conducting materials lose their resistance [66]. In order to cool the conducting material down to this temperature, a cooling system is required. The cost of such a system is relatively high and the cooling process lower the efficiency of the overall system. Hence, this technology is not yet commercially available and still at the demonstration stage [60–63, 65].

Thermal energy storage

Thermal energy storage systems store energy in the form of heat in an insulated repository. Types of thermal storage technologies that are commercially available includes: sensible heat storage and latent heat storage. In sensible heat storage,

thermal energy is stored in either liquid or solid medium (such as water, sand or rocks) through change of temperature of the storage medium. In latent heat storage, phase change materials such as ice and molten salt are used as the storage medium. The energy exchanged when a material changes its phase is called latent heat. There is no change of temperature during energy transfer in this process. In thermo-chemical storage, heat is stored in chemical compounds using reversible chemical reactions. This technology is still in the early stages of development [60, 61, 63, 65].

Hydrogen energy storage

The excess energy available from renewables can be used to produce hydrogen through electrolysis of water. This hydrogen can be stored for several days, weeks or even several months. Stored hydrogen can also be transported. When needed, stored hydrogen can be used to generate electricity using fuel cells [60, 61, 63, 65].

Battery energy storage

An electro-chemical battery converts energy generated during a chemical reaction into electrical energy. A battery is made of one or more series and/or parallelly connected cells. Each cell consists of three main components: positive electrode, negative electrodes, and electrolyte. The chemical reactions of a battery cell can be either irreversible or reversible. The batteries made of irreversible cells cannot be recharged. This type of battery is called a primary battery. Batteries made of reversible cells can be recharged and they are called secondary batteries.

There are mainly two types of secondary batteries: conventional batteries and flow batteries. In a conventional battery, two electrodes may be immersed in a liquid electrolyte or separated by a solid electrolyte. When the two electrodes are externally connected through a load (discharging), the negative electrode oxidizes and creates an electron flow through the external circuit. The positive electrode accepts these electrons and reduces during the chemical reaction. The electrolyte transports ions from the negative electrode to the positive electrode. When an external voltage that is higher than the open circuit voltage across the two electrodes is applied, the electrochemical reactions reverses and the two electrodes are restored to their original state (charging). In flow batteries, the reaction cell is divided into two chambers using a membrane. Two liquid electrolytes are stored in two external tanks and circulated through these two chambers using pumps. During charging, oxidation reaction occurs in one electrolyte while chemical reduction reaction occurs in the other. The membrane prevents the two electrolytes from mixing but allows only selected types of ions to pass through the membrane to complete the redox reaction. During discharging, electro-chemical reactions reverse. The capacity of a flow battery is determined by the volume of the electrolyte.

A variety of battery technologies are available and the characteristics of these bat-

tery types mainly depend on the materials used for electrodes and the electrolyte. Table 2.1 gives a summary of characteristics and a comparison of different popular battery technologies [6, 60–63, 65].

Table 2.1: Characteristics of different battery technologies.

Type	Characteristics
Flow batteries	
(1) Vanadium Redox	• Specific energy: 10-25 Wh/kg. • Efficiency: 80-85%. • Service life: 15 years. • Cycle life: 10000-12000 cycles at 100% DoD. • Fast response, 1 ms from charge to discharge.
(2) Polysulphide Bromide	• Specific energy: 10-15 Wh/kg. • Efficiency: 75%. • Service life: 15 years. • Cycle life: 2000 cycles. • Fast response time of 20 ms, if electrolyte is retained charged in the cell stack. In normal conditions, response time is 0.1 s.
(3) Zinc Bromine	• Specific energy: 30-50 Wh/kg. • Efficiency: 60-75%. • Service life: 15 years. • Cycle life: 2000 cycles.
Conventional batteries	
(1) Zinc-Air	• Specific energy: 130-200 Wh/kg. • Specific power: 100 W/kg. • Efficiency: 50-60%. • Service life: 15 years. • Cycle life: 1000+ cycles.
(2) Lead Acid	• Specific energy: 30-50 Wh/kg. • Specific power: 75-300 W/kg. • Efficiency: 70-80%. • Service life: 5-15 years. • Cycle life: 500-1000 cycles.

(3) Nickel Cadmium (NiCd)	• Specific energy: 50-75 Wh/kg. • Specific power: 150-300 W/kg. • Efficiency: 70%. • Service life: 10-20 years. • Cycle life: 2500-3000 cycles at 100% DoD.
(4) Nickel Metal Hydride (NiMH)	• Specific energy: 70-100 Wh/kg. • Specific power: 200-300 W/kg. • Efficiency: 70%. • Service life: 5-10 years. • Cycle life: 3000 cycles at 100% DoD.
(5) Sodium Sulphur (NaS)	• Specific energy: 150-240 Wh/kg. • Specific power: 150-230 W/kg. • Efficiency: 80-90%. • Service life: 15 years. • Cycle life: 2500 cycles at 100% DoD. • Operation temperature: 300°C .
(6) Lithium-Ion (Li-ion)	• Specific energy: 75-200 Wh/kg. • Specific power: 150-315 W/kg. • Efficiency: 85-95%. • Service life: 5-15 years. • Cycle life: 1000 to 10000 cycles.

Among the battery technologies listed in Table 2.1, lead-acid is the oldest and most commercially mature technology. Lead-acid batteries are relatively cheap and safe, therefore used in various applications ranging from utility scale applications to residential applications. Even though the cost is low, as can be observed from the table, its specific energy density and cycle life are relatively low compared to the other conventional battery technologies. Lead-acid batteries are quite heavy and last only a few years when subjected to daily cycling. Lithium-ion is the other technology that is used in a wide variety of applications including consumer electronics, vehicle batteries, grid-scale storage, and residential storage. Lithium-ion has superior characteristics over lead-acid. Its specific energy density, efficiency, and cycle life are better than lead-acid. However, the cost of lithium-ion batteries is much higher. Yet when considering the levelized cost, lithium-ion is more economically attractive due to its higher efficiency and cycle life. The cost of lithium-ion packs has decreased over the past several years dramatically. There has been a 73% drop in the cost of lithium-ion packs from 2010 to 2016. According to analysts at Bloomberg New Energy Finance, the price of lithium-ion packs may drop to $73/kWh by 2030 from $273/kWh in 2016 [67]. This will make this technology affordable for all kinds of customers, consequently the energy storage market will

grow significantly in the coming years.

2.4 Overview of Control Strategies of Distributed Battery Energy Storage Systems

Among the energy storage technologies mentioned above, battery energy storage (BES) is the technology that can be deployed at any level of the grid and at any geographic location with capacities ranging from a few kWh to several MWh. This technology is therefore used in a variety of applications ranging from large-scale utility scale applications to small-scale applications like residential energy storage systems. As mentioned earlier, significant growth of the BES market is expected in the coming years. This will facilitate the safe integration of a large amount of renewable energy systems into the grid.

The main function of BES is to store active power and release it when needed. Most of the applications listed in Section 2.3.1 are related to the active power storage capability of BES systems. However, as BES systems are connected to the grid via power electronic converters, they are capable of providing services related to reactive power as well. Fig. 2.6 illustrates the active and reactive power (P-Q) capability curve of a BES system. The shaded area corresponds to the operating region of the battery converter. The converter is able to operate at any point within the circle with radius S_{max}, if there is no limitation of power factor or maximum reactive power (Q_{max}).

The P, Q operating points of the battery converter in a certain application need to be controlled according to its specific use. These set points can be locally decided based only on the local information. In that case, a local objective can be fulfilled. Otherwise, the set points can be decided by an external controller. When controlling via an external controller, higher-level objectives can be achieved. Depending on the type of the control structure the information and the infrastructure needed, the complexity of the control system may vary. In general, four different control architectures can be found in the power system. Those are: local control, centralized control, decentralized control, and distributed control. Fig. 2.7 illustrates the first three control architectures.

2.4.1 Local control

In local control architecture, the local controller decides the set points based only on local information. For example, consider the local controller of a distributed BES system co-located with a load and a PV system. The local information available for this case would be voltage and current measurements at the load, PV system, and the point of common coupling (PCC). The set points determined by the local controller would be the charging/discharging power set points of the BES system

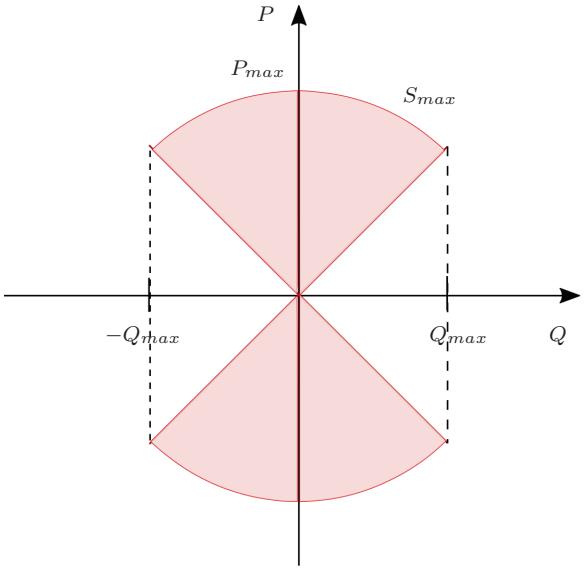

Figure 2.6: P-Q capability curve of a BES system. Shaded area represents the operating region of the battery converter.

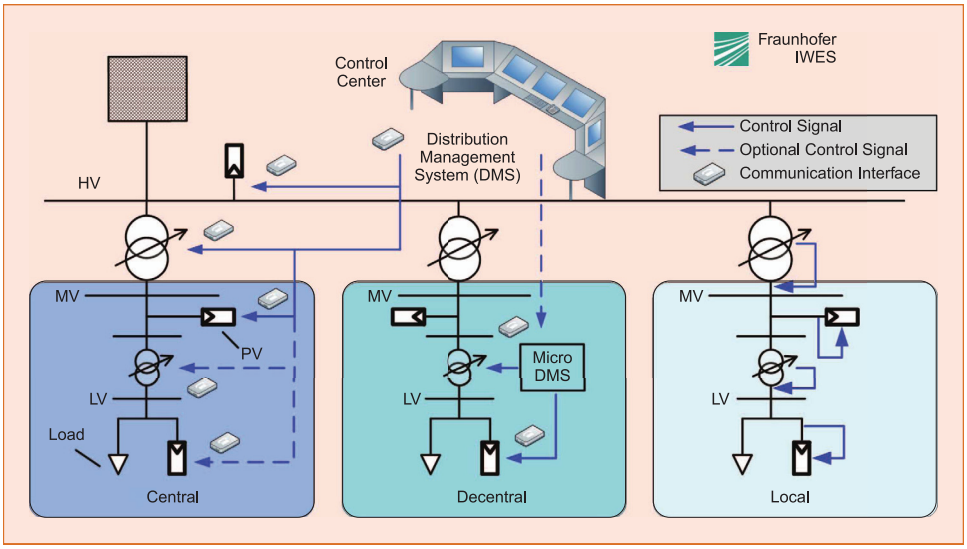

Figure 2.7: Overview of different control architectures used in the power system [4] (source: Fraunhofer IWES).

and the reactive power set point of the converter. In this control architecture, the controller is not aware about the state of the network outside the PCC. So, there is no coordination between the systems because each system takes decisions independently based only on the local information. This control structure may not result in optimized operation for an overall grid section. Nevertheless, local control algorithms have the fastest response times compared to the other two control structures. Also, this approach needs lower investment mainly because it does not need communication infrastructure.

The simplest local control method for a BES system co-located with load and renewable based generation is rule-based control. In this method, instantaneous battery charging/discharging set points are decided based on certain rules. For example; the battery should be charged from the excess power available from the local generator and should be discharged in the evening to supply the load. Likewise, depending on the requirement, rules can be defined or real-time algorithms can be developed to determine the instantaneous power set points of the BES systems. Day-ahead scheduling using optimization is another method to determine the BES set points. In this method, BES set points over a selected time interval into the future are calculated by solving an optimization problem. Unlike rule-based control, with this control; the operation of the BES system can be optimized with respect to a given objective. To solve the optimization problem, at least the following information about the system is needed: a model of the complete system, forecasts of the uncontrollable loads and generation over the selected time interval into the future, and day-ahead electricity prices. The realization of the objective is primarily depends on the accuracy of the forecasts. The optimization problem can be linear or non-linear depending on the complexity of the system, the objective function, constraints and the types of variables involved (continuous variables and/or integer variables). Therefore, an appropriate optimization technique needs to be chosen according to the problem's complexity.

Ref. [68–70] present different local control algorithms for smoothing out the power exchanged with the grid from PV or/and wind energy systems. These real-time algorithms calculate the instantaneous power set points of the BES system based on real-time measurements from the systems connected to PCC.

Ref. [71, 72] present local control algorithms for BES systems to improve the voltage profile of a distribution system having high PV penetration. In these methods, charging operation of the BES system is determined by the voltage at PCC. That is, the BES is charged if the voltage at PCC exceeds a predefined threshold. In [71], the BES charging power can be either the total PV generation or the excess PV power. In [72], the charging power set points are determined based on the droop coefficient. The droop coefficient defines the relationship between the PCC voltage and the BES power set points.

Ref. [73–81] present local control methods using optimization-based day-ahead scheduling for determining the charging/discharging power set points of BES systems. These BES systems are usually co-located with various types of loads (uncon-

trollable or/and controllable) and renewable/non-renewable sources based generations. The main objective of the BES system in Ref. [73–78] has been to minimize the operating cost. In Ref. [73], the control problem has been formulated as a linear optimization problem, therefore, linear programming has been used to determine the BES system's control set points (hourly average power set points) over a 24-hour period. The control problems in Ref. [74, 75] also involve integer variables. Ref. [74] considers the scheduling of controllable loads whose behaviour is discrete and Ref. [75] considers a thermal generator whose cost is represented as a summation of piecewise linear segments. Therefore, integer variables are used. In these cases, the optimization problems have been solved using mixed-integer linear programming. Ref. [76–78] formulate the control problems as non-linear optimization problems, where Ref. [76, 77] adopt dynamic programming while [78] uses genetic algorithm to solve the problems. In Ref. [79], the main purpose of the BES system is to reduce the peak load on the system. This control problem has been solved using linear programming as the optimization problem is linear. The BES control method presented in Ref. [80] attempt to minimize the energy exchanged with the grid to minimize the daily operational cost and power feed-in to the grid. In this work, the optimization problem has been solved using quadratic programming. The control objective of ref. [81] is to smooth out the effective load profile (seen by the grid) of a residential energy system comprising loads, a PV system, and a BES system. The objective function of the optimization problem has been set to minimize the energy cost over the planning horizon. The desired objective, i.e. smoothing out the effective load profile, has been indirectly achieved by adding a capacity dependent tariff to the retail electricity price. There, mixed integer linear programming has been adopted to solve the optimization problem.

2.4.2 Centralized control

In a centralized control structure, the control actions of each individual systems are determined by a central controller. The central controller considers the operating conditions of each individual system in order to derive the new set points of the sub systems. Therefore, the central controller should aware of the state of the whole system that is being monitored and controlled, as well as its controllable entities. For that, the communication infrastructure needs to be integrated into the power grid and in the devices participating in this control structure. In this way, the operation of a whole network section can be optimized for a given objective. The complexity of this control structure increases with the increase of the system size and the number of controllable elements. The controllers may experience delays in communication. Also, a failure of communication between the controller and an element may adversely affect the operation of the whole system. Although, the centralized control structure results in system wide optimum control, the scalability of this structure is poor due to increased complexity [82].

Ref. [83–85] present centralized control strategies for distributed BES systems, which are based on day-ahead scheduling using optimization. In these approaches,

the objective is to optimize the operation of a whole section of the distribution network. A central controller solves the optimization problem to calculate the day-ahead set points of each BES unit in the system. The corresponding set points are then sent to these systems. In Ref. [83], the optimal set points of the BES units that can flatten the load on the network over the planning horizon have been found. In [84], the objective function consists of multiple objectives: minimizing network power loss, minimizing battery cyclic cost, and minimizing voltage deviations. The optimal BES set points that can minimize the above objectives have been found using a hybrid optimization technique employing an interior point and pattern search method. The objective in Ref. [85] is to minimize the energy cost for the distribution system operator. Maintaining voltage quality (voltage magnitude and voltage unbalance) within acceptable limits is one of the requirements, which has been added as a constraint in this optimization problem. Ref. [86, 87] present real-time centralized control schemes for distributed BES systems. The aim of these control schemes is to maintain the voltage profile within acceptable levels using BES systems. The central controller requests charging/discharging based on the voltage measurements at certain buses. In Ref. [86], the central controller broadcasts charging/discharging signal to all BES units, and BES units react accordingly if certain local conditions are satisfied. In Ref. [87] the central controller also calculates the required charging/discharging set points of each BES units.

2.4.3 Decentralized control

In a decentralized control structure, the system being monitored and controlled is divided into several subsystems and each subsystem is controlled by separate controllers. The subsystem's controller only monitor and control the elements attached to that subsystem. The control actions only depend on the outputs from the sub system therefore, the complexity of the control problem is lower. There are no interactions among the subsystem controllers. However, the subsystem controllers may communicate with a central controller. In that way, the decentralized controlled subsystem can be a part of a centralized control structure. This way, the computational burden on the centralized controller can be distributed among the subsystem controllers, which also reduces the communication requirement [82]. An example of such a system can be an LV network supplied by a distribution transformer, which is the subsystem while a feeder in the MV network is the network section controlled by the central controller. Compared to centralized control, decentralized control greatly reduces the computational burden and reduces the complexity of the control algorithm. Unlike a centralized structure, the distributed control structure can be easily scaled up for larger systems [88].

From the high voltage or medium voltage network's perspective, the control schemes presented in Ref. [83–87] can be considered as decentralized control schemes. This is because the so-called centralized control scheme of an LV network presented there can be a part of a centralized control scheme in the MV network.

2.4.4 Distributed control

In the above three control architectures, the control decisions are either taken by individual systems independently or solely by a central entity. In those methods, there is no communication between the systems or subsystems. In distributed control architecture, systems can communicate with other systems in the network. One system may not share information with all other systems, but share information only with a few neighbouring systems. For this, necessary communication links between the systems need to be established. In this method, the control algorithm is usually initiated by a leader. This leader may monitor the status of the network at one or several critical nodes in the network. The control decisions of each individual system are usually taken by the local controller based on local information and information about the outside network, which are received by the neighbouring systems.

Ref. [89–92] present distributed control schemes for BES systems, which are coupled with PV systems. In these works, The consensus algorithm has been used to coordinate the operation of the BES systems. In the consensus algorithm, the control algorithm is initiated by a virtual leader. This leader can be a control or monitoring system located at some critical node in the system. The virtual leader sends necessary information to the neighbouring system(s) through communication links. The local controllers of BES systems determine the control set points based on this information and the local conditions. It also generates required information to be sent to its neighbours for consecutive decision making. The objective of smart coordination of BES system operation in Ref. [89–91] has been to regulate the feeder voltage within acceptable levels while in Ref. [92] the objective has been to maintain the balance between supply and demand.

In the distributed control method presented in Ref. [93, 94], a central controller is involved in making certain decisions. These decisions are based on real-time information from the network. In Ref. [93], the BES systems in the network have been grouped and a master unit is assigned to each group. A master unit can communicate with the central controller and the other BES systems in its group. The objective of coordinating the BES operation has been to regulate the voltage. In this method, the central controller determines the charging/discharging set points of each group. These set points are then sent to the master units in each group. The master units then decide how this set point is shared among the BES units in their groups. In Ref. [94], the central controller only decides which BES system to be used for voltage support. The selected BES system's local controller then decides the required BES set points and communicates the results back to the centralized controller for subsequent decision making. The objective of the distributed control scheme presented in Ref. [83] has been to flatten the aggregate power usage profile of the distribution network. In this work, BES set points have been found using an optimization based day-ahead scheduling. The optimization problem is solved by local controllers. The central controller broadcasts the day-ahead electricity prices to the residential energy systems. This price profile is an input to the local

optimization problem. The optimization results are then communicated back to the central controller to calculate the aggregate load profile on the network. The central controller updates the electricity prices according to this profile and broadcasts the updates prices. This process is continued until steady-state is reached. In this way, both the communicational and computational burden has been reduced by distributing the tasks among the central and local controllers.

Chapter 3

Local Control Strategies for Residential Storage Systems: Grid-Supportive Operation

This chapter focuses on a local control strategy for battery energy storage systems in residential applications. This control strategy aims to support the grid for over-voltage mitigation while fulfilling the local requirements of the storage owner. It also presents a reactive power control strategy for mitigating the over-voltage issues that can work in coordination with the active power control of battery energy storage systems. The chapter starts with the details of modelling a grid-connected residential energy system comprising a load, PV system, and a battery energy storage system. Details of the control algorithm are then presented followed by the results from a simulation study.

3.1 Introduction

The recent growth of the market for battery energy storage in residential applications has been primarily driven by the prosumers' urge to increase the consumption of self generated energy. Using a BES to achieve a 100% self-consumption rate may not be economically attractive, because of seasonal variations of PV generation and the high cost of batteries. PV systems produce more energy during summer and a little in winter. Therefore, a BES sized to achieve a 100% self-consumption rate during the summer months is over sized for the winter months. When considering the yearly performance of the PV system and the cost of the BES system, the economical option would be an averaged-sized BES unit. The electricity tariff also affects the optimum size of the BES unit. Smart metering technology facilitated introducing time-of-use and real-time-pricing electricity tariff schemes at the resid-

ential level. In some countries a peak demand charge has also been introduced for residential customers. Customers who are subjected to the above electricity tariffs, can maximize their savings by utilizing the stored energy to supply the local load mainly during the high tariff period. The stored energy can also be used to limit the power drawn from the grid to a desired limit to avoid high peak demand charges. Besides, when the difference between the lowest and highest electricity prices is significantly high, charging from the grid during the low tariff period to supply the load in high tariff period may also be an economical option. The optimal capacity of the BES depends on the application and needs to be carefully determined by considering all relevant parameters specific to the application. Optimum sizing of storage for different applications has been addressed in the literature [95–99]. The key parameters that need to be considered when sizing a BES unit for residential application with PV are the cost of the BES system, annual variation of load and local production, utility electricity tariff, sell back rates, and battery ageing.

The charging/discharging operation of the BES unit has to be scheduled strategically in order to obtain maximum economical benefits from the BES. For a residential application, economic benefit is usually quantified by cost saving in the customer's electricity bill. Reference [79] proposes an optimum dispatch schedule for a BES unit coupled with a PV system. The primary application of the BES has been peak shaving. The net energy exchanged with the grid over a certain planning horizon has been considered as objective function, and the dispatch schedule that minimizes the objective function has been found using linear programming. Reference [76] presents optimal control strategies for BES units considering different objectives such as maximizing battery life, maximizing self-consumption, and minimizing energy cost. They have used dynamic programming to solve the optimization problem.

All of these control strategies aim to maximize economic benefits for the BES owner and do not intentionally contribute to improving the voltage quality of the grid. As mentioned in Section 1.2, high levels of PV penetration in distribution grids can cause severe reverse power flow issues resulting transformer over-loading and voltage quality violations. The presence of residential storage lowers the risk of voltage quality violation and transformer over-loading issues, however without proper grid-supportive operational strategies effective support to the grid is not guaranteed. A grid-supportive operational strategy for residential BES has been presented in [80]. The method aims to lower the reverse power flow in the distribution grid with proper scheduling of BES units. The optimization problem attempts to minimize the total energy supplied to/by the grid over the planning horizon by the residential energy system. The optimization problem has been solved using quadratic programming. The method also attempts to maximize economic benefits by introducing selectable weights in the objective function which are calculated based on greedy-search heuristic algorithm. However, according to the simulation results presented, the charging time of the storage is sensitive to the utility electricity tariff. As a result, the storage charges during the times of high utility electricity prices. The peak utility electricity tariff period may not always coincide with the times of high PV penetration periods. Therefore, the proposed method

may not be effective in supporting the grid to reduce the risks of over-voltages in some cases.

This chapter presents a grid-supportive operational strategy for residential BES units coupled with PV systems. The aim of the proposed method has been to effectively support the distribution system operator to lower the risks of transformer over-loading and voltage violations without adversely affecting the local objectives of the BES owner. The BES control method mainly relies on local information. Control of active power injection to the grid using BES units may not be sufficient to solve the over-voltage problem completely when the cumulative storage capacity available in the distribution system is not sufficient. In that case a secondary solution is needed. This chapter also presents a secondary solution which is based on reactive power support from the PV inverters and battery converters.

3.2 The Residential Energy System

A household with a local generation source and energy storage can be defined as a small-scale energy system. Such a residential energy system may consist of household electric loads, a PV system, a BES system, a controller, and a smart meter. Depending on the connection point of the battery bank to the electrical system, two different configurations of residential energy systems can be found: DC- and AC-coupled systems [100]. In an AC-coupled system, both PV array and the battery bank are connected to the AC side of the electrical system via separate power electronic converters, as shown in Fig. 3.1a. The converter connecting the PV array to the grid is an inverter with maximum power point tracking (MPPT) functionality. The converter connecting the battery bank to the AC system is bi-directional (acting as both inverter and rectifier). During power outage the battery converter disconnects the residential energy system from the grid and changes the operation to off-grid mode. The PV converter synchronizes to the voltage and frequency generated by the battery converter.

In a DC-coupled system, the battery bank is connected to an intermediate DC link directly or via a bidirectional DC-DC converter. Fig. 3.1b shows a DC-coupled system where the battery bank is directly coupled to the DC link. The PV array is connected to the intermediate DC link trough a DC-DC converter. The DC-DC converter is usually known as solar charger and consists of MPPT functionality. This DC system is then connected to the AC system via a grid converter. The grid converter can be either uni-directional or bi-directional. Charging the battery bank from the grid is possible with a bi-directional grid-converter. The grid converter is responsible for continuity of supply during a power outage. It disconnects the residential energy system from the grid and changes the operation to off-grid mode. There are converters in the market that integrates both the solar charger and the grid converter in to one box.

AC-coupling of a battery is convenient when adding a battery bank to an exist-

ing PV system. This is because DC-coupling requires replacement of the existing inverter. Moreover, AC-coupled systems are easily expandable without additional cost. In off-grid mode, the control and power management of AC-coupled systems are more complicated as two inverters need to be synchronized with each other. There are debates about the power conversion efficiencies of the two system configurations. Some people claim that the DC-coupled system is more efficient due to a lower number of conversion stages when charging the battery from the PV system. However, when the load is supplied by the PV system, the power still has to go through two conversion stages. Conversely, in an AC-coupled configuration the power has to go through one conversion stage. Therefore, this claim may not be true always. The overall efficiency of the system during one charging/discharging cycle will depend on how much load is supplied directly by the PV system, the energy injected into the grid, and the portion of the load supplied by the battery bank.

3.3 The Home Energy Management System

As a part of demand response programmes, time-based electricity tariffs such as time-of-use pricing, critical peak pricing, variable peak pricing, and real time pricing have been introduced to retail customers [101–104]. Demand response programmes encourage customers to shift electricity consumption during peak period to off-peak periods. Unlike flat rates, time-based rates can result in high electricity bills for customers unless electricity usage is properly managed. A system that manages the electricity usage of the household in order to lower the electricity bill without affecting customer comfort is called a home energy managements system (HEMS). Recently, the demand for HEMSs has been on the rise as consumers are looking for methods to reduce their electricity bills. The HEMS manages the electricity usage of the household by effectively monitoring and controlling the load, the production, and the storage operation. It can communicate with household devices and the DSO, as needed, and receive information such as electricity prices and weather forecasts. The HEMS determines the optimal operation schedule of the flexible loads and the storage that results in maximum savings in the electricity bill.

In distribution grids with high PV penetration, the DSO will benefit by charging customer-owned storage units at times of high reverse power flow in the distribution grid. Charging storages reduces the reverse power flow in the distribution grid, therefore also reducing the risk of over-voltage issues. The HEMSs can be informed by the DSO about the times when the grid is at high risk of over-voltage issues. This information can be included in the scheduling algorithm so that the storage operation, especially the charging of the storage can be scheduled accordingly.

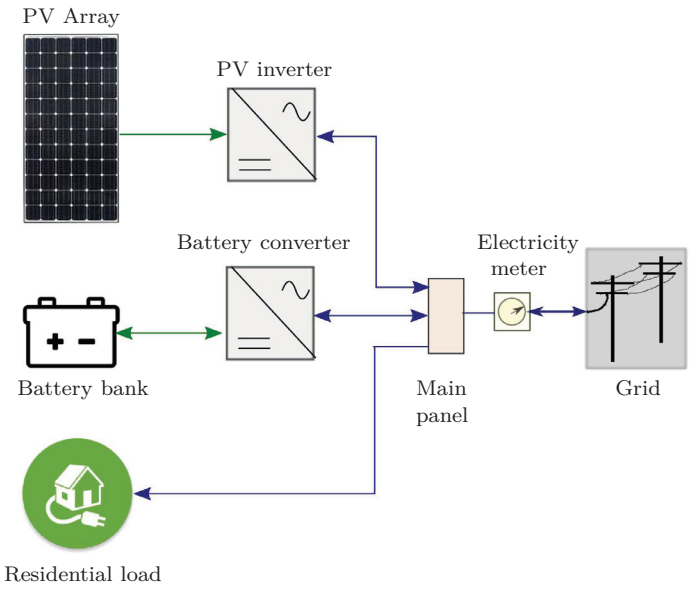

(a) AC-coupled system

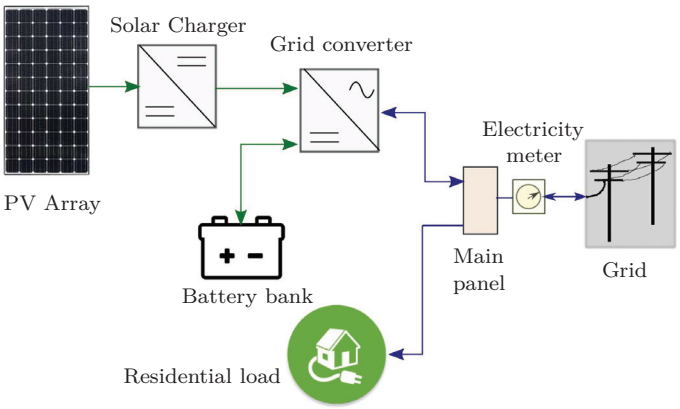

(b) DC-coupled system

Figure 3.1: Residential energy system configurations.

3.3.1 System modelling

The main components of a residential energy system are the loads, the PV system, the battery bank, and the power electronic converters. For energy management studies, it is sufficient to model the components with their steady state behaviour. The focus of this work is to investigate grid-supportive operational strategies for residential battery energy storage units. Therefore, the BES unit is considered to be the controllable load while all other loads have been treated as uncontrollable but predictable. The power production from the PV system is also uncontrollable but considered predictable.

3.3.1.1 PV system

The maximum power point (MPP) power of a PV system for a given irradiance and an ambient temperature is given by

$$P_{pv} = P_{mpp,STC}\left(\frac{G_T}{1000}\right)[1 + \alpha_p(T_c - 25)] \tag{3.1}$$

where $P_{mpp,STC}$ is the MPP power of the PV system at standard test conditions (a cell temperature of 25^{o}C and an irradiance of 1000 W/m^2), G_T is the irradiance, α_p is the module's temperature coefficient of MPP power, and T_c is the temperature of the PV cells. The cell temperature can be estimated from the irradiance along with the ambient temperature and the normal operating cell temperature (NOCT) as follows.

$$T_c = T_{amb} + G_T\left(\frac{NOCT - 20}{800}\right) \tag{3.2}$$

where T_{amb} is the ambient temperature. The NOCT is the operating temperature of the cell at an irradiance of 800 W/m^2 and an ambient temperature of 20 ^{o}C. The NOCT is usually provided by the manufacturer.

3.3.1.2 Battery energy storage

The complete modelling of a battery for a long-term study includes the modelling of the battery voltage, capacity, and lifetime. The battery voltage models presented in the literature can be mainly divided into two types: electrochemical based and electric-circuit based models. Molecular level physics based electrochemical models typically represent the dynamic behaviour of a battery with high accuracy. However, due to the high complexity of these models, they are not suited for power and energy management studies. The high level electric circuit based models that can accurately predict the behaviour of the battery require inputs that are not typically available on data sheets [105–108]. The electrochemical based model developed by Shepard in 1965 is able to model the battery voltage during discharging [109]. The parameters of this model can be estimated using the information

available on the data sheets. There have been improvements to this model over time by other researchers [110, 111]. The electrochemical model presented in [111], which is an improved version of the Shepard model, is used in this work to model the battery voltage. According to this model, the terminal voltage of the battery during discharging is

$$\begin{aligned} V_{bat} =& E_o - K\left(\frac{Q_{nom}}{Q_{nom}-q}\right)q - K\left(\frac{Q_{nom}}{Q_{nom}-q}\right)i_{bat} + A\ exp(-Bq) - R_{bat}\ i_{bat} \\ q =& \int i_{bat}\ dt \end{aligned} \tag{3.3}$$

where,

V_{bat}	Terminal voltage (V)
E_o	Battery constant voltage (V)
K	Polarization voltage (V)
Q_{nom}	Battery nominal capacity (Ah)
A	Exponential zone amplitude (V)
B	Exponential zone time constant inverse $(\text{Ah})^{-1}$
R_{bat}	Internal resistance of the battery (Ω)
i_{bat}	Battery current (A)
dt	Time step (hr)

The parameters E_o, K, A and B can be calculated from the discharge characteristics given in the battery data sheet [110]. The assumptions of the model are: the internal resistance is constant and does not vary with the state of charge (SoC) of the battery, the capacity of the battery does not change with the amplitude of the current (No Peukert effect), the model parameters are deduced from the discharge characteristics and assumed to be the same for charging, self-discharge of the battery is neglected, and the battery has no memory effect. The model gives negative voltages at regions of very low SoC, and very high voltages when the battery is over-charged. However, in practical applications the SoC of the battery is maintained well above zero SoC state and over-charging of the battery is avoided. Therefore, the behaviour of the simulated system is not affected by the above limitations.

The SoC of the battery during charging is calculated using the coulomb counting method as follows.

$$SoC(t_2) = SoC(t_1) + \frac{1}{Q_{nom}} \int_{t_1}^{t_2} (\eta_{bat,chrg}\ i_{bat} - i_{sd})\ dt \tag{3.4}$$

where $\eta_{bat,chrg}$ is the coulombic efficiency during charging and i_{sd} is the self discharging current. In this work, we assumed the self-discharging current is zero.

The available capacity of lead-acid batteries varies significantly with the discharging current. The capacity decreases as the charging rate is increased. The Peukert's

law describes the relation between the discharge current and the available capacity.

$$T = \frac{Q_p}{I^n} \tag{3.5}$$

where Q_p is the battery capacity at 1 Ah discharge rate, T is the time to discharge the battery, I is the actual discharge current, and n is the Peukert constant. The Peukert constant of various lead-acid battery types takes the values in the range 1.05-1.6. The Peukert constant of lithium-ion battery types is close to 1. Therefore, the capacities of lithium-ion batteries are not significantly affected by the discharging current.

The effect of discharging current on the battery capacity can be included in the SoC variation equation during discharging as follows.

$$\begin{gathered} SoC(t_2) = SoC(t_1) - \frac{1}{Q_{nom}} \int_{t_1}^{t_2} \frac{i_{bat} - i_{sd}}{\eta_{bat,dischrg}}\, dt \\ \eta_{bat,dischrg} = f(i_{bat}) \end{gathered} \tag{3.6}$$

where $\eta_{bat,dischrg}$ is the coulomb efficiency of the battery during discharging and it is a function of the battery current. For lithium iron batteries $\eta_{bat,dischrg} \approx 1$. For lead-acid batteries the relationship between $\eta_{bat,dischrg}$ and the discharge current is derived using the information given in the battery data sheet as follows.

Eq.(3.6) can be rearranged for a full discharge at the constant discharge current i as follows.

For a full discharge;

$$\begin{gathered} SoC(t_2) - SoC(t_1) = 1 \\ \eta_{bat,dischrg} = f(i_{bat}) = \frac{i_{bat}\, T}{Q_{nom}} \end{gathered} \tag{3.7}$$

The time to fully discharge the battery (T) at different discharge currents can be found on the battery data sheet. This data is used to calculate $\eta_{bat,dischrg}$ at different discharge currents from Eq.(3.7). Fig. 3.2 shows the plot of $\eta_{bat,dischrg}$ vs i_{bat} for a PowerSafe SBS EON lead-acid battery with nominal capacity of 190 Ah and nominal voltage of 12 V. The discharging current of this battery at its nominal capacity is 19 A. The available battery capacity at discharging currents below 19 A is higher than the nominal capacity. Therefore, the efficiency also is above 100% at currents below 19 A as shown in the figure. The following mathematical model has the best fit to the data points plotted in the figure.

$$\eta_{bat,dischrg} = -0.06857\, i_{bat}^{0.4455} + 1.259 \tag{3.8}$$

3.3.1.3 Power electronic converters

Power loss in the converters are represented by their efficiency characteristics. A typical efficiency characteristic of a power electronic converter as a function of normalized output power is shown in Fig. 3.3. This characteristic can usually be found

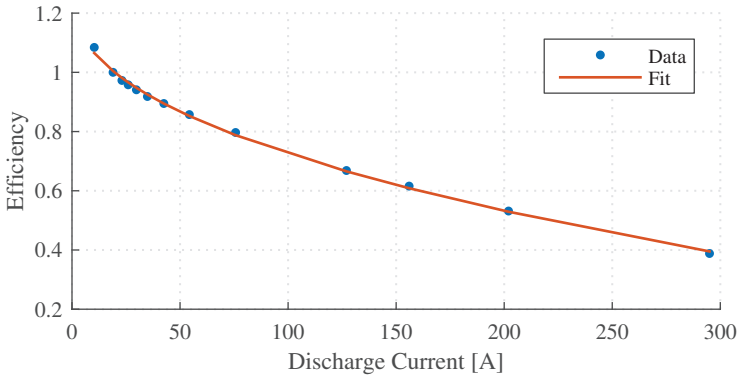

Figure 3.2: Discharging efficiency of the battery.

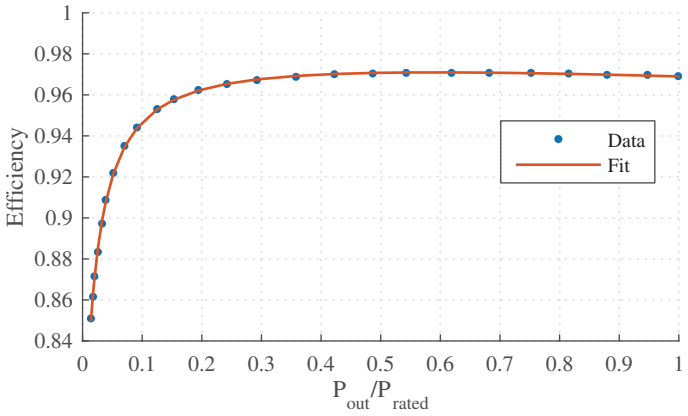

Figure 3.3: Typical efficiency characteristic of a power electronic converter.

in the product data sheet. The efficiency data can be fitted to a rational function with a first or second order polynomial numerator and a first order polynomial denominator. The efficiency characteristic shown in Fig. 3.3 is represented by the rational function

$$\eta_{conv} = \frac{a_1 P_n^2 + a_2 P_n + a_3}{P_n + b_1}, \tag{3.9}$$

where $P_n = \dfrac{P_{out}}{P_{rated}}$, P_{out} is the converter output power, P_{rated} is the converter rated output power, and the constants $a_1 = -0.01196$, $a_2 = 0.9851$, $a_3 = 0.01415$, $b_1 = 0.01888$.

3.3.1.4 System representation

In this chapter, both AC- and DC-coupled configurations shown in Fig. 3.1 are considered for modelling. The systems should satisfy the physical law of power balance. Adopting the sign convention where discharging of the battery and the power injection into the grid is considered positive, the system power balance can be written as follows.

For the AC-coupled configuration, the power balance equation at discrete time t when the battery is discharging $\big(P_{bat}(t) \geq 0\big)$ is

$$\eta_{pv,inv}(t)\ P_{pv}(t) + \eta_{batC,inv}(t)\ P_{bat}(t) - P_{grid}(t) - P_{load}(t) = 0 \tag{3.10}$$

and when the battery is charging $\big(P_{bat}(t) < 0\big)$ is

$$\eta_{pv,inv}(t)\ P_{pv}(t) + \eta_{batC,rec}(t)\ P_{bat}(t) - P_{grid}(t) - P_{load}(t) = 0 \tag{3.11}$$

where P_{pv} is the power production from the PV system, P_{bat} is the charging/ discharging power of the battery, P_{load} is the residential power demand, and $\eta_{pv,inv}$ is the efficiency of the PV inverter. $\eta_{batC,inv}$ and $\eta_{batC,rec}$ are the efficiencies of the battery converter when it is operating in inverter mode and rectifier mode respectively, where $\eta_{batC,inv} = \frac{P_{ac,conv}}{P_{dc,conv}}$ and $\eta_{batC,rec} = \frac{P_{dc,conv}}{P_{ac,conv}}$. $P_{ac,conv}$ and $P_{dc,conv}$ are AC and DC side power of the converter respectively.

The battery power is

$$P_{bat}(t) = V_{bat}(t)\ i_{bat}(t) \tag{3.12}$$

For the DC-coupled configuration, the power balance equation at discrete time t when the grid converter is operating as an inverter $\big(\eta_{pv,inv}(t)P_{pv}(t) + P_{bat}(t) \geq 0\big)$ is

$$\eta_{pv,inv}(t)\ P_{pv}(t) + P_{bat}(t) - \eta_{gC,inv}(t)\ \big[P_{grid}(t) - P_{load}(t)\big] = 0 \tag{3.13}$$

and when the grid converter is operating as a rectifier $\big(\eta_{pv,inv}(t)P_{pv}(t)+P_{bat}(t) < 0\big)$ is

$$\eta_{pv,inv}(t)\ P_{pv}(t) + P_{bat}(t) - \eta_{gC,rec}(t)\ \big[P_{grid}(t) - P_{load}(t)\big] = 0 \tag{3.14}$$

where $\eta_{gC,inv}$ and $\eta_{gC,rec}$ are the efficiencies of the grid converter when it is operating in inverter and rectifier mode respectively.

3.3.1.5 System constraints

The system constraints include a set of physical constraints imposed by the operating limits of the devices and a set of external constraints defined by the user or the DSO. The operational constraints of the battery include maintaining the SoC within certain limits while maintaining battery voltage and current below rated values. The process of fully charging a battery usually goes through two stages, namely constant current charging and constant voltage charging. During the constant current charging stage, the battery is charged at constant current until the

battery voltage reaches the charging voltage threshold. However, when charging the battery from a PV system, a constant current may not be available as power production from the PV system is dependent on an intermittent source. Therefore, at this stage, the battery is charged from the available current. Once the battery voltage reaches the threshold level, the charging process seamlessly enters the constant voltage charging stage. During constant voltage charging, the battery voltage is maintained at the voltage threshold and the battery current gradually drops. The battery is considered fully charged when the current drops to a set level. Constant voltage charging is a slow process, therefore it takes several hours to reach 100% SoC. When charging from solar, the battery may not reach 100% SoC as the PV system may not be able to provide the required charging current until the battery is fully charged. Choosing a higher charging voltage threshold may be a solution for increasing the usable capacity of the battery. However, high voltages shorten a battery's lifetime. Charging lead-acid batteries at high voltages causes corrosion, gassing, and severe overcharge. High voltages during the fully charged state stresses a lithium-ion battery resulting in faster degradation. Therefore, it is not recommended to fully charge lithium-ion batteries. The lifetime of lithium-ion batteries can be prolonged by choosing a lower voltage threshold or eliminating constant voltage charging altogether. From experiments it has been found that charging lithium-ion batteries to 85% provides a longer service life than charging them to 100% [112]. Conversely, fully charging lead-acid batteries is essential to prevent build-up of lead sulphate crystals, which accelerate the battery's degradation. However, fully charging may not always be realized when lead-acid batteries are used with renewable sources such as solar. For this reason, lithium-ion batteries are comparatively better suited for applications with renewables where the batteries are cycled on a daily basis. Fully discharging batteries is also not recommended, because many cell chemistries are not able to tolerate deep discharge and cells may be permanently damaged if fully discharged.

When formulating the battery constraints for the optimization algorithm, we have eliminated the constant voltage charging stage. This assumption is acceptable for lithium-ion batteries, as mentioned above. For lead-acid batteries, real-time corrections can be made to fully charge the battery if excess energy is available for charging it. The operational constraints of the battery bank are

$$-I_{chrg,max} \leq i_{bat}(t) \leq I_{dischrg,max} \tag{3.15}$$

$$SoC_{min} \leq SoC(t) \leq SoC_{max} \tag{3.16}$$

where $I_{chrg,max}, I_{dischrg,max}$ are the charging and discharging current limits of the battery bank, SoC_{min}, SoC_{max} are the minimum and maximum limits of the battery SoC.

The operational constraint of the battery converter in an AC-coupled system is

$$-P_{batC,rated} \leq P_{bat}(t) \leq P_{batC,rated} \tag{3.17}$$

where $P_{batC,rated}$ is the power rating of the battery converter.

The operational constraints of the grid converter in a DC-coupled system are

$$\begin{aligned} \eta_{pv,inv}(t)\ P_{pv}(t) + P_{bat}(t) &\leq P_{gC,rated} \\ P_{grid}(t) + P_{load}(t) &\geq -P_{gC,rated} \end{aligned} \tag{3.18}$$

where $P_{gC,rated}$ is the power rating of the grid converter.

The DSO defined constraints include the maximum power that can be drawn from the grid and the maximum power that can be fed into the grid.

$$P_{grid}(t) \geq -P_{buyG,max}(t) \tag{3.19}$$

$$P_{grid}(t) \leq P_{sellG,max}(t) \tag{3.20}$$

where $P_{buyG,max}$ is the maximum power that can be bought or drawn from the grid, and $P_{sellG,max}$ is the maximum power that can be sold or fed into the grid.

3.3.2 Control objectives

The main purpose of buying a BES unit for a residential household with a PV system is usually maximizing the consumption of self-generated energy in a way in which the economic benefits are maximized. It is to the advantage of the DSO to charge these storage units during times when their network experiences excessive reverse power flow that may create over-voltage issues. The proposed scheduling algorithm takes in to account both these concerns. It attempts to make a compromise between grid-supportive storage operation and fulfilling storage owners' objectives.

3.3.2.1 Electricity cost

The electricity bill of a residential customer normally consists of a service fee and a consumption charge. The service fee is usually a fixed charge per billing period, which covers the costs that are not dependent on energy use, such as grid maintenance cost, administration cost, taxes and levies. The consumption charge is the charge for the total amount of energy that has been used by the customer over the billing period. In addition, a demand charge may also be applied. The demand charge is a fee that is charged for the maximum power drawn from the grid over a billing period. The energy tariff can be either a flat rate or a time-based rate. The flat rate is the most widely adopted electricity tariff where a constant price is charged for each kWh consumed. However, with the deployment of smart meters, flat rates have been increasingly replaced by time-based rates where the cost per kWh is dependant on the time of using that kWh. Time-based tariffs are designed to suppress the peak demand on the grid by encouraging customers to reduce their electricity usage during peak hours. Time-based pricing options for residential consumers include: [113]

- Time-of-use pricing (TOU): Fixed electricity prices for different time blocks within a time period.
- Real time pricing (RTP): An hourly rate depending on the day ahead real-time price of electricity.
- Critical peak pricing: High electricity price periods for certain days within a year.

Real time prices change more frequently than time-of-use prices. For example, real time prices might change on an hourly basis, while TOU prices might be adjusted for time blocks during the day.

The sell back options available for residential customers with PV are net metering, feed-in tariff (FIT), and net purchase and sale [114, 115]. Under FIT, the utility buys all the electricity produced by the PV system for a fixed price while the customer buys electricity from the utility for supplying his load. In the net metering mechanism, the customer is billed for the net energy consumption over a billing period. If the generation from the PV system over the billing period has exceeded the consumption, the excess generation can be rolled over to the next billing period. In the net purchase and sale system, the bill is calculated on a moment-to-moment basis. The customer is billed for the electricity taken from the grid at each time step with the buying price applied for that time, if the consumption is higher than the PV-generation. When the generation is higher than the consumption, the utility buys the excess electricity for the sell back price applicable to that time.

It makes economically no sense to couple a BES to a PV system in a household that is subjected to either FIT or net metering. Because in FIT, as all the generation is sold to the grid for a fixed price, there is no use in storing it. In net metering, the grid acts as a storage for the excess energy produced from the PV system, because the bill is made for the net energy transferred with the grid by the end of a billing period. However, if demand charge makes a significant contribution to the electricity bill, installing a BES to reduce the maximum demand might be an economical option for households subjected to net metering.

The energy cost over a certain time interval for all types of customers except those with FIT can be calculated from the following equation. Since there is no economic sense to installing BES when the sell-back option is FIT, that is not discussed in this thesis.

$$C_{energy} = \sum_{k} P_{grid}(k)\, \gamma(k)\, \Delta t \tag{3.21}$$

where

$$\gamma(k) = \begin{cases} \gamma_{buy}(k) & ;\text{If } P_{grid}(k) \leq 0 \\ \gamma_{sell}(k) & ;\text{If } P_{grid}(k) > 0 \end{cases}$$

Δt is the sampling interval (hours) and γ_{buy} is the electricity buying rate (\$/kWh), which can either be a flat rate or a time-based rate. γ_{sell} is the electricity selling rate (\$/kWh). Buying and selling rates take different values in purchase and sale schemes while in net metering these two are the same and not dependent on time.

3.3.2.2 Battery degradation cost

A battery losses its capacity over time. A battery is considered dead when its capacity drops to a certain threshold from its original capacity. Normally, this threshold is about 80%, however this may vary depending on the battery chemistry, the application, user preference, and the manufacturer's policy. Cycling of the battery is one of the main reasons for capacity loss. The number of cycles a battery can perform before its capacity drops to the threshold is called the cycle life of the battery. The capacity loss due to cycling is dependent on several factors. The main causes are the operating SoC window over a cycle and the operating temperature [112, 116]. The battery degradation cost is the capacity loss cost when cycling a certain amount of energy through the battery. As capacity fade highly depends on the operating conditions of the battery, calculating an accurate value for battery degradation cost is extremely difficult. However, it is important to know at least an approximated value for battery degradation cost due to cycling in order to avoid unnecessary cycling of the battery. Because, unnecessary cycling will shorten battery lifetime. For example, consider a BES coupled to a PV system that can also be charged from the grid. The BES charges from the PV system during the day-time and uses that energy to supply the evening load. Let us assume the BES reaches its minimum SoC level by midnight. The HEMS decides to charge the battery again from the grid to supply the early morning load, because of the lower electricity price in the night compared to the price in the morning. In that case, the battery performs more than one cycle resulting in higher capacity loss and the cost of this capacity loss may be higher than the electricity bill savings. Charging from the grid is not economically attractive, if the savings made by supplying the early morning load by the battery, which is originally charged from the grid is less than the cost of battery capacity loss during cycling. Therefore, it is important to consider battery degradation cost due to cycling when making decisions such as charging from the grid. Otherwise, even a slight change in the electricity price can result in charging the battery from the grid.

The following section describes a method for calculating an approximated value for battery degradation cost using the data provided in the battery data sheet.

The battery degradation cost per kWh of energy charged/discharged from the battery due to cycling is calculated from the equation

$$\gamma_{bat,cyl} = \frac{\mathrm{BC}}{\mathrm{E}_{bat,ltpt}}, \tag{3.22}$$

where BC is the battery installation and maintenance cost over its lifetime. $\mathrm{E}_{bat,ltpt}$ is the lifetime throughput of the battery. Lifetime throughput is the total amount of energy (kWh) that can be delivered from the battery during its lifetime. Battery ageing tests have been performed in [116] for several battery types to observe the battery capacity loss due to cycling over time. The results have shown a linear relationship between the capacity loss and the number of full equivalent cycles. Based on this linear behaviour, the lifetime throughput of a battery sized to operate

with minimum depth of discharge of DoD_{min} is found as follows.

$$\mathrm{E}_{bat,ltpt} = \left(\frac{\mathrm{E}_{bat,nominal} + \mathrm{E}_{bat,end}}{2}\right) \times \mathrm{DoD}_{min} \times \text{Number of cycles to failure,}$$

where $\mathrm{E}_{bat,nominal}$ is the nominal capacity of the battery when it was new and $\mathrm{E}_{bat,end}$ is the end of life capacity of the battery. The number of cycles to failure of the battery for a given DoD can be found in the data sheet.

The battery degradation cost when delivering a certain amount of energy from the battery is

$$\mathrm{BDC}_{cyl} = \gamma_{bat,cyl}\, E_{bat} \tag{3.23}$$

where E_{bat} is amount of energy delivered from the battery.

3.3.3 BES scheduling algorithm

A scheduling algorithm based on the receding horizon control (RHC) approach is implemented to determine the optimal charging/discharging power set points of the BES. Receding horizon control is a general purpose control scheme that involves repeatedly solving a constrained optimization problem, using predictions of future costs, disturbances, and constraints over a moving time horizon to choose the control action. The objective of the optimization problem to be solved in the BES scheduling problem is chosen to maximize the economic benefits for the BES owner, while complying with the requirements imposed by the DSO. The primary control variables of the RHC problem are the charging/discharging power set points of the BES unit. The PV generation and the local load are the disturbances while the electricity price and the battery degradation cost are the cost parameters. We assume that the HEMS consists of a forecasting module, which is able to predict the residential load and the PV generation over a given planning horizon. The electricity price information is received from the DSO via smart meters.

3.3.3.1 Objective function

The economic benefits of BES for a residential household are usually quantified by savings in the energy bill. However, as discussed in Section 3.3.2.2, frequent cycling of the BES unit can shorten the battery's lifetime. Therefore, in addition to the cost of electricity, the battery degradation cost-the cost that represents the capacity loss of the battery due to cycling- is also added to the objective function as follows.

$$\mathrm{Objf} = C_{energy} - \sum_{k} |\mathrm{BDC}_{cyl}(k)| \tag{3.24}$$

The inclusion of battery degradation cost, however, can decrease the self-consumption rate when the cost of battery capacity loss due to cycling a certain amount of energy generated from the PV system is higher than the cost of buying the same amount

of energy from the grid when needed. The purpose of coupling the BES to the PV system in the first place is to maximally utilize the self generated energy. Since the electricity cost has been chosen as the objective function, we need to increase the self consumption rate in such a way that the cost of electricity over the planning horizon is minimized. Therefore, the battery capacity loss cost due to cycling of energy generated from the PV system to supply the local load is considered zero. The battery capacity loss cost is included when 1) the battery is charged from the grid, and 2) the stored energy in the battery is fed-in to the grid. This is because, in these two cases, there is possibility to 1) buy energy directly from the grid, and 2) sell excess energy directly to the grid without cycling the battery. Without battery degradation cost, even a slight difference between the electricity prices at different time slots can cycle the battery. Inclusion of battery degradation cost prevents such redundant behaviour and allows charging from the grid and feed stored energy into the grid only when there are economic benefits. That is, the battery will only charge from the grid, if the cost of buying energy from the grid during the high tariff period is higher than the cost of buying energy during the low tariff period plus the battery degradation cost for cycling that energy. The stored energy will only be fed-in to the grid if the savings made by selling the stored energy are higher than the battery degradation cost due to cycling that energy.

The battery degradation cost due to cycling of the battery during time step k is calculated as follows for the different operating conditions mentioned above.

1. When BES is charging from the grid $\big(P_{bat}(k) < 0$ and $P_{grid}(k) < 0\big)$:

$$\mathrm{BDC}_{cyl}(k) = \begin{cases} \gamma_{bat,cyl}\ P_{bat}(k)\ \Delta t, & \text{If } P_{net}(k) \leq 0 \\ \gamma_{bat,cyl}\ P_{grid}(k)\ \Delta t, & \text{If } P_{net}(k) > 0 \end{cases}$$

2. When the stored energy in the BES is fed-in to the grid $\big(P_{bat}(k) > 0$ and $P_{grid}(k) > 0\big)$:

$$\mathrm{BDC}_{cyl}(k) = \begin{cases} \gamma_{bat,cyl}\ P_{bat}(k)\ \Delta t, & \text{If } P_{net}(k) > 0 \\ \gamma_{bat,cyl}\ P_{grid}(k)\ \Delta t, & \text{If } P_{net}(k) \leq 0 \end{cases}$$

3. For all other cases:

$$\mathrm{BDC}_{cyl}(k) = 0$$

where the net load, P_{net} is given by

$$P_{net}(k) = \begin{cases} \eta_{pv,inv}(k) P_{pv}(k) - P_{load}(k), & \text{AC-coupled system} \\ \eta_{pv,inv}(k)\ \eta_{gC,inv}(k)\ P_{pv}(k) - P_{load}(k), & \text{DC-coupled system} \end{cases}$$

3.3.3.2 Grid-supportive charging of BES systems

The residential storage units need to be controlled in such a way that the objectives of the BES owner are satisfied while the grid is supported to lower the reverse power

flow. The risk of over-voltages reduces with the reduction of reverse power flow in the grid. The diurnal variation of power generation from a PV system follows the shape of a bell curve as shown in Fig. 3.4. The over-voltage problem primarily occurs around the solar noon, because this is the time period where the production is relatively high. The load on residential feeders in this period is usually low, because the majority of occupants are away from their houses in this period. This leads to higher reverse power flow in the grid and therefore a higher possibility of over-voltage problems occurring. The charging of storage units in this period reduces the reverse power flow in the grid and consequently solves the over-voltage problems.

The DSO can determine in which period of the day the voltage profile may exceed the maximum allowable limit. This period can be identified via off-line power flow studies. From here onwards, we call this period "the critical period". The DSO can force customers to charge their BES units during this critical period. By doing so, the charging operation of the BES units in the system can be coordinated. Depending on the variation of the PV production over a year or the increase in PV penetration level in the grid, the length of the critical period may change. The DSO can update the critical period occasionally when there are significant changes in the PV generation level in the distribution grid.

The requirement to charge the BES unit during the critical period is included in the optimization problem in terms of a grid feed-in limit over the critical period. This feed-in limit is locally decided by the HEMS. Each time the optimization is run, this feed-in limit is set to zero. Setting feed-in limit to zero means, all the excess energy available over the critical period must be transferred to the BES unit. If the usable capacity of the battery is sufficient to store this energy, the power injection into the grid during this period will be zero. However, if the usable capacity is not sufficient, it is not possible to store all the excess energy available during the critical period. In that case, a certain amount of energy has to be transferred to the grid. Consequently, in the optimization problem, the grid feed-in limit needs to be increased. When the forecasted excess energy available over the critical period is higher than the usable capacity of the battery, optimization problem is infeasible. Therefore, the grid feed-in limit is gradually increased until the optimization problem is feasible. In this way, the optimal feed-in limit that can maintain charging of the BES units over the entire critical period can be found. Moreover, if the excess energy available during the critical period is lower than the usable capacity of the battery, charging outside the critical period will also be allowed by the HEMS. Therefore, maximal use of the battery for any weather condition is guaranteed for the customer. From the DSO's perspective, reduction of reverse power flow is achieved over the entire critical period because BES units continue to charge at least until the end of the critical period. This reduces the risk of over-voltage or may completely solve the problem if a sufficient number of BES units are available in the distribution system.

In this method, the grid feed-in limit is decided locally with the use of information about the critical period received by the DSO. This information does not need to

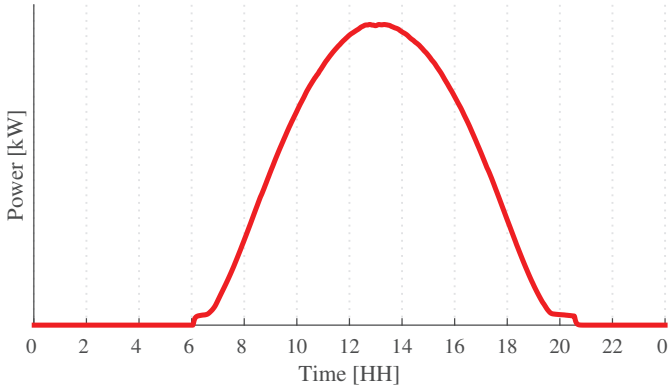

Figure 3.4: Clear sky day power generation profile of a PV system.

be updated regularly. This makes this method a local control strategy, which is supportive to the grid.

3.3.3.3 Receding horizon control

In receding horizon control, an optimization problem is solved at each time step to determine the control set points over a fixed time horizon. The set points corresponding to the first time step are then applied. At the next time step, a new optimization problem is solved with the time horizon shifted one step forward. The new optimization problem is formulated with new initial states and the updated predictions of disturbances and other required inputs [117].

The basic steps of receding horizon control of the residential BES system are mentioned below.

Step 1 : Formulate the optimization problem.

At time t, we consider a time interval extending T steps into the future: $t, t+1, ..., t+T$. We formulate the BES scheduling problem as a receding horizon control optimization problem with the maximization function

$$max\left(\sum_{k=0}^{T-1} P_{grid}(k)\ \gamma(k)\ \Delta t - |\mathrm{BDC}_{cyl}(k)|\right), \tag{3.25}$$

subjected to the constraints reported in Section 3.3.1.5 on page 40. Control set points that need to be computed from the optimization are $P_{bat}(k), P_{grid}(k)$. In order to solve the optimization, we need predictions of average PV generation and the residential load $P_{pv}(k), P_{load}(k)$ for $k = 0, 1, 2, \ldots, T-1$. This data is obtained from the forecasting module.

Step 2 : Solve the optimization problem.

At time t, compute the system control variables: $P_{bat}(k), P_{grid}(k)$ for $k = 0, 1, 2, \ldots, T-1$ by solving the optimization problem.

Step 3 : Execute the control set points.

Apply the set points corresponding to the first time step.

Step 4 : Repeat Steps 1-3 at each time step.

Repeat the process at each time step with updated system initial states, predictions of load and PV generation, and other time dependent model inputs.

3.3.3.4 Optimum scheduling using dynamic programming

The optimization problem is non-linear because the objective function contains conditional terms and some of the constraints are non-linear. We chose dynamic programming to solve this non-linear optimization problem. Dynamic programming is based on the principle of optimality and can be applied to any optimization problem that can be structured into multiple stages, where each stage is comprised of collectives states. The principle of optimality states that an optimal policy has the property that whatever the initial state and initial decisions are, the remaining decisions must constitute an optimal policy with regard to the state resulting from the first decision [118]. In dynamic programming, the complex problem is broken down into a collection of sub problems and the optimal solution of the original problem is found from the optimal solutions of the sub problems. The optimal solution is obtained from recursive optimization with the backward induction process, where the final stage is analysed first and the problem is solved moving back one stage at a time until all stages are included.

Formulation of the optimization problem for solving using dynamic programming requires structuring the system into stages. At each stage the system is represented by a number of states. In the BES scheduling problem, discrete time steps correspond to the system stages and SoC of the BES is chosen as the system state.

stages: $\{0, 1, 2, 3, \ldots, T\}$

states: $\{SoC_1, SoC_2, SoC_3, ..., SoC_i, ..., SoC_n\}$

The problem consists of $T+1$ number of stages with n number of states per stage. The state of the system, i.e. SoC is constrained to operate in the region

$$(SoC_{min}, SoC_{max}).$$

Therefore, $SoC_1 = SoC_{min}$ and $SoC_n = SoC_{max}$

When the SoC is discretized with step size of SoC_{step}, the number of states per stage is

$$n = \frac{SoC_{max} - SoC_{min}}{SoC_{step}} + 1, \quad n \in \mathbb{Z}^+$$

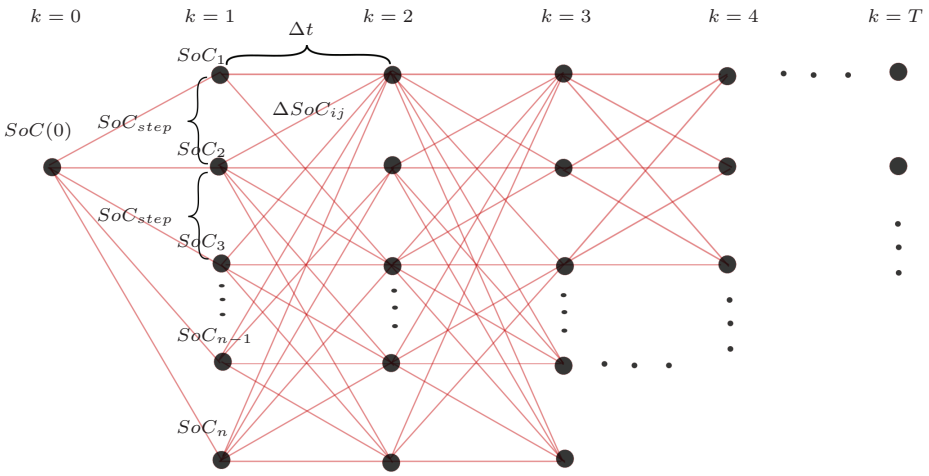

Figure 3.5: Dynamic programming: System stages, states and all possible trajectories between the stages.

where $SoC_{step} = SoC_i - SoC_{i-1}$, $i \in (1, 2, 3, .., n)$.

In dynamic programming, first we need to establish all possible decisions that can be taken at each system state. Fig. 3.5 illustrates the possible decision trajectories for change in SoC from one stage to the next stage over some consecutive stages. In the figure, ΔSoC_{ij} represents the change in SoC along the trajectory from the i^{th} state in the k^{th} stage to the j^{th} state in the $(k+1)^{th}$ stage.

$$\Delta SoC_{ij} = SoC_i(k) - SoC_j(k+1)$$

Every possible changes of SoC from one stage to the next can be represented in matrix form as

$$\mathbf{\Delta SoC} = \begin{bmatrix} \Delta SoC_{11} & \Delta SoC_{12} & \Delta SoC_{13} & \dots & \Delta SoC_{1n} \\ \Delta SoC_{21} & \Delta SoC_{22} & \Delta SoC_{23} & \dots & \Delta SoC_{2n} \\ \vdots & \vdots & \vdots & \ddots & \vdots \\ \Delta SoC_{n1} & \Delta SoC_{n2} & \Delta SoC_{n3} & \dots & \Delta SoC_{nn} \end{bmatrix}$$

The charging/discharging current of the battery that results in a BES SoC change by ΔSoC_{ij} over Δt time interval is

$\Delta SoC_{ij} < 0$ (charging):

$$I_{bat,ij} = \frac{Q_{nom}}{\Delta t} \Delta SoC_{ij}$$

$\Delta SoC_{ij} \geq 0$ (discharging):

$$I_{bat,ij} = \frac{Q_{nom}\, \eta_{bat,dischrg}}{\Delta t} \Delta SoC_{ij}$$

The charging/discharging current of the BES should be below the rated charging/discharging current of the BES. Therefore, the trajectories that violate the BES charging/discharging current limits described by Eq.(3.15) are rejected.

The corresponding terminal voltage of the battery is calculated from Eq.(3.3).

$$\begin{aligned} V_{bat,ij} = E_o - K\left(\frac{Q_{nom}}{Q_{nom} - q_i}\right) q_i - K\left(\frac{Q_{nom}}{Q_{nom} - q_i}\right) |I_{bat,ij}| \\ + A\ exp\big(-Bq_i\big) - R_{bat}\ I_{bat,ij} \end{aligned} \tag{3.26}$$

where

$$\begin{aligned} q_i &= Q_{nom}\ SoC_i\ , && \text{Discharging } (I_{bat,ij} \geq 0) \\ q_i &= Q_{nom}\ (1 - SoC_i)\ , && \text{Charging } (I_{bat,ij} < 0) \end{aligned}$$

The corresponding charging/discharging power of the battery is

$$P_{bat,ij} = V_{bat,ij}\ I_{bat,ij}$$

For an AC-coupled system, the trajectories that violate the battery converter power rating constraint given in Eq.(3.17) are rejected at this point. Once the battery power set points are found for all the feasible trajectories between two stages, the corresponding power supplied to/by the grid for all stages can be calculated for an AC-coupled system from Eqs.(3.10), (3.11) and for a DC-coupled system from Eqs.(3.13), (3.14). In order to calculate the power supplied to/by the grid, we need the predictions of load and PV generation for all stages. We assume this information is obtained from the forecasting module. The trajectories that violate the maximum power that can be drawn from the grid and the grid feed-in limit given by Eqs.(3.19) and (3.20) are rejected at this point. Moreover, for the DC-coupled system, the trajectories that violate the grid converter power rating constraints given by Eq.(3.18) are rejected.

Then, the associated cost over all feasible trajectories can be calculated from the equation

$$\psi_{ij}(k) = -P_{grid,ij}(k)\ \gamma(k)\ \Delta t + |BDC_{cyl,ij}(k)| \tag{3.27}$$

The path from stage 0 to T that gives the largest sum of the costs over the path is the optimum solution of the problem. The optimum path is found using backward induction, as described below.

Initially we do not know the state of the system in the final stage. Therefore, we assume the state of the BES at the final stage, i.e. at $k = T$ is m. State m corresponds to the SoC,

$$SoC_m = SoC_{min} + (m-1)SoC_{step}$$

The associated cost for each state at stage $T-1$ when moving from stage $T-1$ to

state m in stage T is

$$\Phi(T-1) = \begin{bmatrix} \psi_{1m}(T-1) \\ \psi_{2m}(T-1) \\ \vdots \\ \psi_{nm}(T-1) \end{bmatrix}_{n\times 1}$$

$$\lambda^*(T-1) = \text{Indx}\{max[\Phi(T-1)]\}$$

where $\lambda^*(T-1)$ is the state corresponding to the maximum cost of stage $T-1$. Indx gives the index of the maximum value of the matrix Φ. The associated cost of trajectories that violate the constraints can be replaced with large negative numbers. Those trajectories will then never be chosen because the cost assigned to them are smaller than the costs associated to other paths.

The associated cost for each state at stage $T-2$ when moving from stage $T-2$ to T is

$$\begin{aligned}
\phi_1(T-2) &= \begin{bmatrix} \psi_{11}(T-2) & \psi_{12}(T-2) & \psi_{13}(T-2) & \dots & \psi_{1n}(T-2) \end{bmatrix} + \Phi(T)' \\
\phi_2(T-2) &= \begin{bmatrix} \psi_{21}(T-2) & \psi_{22}(T-2) & \psi_{23}(T-2) & \dots & \psi_{2n}(T-2) \end{bmatrix} + \Phi(T)' \\
&\vdots \\
\phi_n(T-2) &= \begin{bmatrix} \psi_{n1}(T-2) & \psi_{n2}(T-2) & \psi_{n3}(T-2) & \dots & \psi_{nn}(T-2) \end{bmatrix} + \Phi(T)'
\end{aligned}$$

$$\Phi(T-2) = \begin{bmatrix} \phi_1(T-2) \\ \phi_2(T-2) \\ \phi_3(T-2) \\ \vdots \\ \phi_n(T-2) \end{bmatrix}_{n\times n}$$

The maximum values in each row of matrix $\Phi(T-2)$ give the largest costs involved when moving from the states $1, 2, \dots, n$ in stage $T-2$ to state m in stage T.

$$\begin{aligned}
\Phi^*(T-2) &= max_{row}\{\Phi(T-2)\} \\
\lambda^*(T-2) &= \text{Indx}\{max[\Phi^*(T-2)]\}
\end{aligned}$$

where Φ^* denotes the maximum cost and max_{row} gives the maximum value in each row.

The associated costs of the paths from states $1, 2, \dots n$ in stage $T-3$ to state m in stage T that has the highest cost can be calculated as follows.

$$\begin{aligned}
\phi_1(T-3) &= \begin{bmatrix} \psi_{11}(T-3) & \psi_{12}(T-3) & \psi_{13}(T-3) & \dots & \psi_{1n}(T-3) \end{bmatrix} + \Phi^*(T-2)' \\
\phi_2(T-3) &= \begin{bmatrix} \psi_{21}(T-3) & \psi_{22}(T-3) & \psi_{23}(T-3) & \dots & \psi_{2n}(T-3) \end{bmatrix} + \Phi^*(T-2)' \\
&\vdots \\
\phi_n(T-3) &= \begin{bmatrix} \psi_{n1}(T-3) & \psi_{n2}(T-3) & \psi_{n3}(T-3) & \dots & \psi_{nn}(T-3) \end{bmatrix} + \Phi^*(T-2)'
\end{aligned}$$

$$\Phi(T-3) = \begin{bmatrix} \phi_1(T-3) \\ \phi_2(T-3) \\ \phi_3(T-3) \\ \vdots \\ \phi_n(T-3) \end{bmatrix}_{n \times n}$$

$$\Phi^*(T-3) = max_{row}\{\Phi(T-3)\}$$

The index of the state corresponding to the maximum cost in stage $T-3$ is

$$\lambda^*(T-3) = \text{Indx}\{max[\Phi^*(T-3)]\}$$

In this way the associated costs of the paths from states $1, 2, \ldots n$ from stage 1 to state m in stage $T+1$ that has the highest cost can be calculated recursively.

$$\begin{aligned} \Phi^*(T-4) &= max_{row}\{\Phi(T-4)\} \\ \Phi^*(T-5) &= max_{row}\{\Phi(T-5)\} \\ &\vdots \\ \Phi^*(1) &= max_{row}\{\Phi(1)\} \end{aligned}$$

The corresponding states that have the maximum cost at each stage are

$$\begin{aligned} \lambda^*(T-4) &= \text{Indx}\{max[\Phi^*(T-4)]\} \\ \lambda^*(T-5) &= \text{Indx}\{max[\Phi^*(T-5)]\} \\ &\vdots \\ \lambda^*(1) &= \text{Indx}\{max[\Phi^*(1)]\} \end{aligned}$$

If the initial SoC state of the BES is l, the maximum cost involved in moving from state l in stage 0 to state m in stage T can be found as follows.

$$\Phi(0) = [\psi_{l1}(0) \quad \psi_{l2}(0) \quad \psi_{l3}(0) \quad \ldots \quad \psi_{ln}(0)] + \Phi^*(1)'$$

$$\Phi^*(0) = max\{\Phi(0)\}$$

$$\Phi^*_{lm} = \Phi^*(0)$$

The corresponding states of the BES that have the maximum values of the costs at each stage is

$$\{l, \lambda^*(1), \lambda^*(2), \ldots, \lambda^*(T-1), m\}$$

The above process is repeated for $m = 1, 2, 3, \ldots, n$. Then, the optimum cost is the maximum of the costs obtained for $m = 1, 2, 3, \ldots, n$,

$$\Phi^* = max\{\Phi^*_{l1}, \Phi^*_{l2}, \Phi^*_{l3}, \ldots, \Phi^*_{ln}\}$$

If $\Phi^* = \Phi^*_{lr}$, then the SoC of the BES in the final stage, i.e. at $k = T$ is,

$$SoC(T) = SoC_{min} + (r-1)SoC_{step}$$

3.4 Reactive Power Support from the Converters

The DSO can use reactive power support from the converters, when the support provided by the BES units is not sufficient for maintaining the voltages within statutory limits. The reactive power support solution needs to be properly co-ordinated with the operation of the BES units, in order to minimize the reactive power utilization. The lower the reactive power the better for the DSO. In the following, we discuss the reactive power support solution adopted in coordination with BES units. Reactive power support is only utilized when the over-voltage problem persists even after charging the BES units.

The basic steps of secondary voltage control of the power system are as follows. The network is divided into distinct control zones, where each zone consists of some kind of voltage regulating sources. A pilot node that can represent the voltage profile over the zone is selected. The voltage profile over the zone is controlled by controlling the voltage regulating sources in response to the voltage measurements at the pilot node. A similar concept can be applied to low voltage networks as well. A distribution network can be divided into small zones, if distribution transformer supplies several long feeders. Otherwise, the whole low voltage grid supplied by a distribution transformer can be treated as one zone. The PV inverters and the converters of the BES units belonging to each zone can provide necessary reactive power for regulating the voltage profile in respective zones. From each zone, one or several nodes that can represent the voltage profile over the zone can be selected. In this thesis, we call these nodes "the critical nodes". Off-line power flow can be used to identify the critical nodes in a distribution grid.

Smart meters located at the critical nodes measure the critical node voltages. These meters can send requests to the converters that are located within the same zone as the critical node. The request type depends on the voltage of the critical node. There can be four different types of requests as described below. Fig. 3.6 illustrates the voltage ranges corresponding to each of the requests.

RQST-1: Increase inductive reactive power.

This request is sent when the critical node voltage exceeds the upper limit of the allowed voltage variation (V_{max}). The allowed voltage range can vary from regulation to regulation. According to European standard-EN50160, 10-minute average values of the supply voltage should be within the range of $\pm 10\%$ of the nominal voltage (V_{nom}).

RQST-2: Decrease inductive reactive power.

This request is sent when the critical node voltage is within the range $V^2_{thres,high} - V^1_{thres,high}$, where $V_{max} > V^2_{thres,high}, V^1_{thres,high} > V_{nom}$. When the voltage is within this region, reactive power support from the converters are no longer needed. Therefore, this request is sent to reduce the reactive power support provided by the converters.

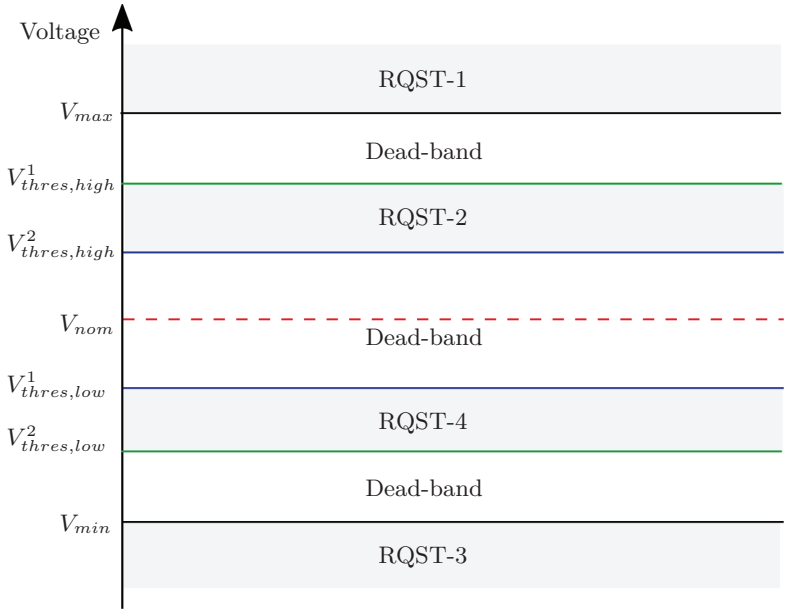

Figure 3.6: Voltage ranges corresponding to different requests generated by the smart meters. No request is generated when the critical node voltage is within the dead-bands.

RQST-3: Increase capacitive reactive power.

This request is sent when the critical node voltage drops below the lower limit of the allowed voltage range (V_{min}).

RQST-4: Decrease capacitive reactive power.

This request is sent when the critical node voltage is within the range $V^2_{thres,low} - V^1_{thres,low}$, where $V_{nom} > V^2_{thres,high}, V^1_{thres,high} > V_{min}$. When the voltage is within this region, reactive power support from the converters is no longer needed. Therefore, this request is sent to reduce the reactive power support provided by the converters.

The smart meter does not generate any request if the critical node voltage is within the dead-bands, $V^1_{thres,low} - V_{max}$, $V^1_{thres,low} - V^2_{thres,high}$ or $V_{min} - V^2_{thres,low}$.

The smart meter continuously monitors the voltage profile of the critical node and broadcasts a message to all the converters located within the zone when it detects an event. The message can be one of the four above depending on the event the meter detects. Fig. 3.7 illustrates the smart meter logic of sending requests. Once a converter receives a message from the smart meter, it reacts accordingly. If the request is to increase reactive power, it decreases the power factor by a fixed step (Δpf). If the request is to decrease reactive power it increases the power factor by a fixed step. The power factor is adjusted by Δpf per request. Fig. 3.8 illustrates the

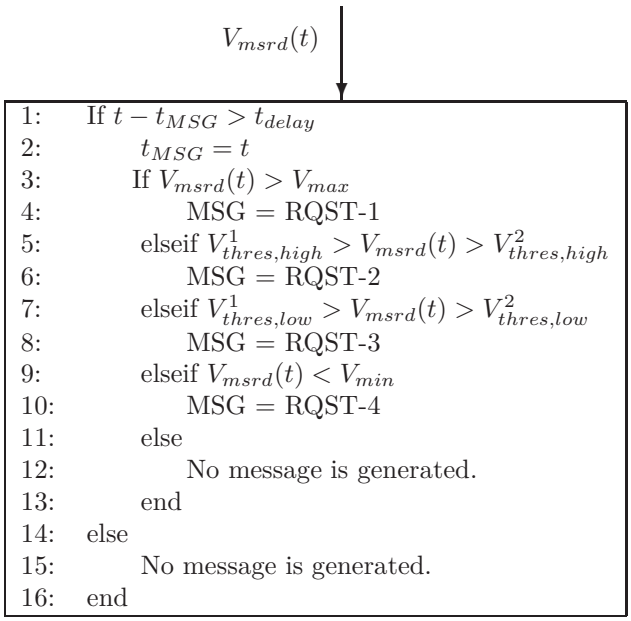

Figure 3.7: The smart meter logic of sending requests to the converters.

1: If MSG = RQST-1
2: $pf = |pf_{old}| - \Delta pf$
3: $pf_{new} = pf$
4: elseif MSG = RQST-2
5: $pf = |pf_{old}| + \Delta pf$
6: $pf_{new} = pf$
7: elseif MSG = RQST-3
8: $pf = |pf_{old}| - \Delta pf$
9: $pf_{new} = -pf$
10: elseif MSG = RQST-4
11: $pf = |pf_{old}| + \Delta pf$
12: $pf_{new} = -pf$
13: end
14: If $pf_{new} < pf_{min}$
15: $pf_{new} = pf_{min}$
16: elseif $pf_{new} < -pf_{min}$
17: $pf_{new} = -pf_{min}$
18: elseif $pf_{new} > 1$ or $pf_{new} < -1$
19: $pf_{new} = 1$
20: end
21: $pf_{old} = pf_{new}$

Figure 3.8: The converter logic of responding to the requests received from the smart meter.

converter logic of responding to the requests. If this adjustment is not sufficient, the smart meter will continue to detect the event. The system takes some time to respond to the messages generated by the smart meter. Therefore, the meter should wait until the system responds to the last message, before generating an another message. The waiting time (t_{delay}) has to be determined based on the communication delay and the response time of the converter to the requests. If the meter continues to detect the event even after this waiting time, it broadcasts an another message.

3.5 Case Study

A simulation study was carried out to evaluate the performance of the proposed grid-supportive BES operational strategy and the reactive power support strategy. A Matlab code was developed to simulate the detailed residential energy system model described in Section 3.3 and the reactive power support strategy. A power flow model of the modified IEEE European low voltage test feeder [119] was developed in openDSS to evaluate the impact of the proposed BES operational strategy on the grid. OpenDSS is an open and free software developed by EPRI to solve power flow, perform harmonics analysis, and calculate fault currents in electrical distribution systems. OpenDSS is able to solve unbalanced networks. Moreover, it can be driven from MATLAB through a COM server [120].

The modifications made in the IEEE European low voltage test feeder include

- 10 different type of conductors have been used to construct the distribution system. It was found that the R/X ratios of some conductors were considerably too high (>10), therefore those conductors were replaced by a conductor type having a lower R/X ratio (<10).
- The lengths of the lines were increased by a factor of 3 to make the network weaker.

The majority of residential customers are connected to the grid via a single phase connection. PV systems with a capacity up to 4.6 kVA can also be connected to the grid via a single phase inverter. Therefore, there can be several PV systems connected to the grid via single phase inverters. Distribution grids are usually unbalanced to a certain extent due to these single phase loads and PV generators. Therefore, in this work we have considered three phase representation of the distribution grid and its unbalanced nature. The single line diagram of the modified IEEE European low voltage test feeder is shown in Fig. 3.9. The main feeder and the laterals are at the voltage level of 416 V (phase-to-phase). The considered distribution network serves 56 single phase customers located at the nodes indicated in the figure. The loads were modelled as constant PQ loads and represented by the load profiles obtained from an Italian distribution grid located in the city of Brescia [121]. The load data was available with a 1 minute time resolution. 56 customers were represented by

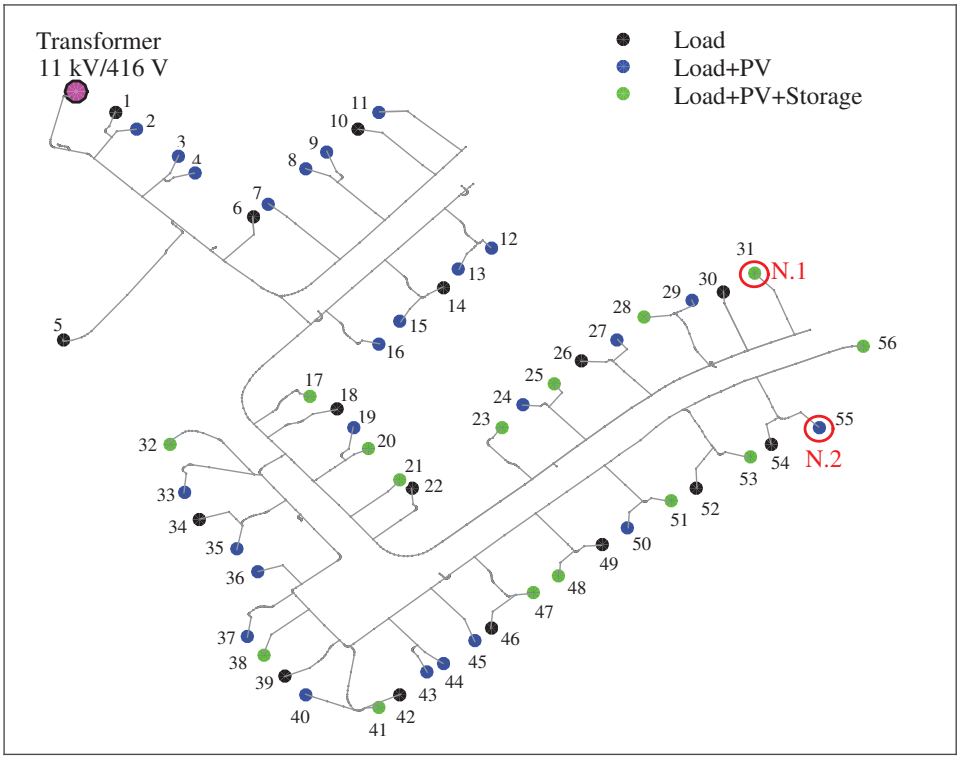

Figure 3.9: Single phase layout of the low voltage network, the modified IEEE European low voltage test feeder.

56 distinct load profiles. Both single phase customers and three phase customers were considered. The power factor of the load was set to 0.99. 40 customers out of the 56 were considered to have roof-top photovoltaic systems. The locations of the customers having PV systems are shown in the figure. The rated capacity of each PV system is 4.0 kW. PV systems connected to the grid via single phase inverters as well as three phase inverters were considered. Measurements recorded from residential PV systems connected to an Italian low voltage network located in the city Brescia were used as the basis for the PV generation profiles. The PV generation data was available with 1 minute time resolution. Hourly averages of the load and PV generation were derived from these load and PV data sets. These hourly averages were used as the forecasted load and PV generation profiles in the optimization strategy.

Out of the total 40, 15 PV system owners were considered to have lithium-ion based BES systems. All the considered BES units were connected to the grid via three phase inverters. In this study, the residential energy systems were represented by AC-coupled configuration. The battery model presented in Section 3.3.1.2 is used only for calculating the optimal BES set points using the optimization strategy

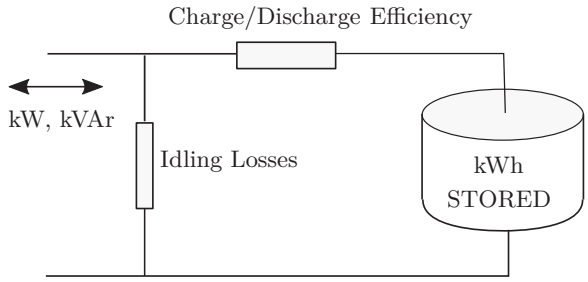

Figure 3.10: Model of the OpenDSS storage element.

presented in Section 3.3. In the power flow study, the openDSS model of the battery shown in Fig. 3.10 is used. The nominal capacity of all the BES considered is 10 kWh/208 Ah. The technical parameters of these BES units corresponding to the detailed model used in the optimization strategy are listed in Table 3.1. The openDSS battery model is based on energy (kWh) not coulomb (Ah). The energy efficiency of batteries is usually lower than the coulomb efficiency. Therefore, charging and discharging efficiencies of the battery model used in the power flow study were set to 0.95%.

The critical nodes in the distribution grid and the critical period were first identified via running off-line power flow over a 24-hour period. This off-line power flow was performed with the considered load and the PV generation but without BES units. Since, the network has two long laterals, one critical node per lateral, N.1 and N.2 were chosen. The locations of these nodes are shown in Fig. 3.9. The node in each lateral that experiences the largest voltage deviation from the nominal voltage is selected as the critical node. The period from 0800-1400h was identified as the critical period.

The BES units in the system were divided into two groups, where each group consists of about half of the BES units. Since there are 15 BES units in total, 7 units were allocated to one group while the other 8 units were allocated to the other group. Group-1 consists of the BES units connected to the nodes: 20, 23, 28, 32, 41, 48, 53 and group-2 consists of the BES units connected to the nodes: 17, 21, 25, 31, 38, 47, 51, 56. The grid feed-in limit is active from 0800h-1300h for the residential energy systems belonging to group-1, while for the other group the grid feed-in limit is active from 0900-1400h. As a result, only about a half of the BES units are forced to charge during the first and last hours of the critical period. The reverse power flows during these hours are lower than the reverse power flow during the rest of the hours of the critical period (0900h-1300h). Therefore, charging of all the BES units may not be necessary to solve the over voltage issues in these hours. The total length of the critical period considered in this study is approximately 6 hours. However, we decrease the charging period of the BES units by deceasing the time interval in which the grid feed-in limit is active. If the excess energy available from the PV system in this period is higher than the usable capacity of the battery, the battery will charge only during the period the feed-in limit is

Table 3.1: Parameters of the BES systems considered in the optimization model.

Parameter	Value
Battery Bank	
Battery type	Lithium-ion
Nominal Ah capacity	208 Ah
Nominal kWh capacity	10 kWh
E_o	48 V
K	0.0024 V
A	4.078 V
B	0.32138 Ah^{-1}
R	0.025Ω
$\eta_{bat,dischrg}$	0.98
$\eta_{bat,chrg}$	0.98
$I_{chrg,max}$	100 Ah
$I_{dischrg,max}$	120 Ah
SoC_{min}, SoC_{max}	20%, 95%
Converters	
$\eta_{pv,inv}$	$\frac{0.9589P_n - 0.00717}{P_n - 0.00459}$
$P_{batC,rated}$	4.5 kW
$\eta_{batC,inv}$	$\frac{0.9388P_n - 0.002302}{P_n + 0.007545}$
$\eta_{batC,rec}$	$\frac{0.9907P_n - 0.006077}{P_n + 0.006633}$

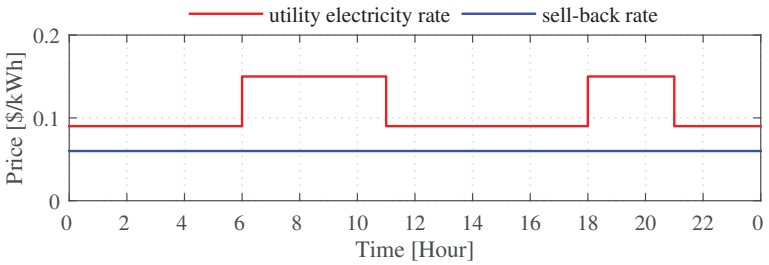

Figure 3.11: Electricity Tariff.

active. The charging power of the BES units can be increased by decreasing the length of the charging period. As a result, more reduction in reverse power flow can be achieved during high PV generation hours.

A 24-hour period was chosen as the planning horizon in the optimization problem with a sampling interval (Δt) of 1 hour. The sampling interval of the power flow simulation was 1-minute. As mentioned earlier, the hourly averages of 1 minute measurements of the load and the PV were used as the forecasted inputs to the optimization problem. The considered time-of-use electricity tariffs during the day are shown in Fig. 3.11. The battery degradation cost is 0.2 $/kWh. The secondary side manual tap setting of the distribution transformer was set to 1.04375pu for preventing under-voltage problems.

3.6 Simulation Results

Simulations were performed over a 48-hour period with a 1-minute time resolution. The optimization was run every hour by each HEMS independently for scheduling the BES for the coming 24 hours. From the optimization, the hourly dc side power set points of the BES systems were calculated. The control set points calculated from the Matlab code, i.e. the BES set points and the power factor set points of the converters were sent to openDSS to run the power flow at each time step. The results obtained from running the power flow were then sent back to Matlab for making decisions for the next time step.

3.6.1 The home energy management system

Fig. 3.12a illustrates the performance of an exemplary residential energy system over a 48 hour period. In this figure, the hourly forecasts of the load, PV production and the corresponding optimal battery set points and the power supplied to/by the grid are shown. The corresponding 1-minute variations of the load and the PV generation are shown in Fig. 3.12b. The short term fluctuations of the load and the PV generation observed in Fig. 3.12b are not represented in the hourly

averages shown in Fig. 3.12a. As the optimization problem's sampling interval is 1 hour, the optimal set points calculated from the optimization, P_{bat} and P_{grid} are also the hourly average set points. The variables, $P_{bat}(k)$ and $P_{grid}(k)$ depend on each other. Therefore, if we chose to operate the battery at the optimal set points calculated from the optimization, the short term fluctuations will be compensated by the grid or vice versa.

The performance of the residential energy system when P_{bat} is operated at the set points calculated from the optimization is shown in Fig. 3.12b. From the figure, it can be observed that the short-term fluctuations of the load has resulted drawing energy from the grid in some time slots, for example from 0900h-1400h in day-1 and 1800h-2200h on both days. But, according to the optimization results, the residential energy system should not draw power from the grid in the period from 0900h-1400h in day-1. Moreover, in the time slots from 1800h-2200h the load should be fully supplied by the battery. In this case, the customer will be billed for the compensated energy from the grid based on the time-of-use tariff in those time slots. As a result, at the end of the day the customer will not realize the expected cost savings.

By contrast, the performance of the residential energy system when P_{grid} is operated at the set points calculated from the optimization is shown in Fig. 3.13b. In this case, the short-term fluctuations are compensated by the battery. Therefore, the system does not draw energy from the grid as before. However, the battery performs short charge/discharge cycles, which will have an adverse effect on the cycle life of the battery. The battery handles more energy compared to the previous case, therefore the battery losses and the converter losses will be higher compared to the previous case.

In conclusion, both these methods have drawbacks, hence there is no clear superior method. Therefore, we have chosen the following method that is a combination of the above two methods to compensate for the short-term fluctuations.

The steps of the algorithm used for correcting instantaneous $\tilde{P}_{bat}$ and $\tilde{P}_{grid}$ set points in response to the short-term fluctuations of the load and the PV generation are as follows.

I The original instantaneous set points within the k^{th} time slot:
$\tilde{P}_{grid} = P_{grid}(k)$, $\tilde{P}_{bat} = P_{bat}(k)$,
where the variables with "tilde" correspond to the instantaneous set points.

II Initially, $\tilde{P}_{grid}$ is kept at the set points calculated from the optimization.
$\tilde{P}_{grid} = P_{grid}(k)$

III From the optimization results, it is checked whether charging the BES from the grid is recommended or not.
Charging from the grid in time slot k is recommended if $|P_{grid}(k)| > P_{load}(k)$ when $P_{grid}(k) < 0$.

IV Short-term fluctuations that cause charging from the grid in the time slots,

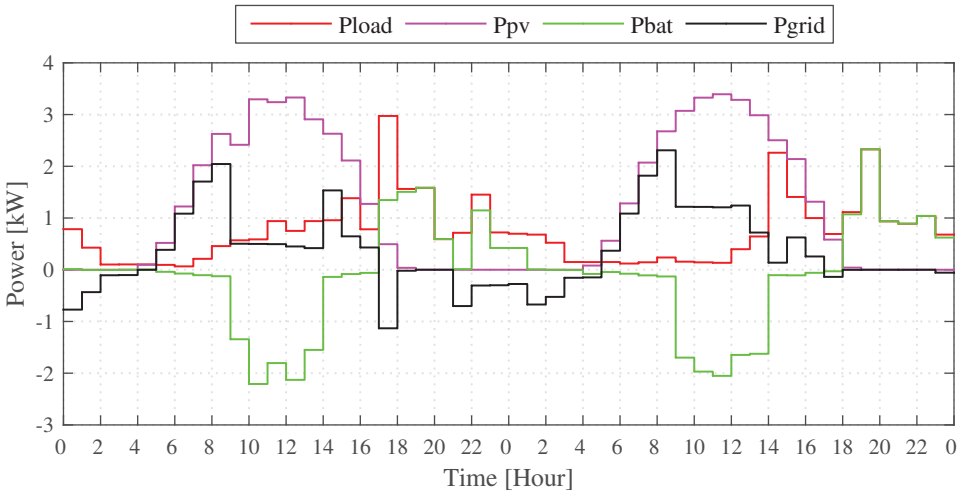

(a) Average load forecasts, PV forecasts and the calculated BES power set points and the grid power set points.

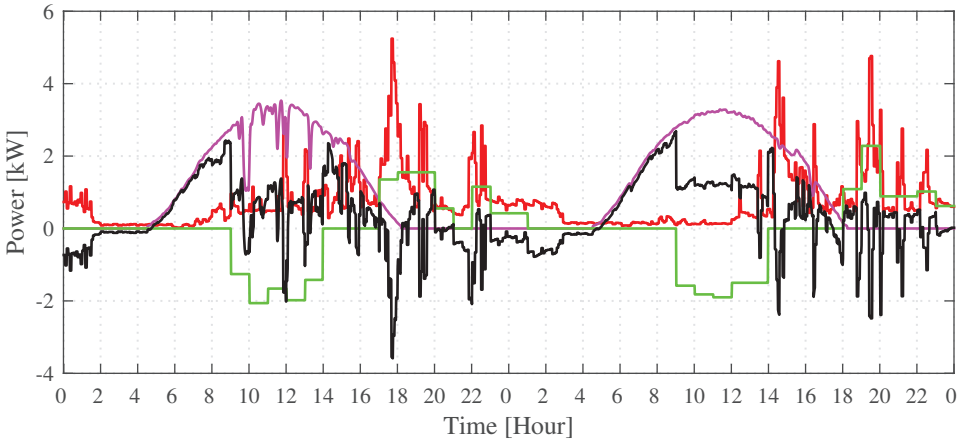

(b) Power flow when P_{bat} is chosen to operate at the set points calculated from the optimization with 1 min time resolution.

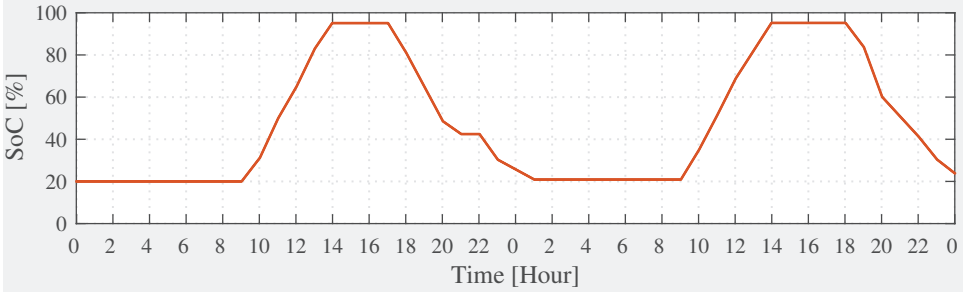

(c) SoC variation.

Figure 3.12: Performance of an exemplary HEMS when P_{bat} is chosen to operate at the set points calculated from the optimization.

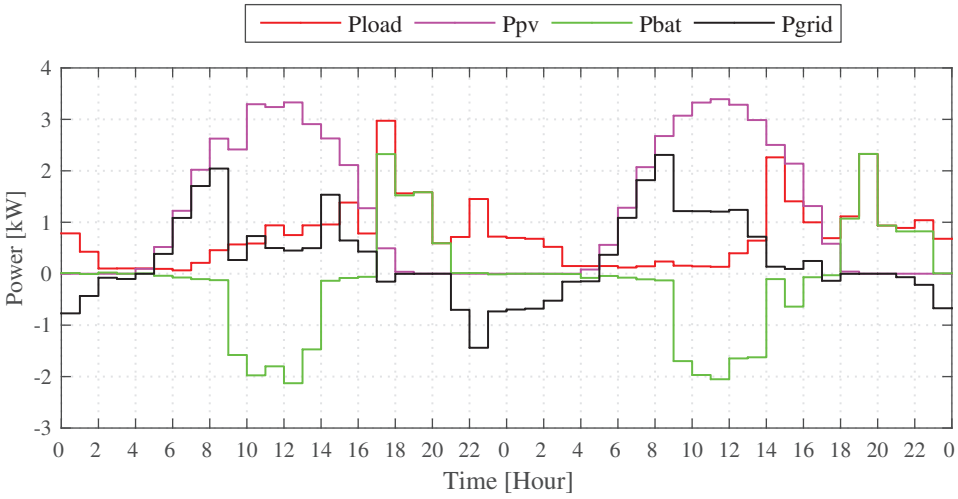

(a) Average load forecasts, PV forecasts, and the calculated BES power set points and the grid power set points.

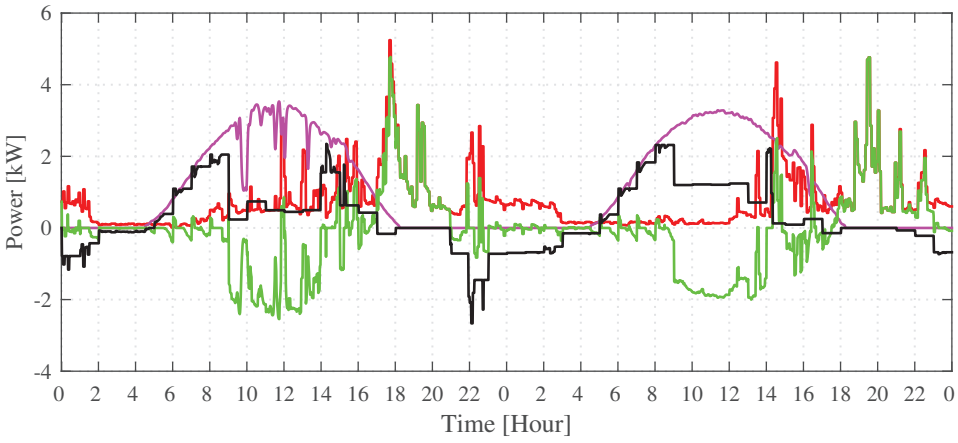

(b) Power flow when P_{grid} is chosen to operate at the set points calculated from the optimization with 1 min time resolution.

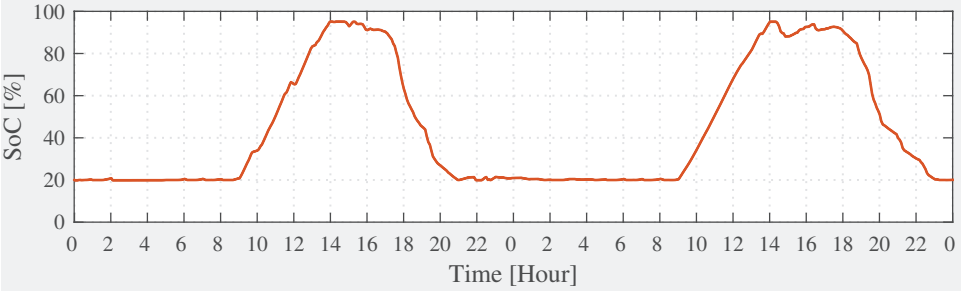

(c) SoC variation.

Figure 3.13: Performance of an exemplary HEMS when P_{grid} is chosen to operate at the set points calculated from the optimization.

other than the time slots recommended by the HEMS is prevented. Therefore, at this point P_{grid} is modified. The condition for modifying the grid set point is as follows.
If $\tilde{P}_{grid} < -\tilde{P}_{load}$ then $\tilde{P}_{grid} = -\tilde{P}_{load}$.

V After the above corrections, the new $\tilde{P}_{bat}$ is calculated with the use of the updated $\tilde{P}_{grid}$ and the measured load and the PV inverter's power output using the power balance equations given in Section 3.3.1.4.

VI Short-term fluctuations that cause charging or discharging of the BES are prevented in the time slots the battery is supposed to be idle. The time slots the battery is supposed be idle are found from the optimization results. At k^{th} time slot if $P_{bat}(k) = 0$, then the battery should be idle.
The $\tilde{P}_{bat}$ set point calculated at this step is finally sent to the battery converter.

The performance of the HEMS when the above set point correction method is included is shown in Fig. 3.14. This set point correction method has been able to avoid short charging/discharging cycles compared with the case in Fig. 3.13b. Moreover, power is not drawn from the grid to compensate for fluctuations. Therefore, there is no charge for the compensated energy as in the case shown in Fig. 3.12b. During day-1 the load in the high tariff period (1800h-2100h) is higher than the energy stored in the battery. Therefore, the whole stored energy is utilized to supply the local demand during the high tariff period. But in day-2, some of the load outside the high tariff period has also been supplied by the battery. This is because the load during the high tariff period is lower than the stored energy in the battery bank.

In the optimization, we introduced a grid feed-in constraint that forces charging of the batteries during the critical period. As a result, we can see the battery starts charging at the beginning of the critical period (0900h) and reaches maximum SoC by the end of the critical period (1400h). Therefore, in this case the usable capacity of the battery is fully utilized during the critical period. The excess energy available during the critical periods in both days is higher than the usable capacity of the battery. In order to maintain charging during the whole critical period, part of the power has to be fed-in to the grid. As shown in the figure, the HEMS has adjusted the grid feed-in such that the battery reaches its fully charged state by the end of the critical period. Hence, the battery provides support to the grid during the whole critical period by reducing power injection into the grid. As the power injection into the grid is reduced, the reverse power flow in the grid will also reduce during the whole critical period. Consequently, the risk of over-voltage will reduce too.

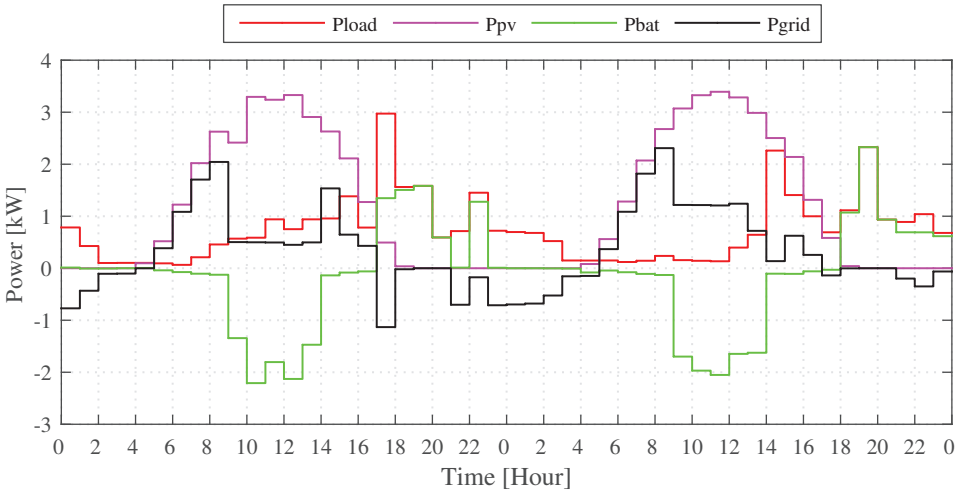

(a) Average load forecasts, PV forecasts and the calculated BES power set points and the grid power set points.

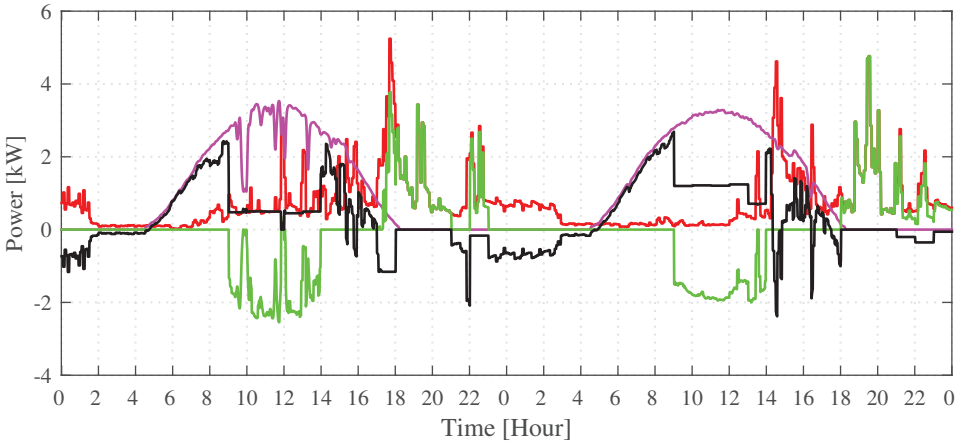

(b) Load profiles, PV profiles, BES power set points and the grid power set points with 1-minute resolution.

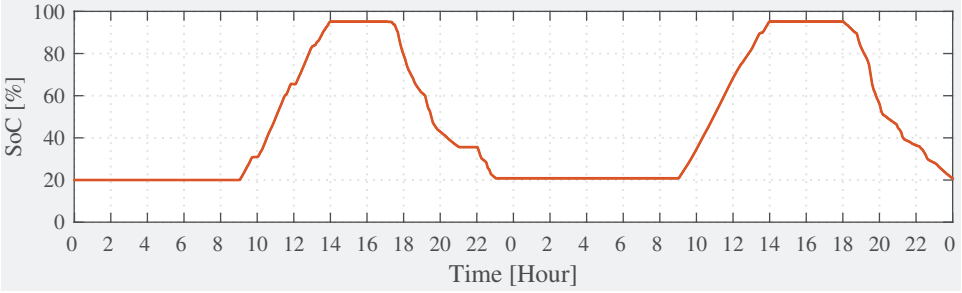

(c) SoC variation.

Figure 3.14: Performances of an exemplary HEMS with adjustments for short term fluctuation of load and PV.

3.6.2 Impacts on the grid

In this section, the grid side impacts of the proposed grid-supportive charging strategy along with the reactive power support solution are presented. Fig. 3.15 shows the voltage profiles of the two critical nodes and the voltage unbalance rates (the ratio between the negative sequence voltage and the positive sequence voltage), when there are no BES units nor reactive power support from the converters. As can be seen, due to the single phase loads and generators, the voltage magnitudes are relatively unbalanced, even though the voltage unbalance rates (VUR) are below the statutory limit of 2%. According to the European standard EN50160, 10-minute average values of the supply voltage should be within the range of $\pm 10\%$ of the nominal voltage. The voltage profiles shown are the 10-minute moving averages computed from 1-minute voltage measurements. As shown in the figure, the voltages of some phases at both critical nodes exceed the maximum limit during the critical period. Voltage fluctuations can also be observed due to the fluctuations of the load and the PV generation. Fig. 3.16a shows the improved voltage profiles at these nodes with the proposed BES operational strategy and the reactive power support method. Fig. 3.16b shows the corresponding VURs. The proposed control strategy has solved the over-voltage issues, however this control strategy has no significant impact on the VUR. That is because all the considered BES units are three phase units and they share the charging/discharging power equally among the phases. Therefore, the aggregate power transferred to/from the BES units via each phase is equal as depicted in Fig. 3.17.

Fig. 3.18 shows the SoC variations of 15 BES units. From the figure, it can be seen that the BES units in group-1 start charging at 0800h and the majority of them reach maximum SoC level (95%) by 1300h. Only one storage unit continues charging after 1300h. This is because the excess energy available from the corresponding PV system during the period from 0800h-1300h is not sufficient to charge the battery up to 95% SoC. Therefore, the HEMS allows charging outside the corresponding critical period. The BES units in group-2 start charging at 0900h and continue charging until 1400h. These BES units reach maximum SoC level by 1400h. From the results we can see that the BES units provide maximum support to the grid by charging during the period the DSO wants. When the excess energy available during the charging period specified by the DSO is not sufficient to charge the battery fully, the HEMS also schedules charging outside the critical period. Therefore, the maximum potential of the BES is utilized over a planning horizon.

Fig. 3.19 compares the active power flow through the distribution transformer in the base case with the case when the BES units are operated with the proposed strategy. The positive power in the figure corresponds to the power flow into the distribution system and the negative power corresponds to the power flow from the distribution system to the medium voltage grid. As can be seen in the figure, the reverse power flow has been shaved at about a three phase average of 25 kW in both days due to charging of BES units.

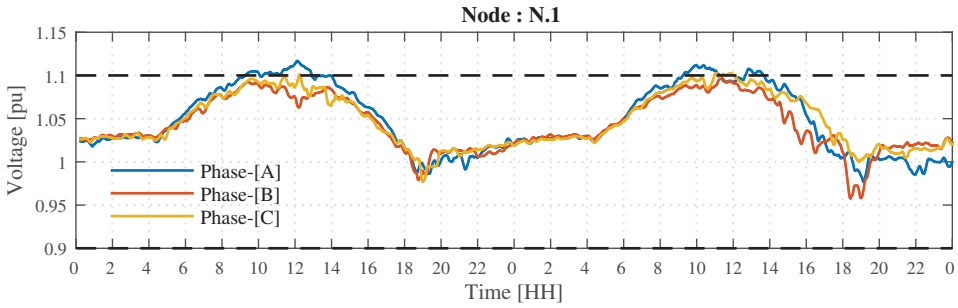

(a) Supply voltage variations.

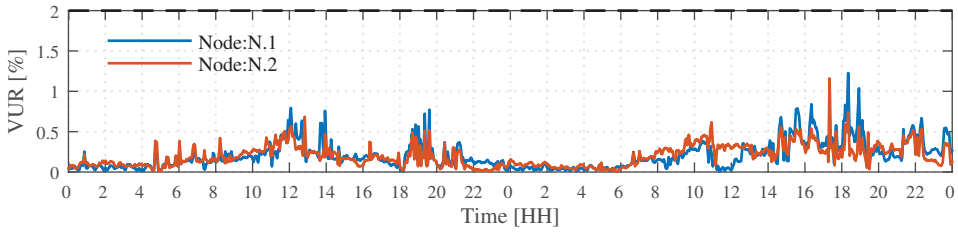

(b) Voltage unbalance rates.

Figure 3.15: Quality of the voltage at the critical nodes when there are no BES units in the system and reactive power support from the converters is not available (Base case).

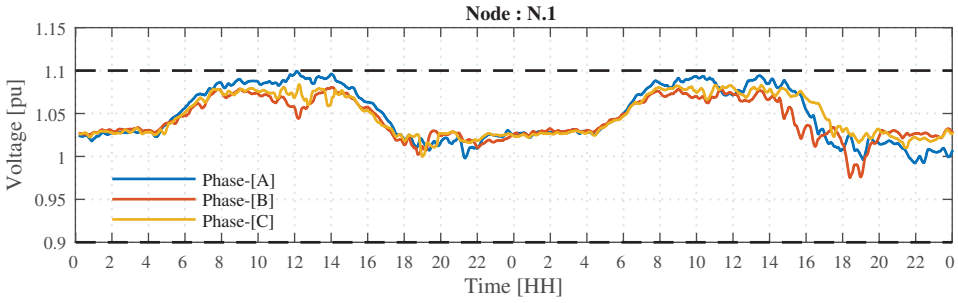

(a) Supply voltage variations.

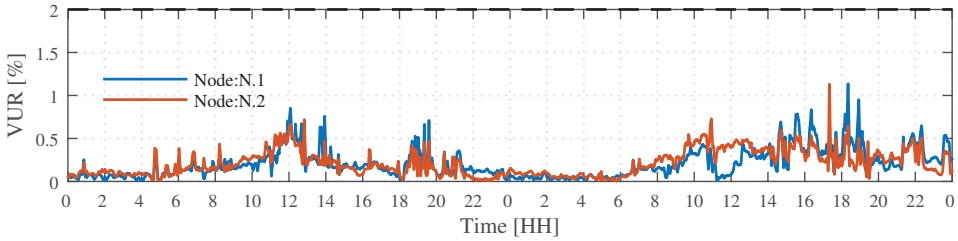

(b) Voltage unbalance rates.

Figure 3.16: Quality of the voltage at the critical nodes when there are BES units in the system and the reactive power support from the converters is active.

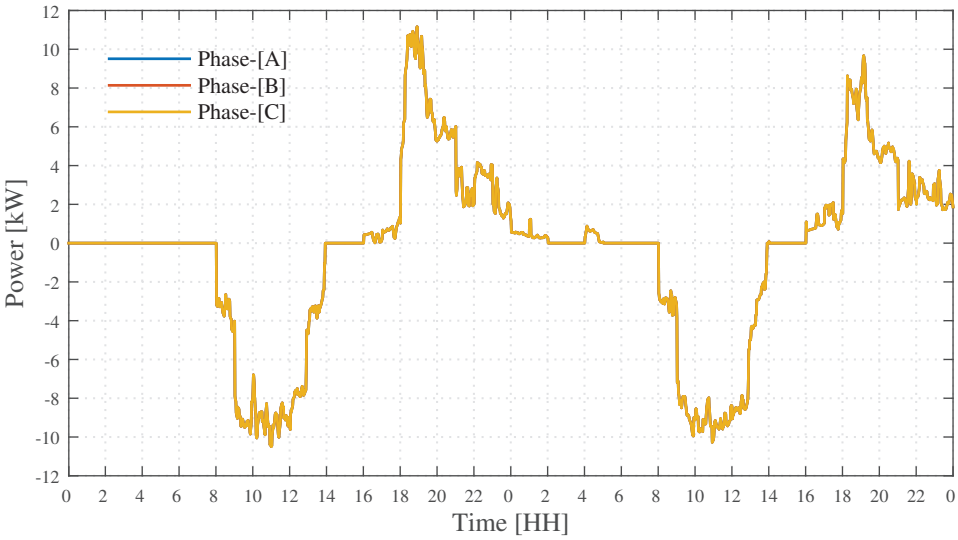

Figure 3.17: Aggregate power transferred to/from the BES units in each phase.

In this study, it is considered that the reactive power support is provided only from the PV inverters. Since AC-coupled systems have been considered, there is a possibility to provide reactive power support from the battery converters as well. As customers possessing BES units provide reactive power support to the grid from the PV inverters, it was assumed that the reactive power support from the battery converters is not compulsory. The battery converters can easily be integrated into the reactive power support method if needed. In the studied network, there are two long laterals. Therefore, for the purpose of voltage control, the network was divided into two control zones where each lateral represents a zone. The PV inverters were then allocated to each zone according to the electrical distance from the critical nodes to the PV nodes. The reactive power support from the PV inverters located closer to the transformer have a little impact on the voltage profile of the network. Therefore, they were discarded.

Fig. 3.20 illustrates the power factor variations of the converters in two control zones. As shown in the figure, the reactive power support from the converters has also been utilized for completely solving the over-voltage issues. This is because the reduction in active power flow due to charging of BES units is not sufficient to solve the over voltage issues in some phases. For example, in day-1, the voltage profile in phase-[A] at node-N.1 reaches the upper limit at about 1200h. The voltages shown are the 10-minute moving averages computed from the 1-minute measurements. The smart meter's setting was set such that a request is generated when the 5-minute moving average of the voltage violates the limits. At this time, the 5-minute moving average of the voltage exceeds the upper limit, although the 10-minute average is lower than the upper limit. Therefore, the reactive power support from the PV inverters in zone-1 is activated. The smart meter located at

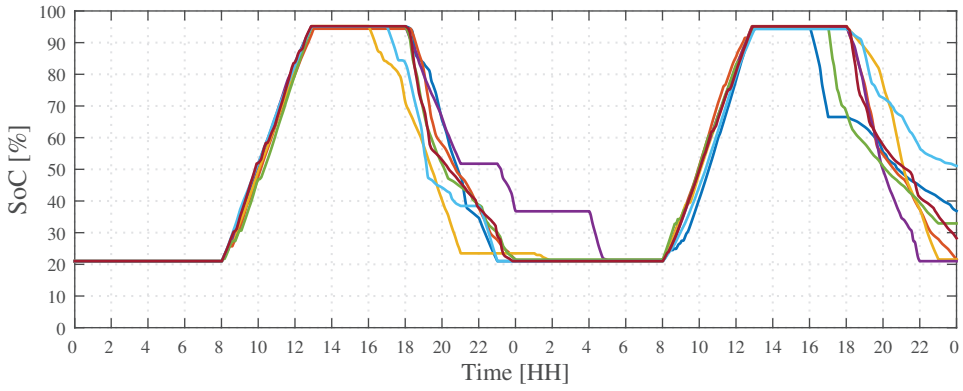

(a) SoC variation of BES units in group-1.

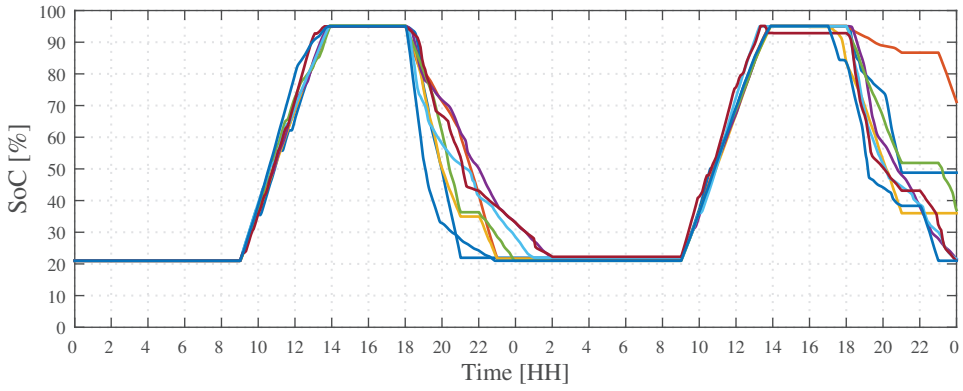

(b) SoC variation of BES units in group-2.

Figure 3.18: SoC variation of the BES units.

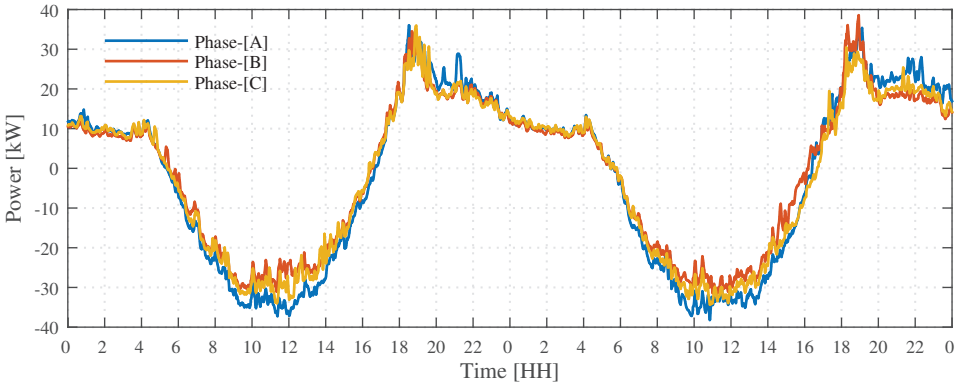

(a) Base Case.

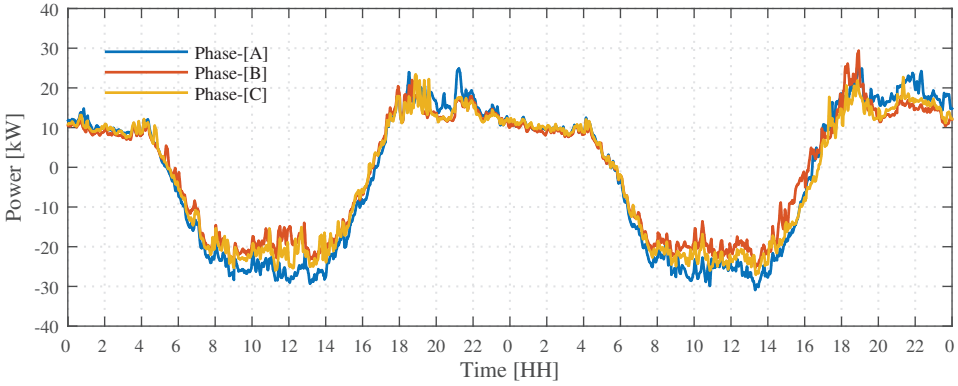

(b) When there are BES units in the system and the reactive power support from the converters is active.

Figure 3.19: Active power flow through the transformer.

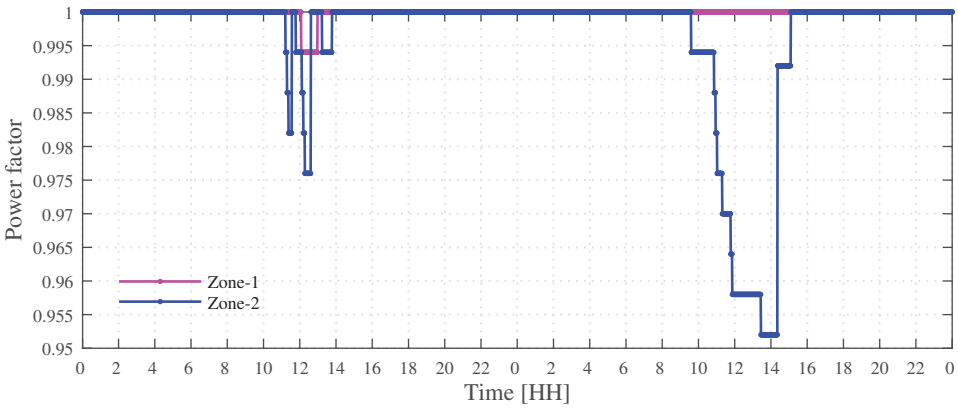

Figure 3.20: Power factor variations of the PV inverters when the reactive power support from the converters is active.

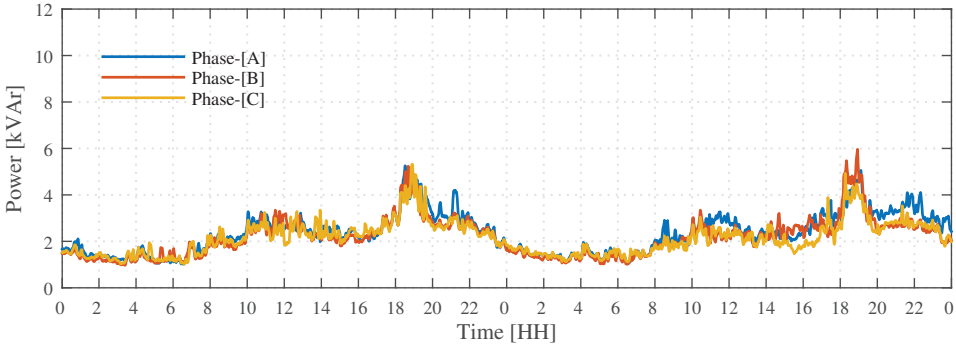

(a) When there are BES units in the system and the reactive power support from the converters is active.

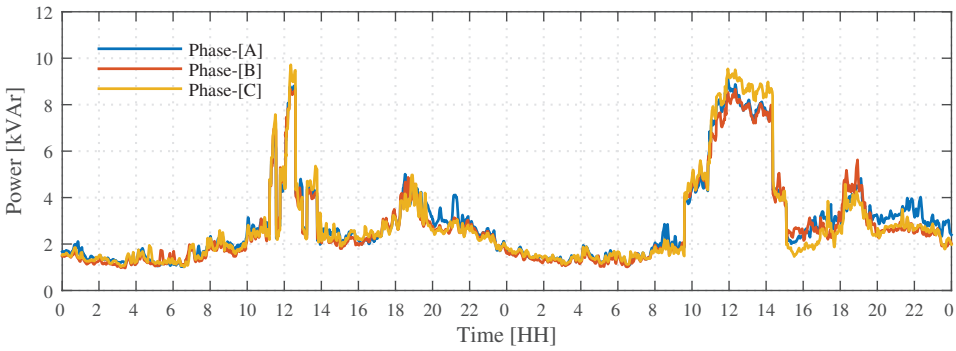

(b) Reactive power.

Figure 3.21: Reactive power on the transformer.

node-N.1 broadcasts a message to all corresponding inverters requesting that they decrease the power factor. The inverters respond by decreasing the power factor by 0.006 per request. At this time, decreasing the power factor by one step solves the over-voltage issue at node-N.1. The smart meter also broadcasts a message when the critical node voltage drops below 1.08 pu. That message asks PV inverters to reduce the reactive power support provided. The PV inverters respond to this message by decreasing the power factor by 0.04 per such message. The voltage profile of phase-[C] at node-N.2 also reaches the upper limit at several time points, therefore reactive power support from the converters in zone-2 is also utilized to maintain the voltage profile within the allowed range. The corresponding power factor variation of the PV inverters in zone-2 is also shown Fig. 3.20.

The proposed grid supportive charging strategy in combination with the reactive power support method is able to maintain the voltage profile of the grid within acceptable levels. As the local controller determines the optimal charging/ discharging set points of the BES unit, the objective function can be locally decided by the BES owner. To calculate the optimal BES set points, the local controller does not need any information about the network or the voltage profile of the other nodes in the network. Scheduling the BES units to charge during the critical period reduces the reverse power flow in the grid during the times of high PV feed-in to the grid. Therefore, it helps the utility to reduce the risks of over-voltage. In this case, we have considered 15 BES units with a capacity 10 kWh. When the number of residential BES units increases, further reduction in the reverse power flow during the critical period can be realized. Consequently, the amount of reactive power support required will decrease. This method is aimed to optimally utilize the available BES units to solve the over-voltage issues. The reactive power support is the secondary solution and only used if reduction of reverse power flow due to charging of BES is not sufficient to solve the over-voltage issue completely.

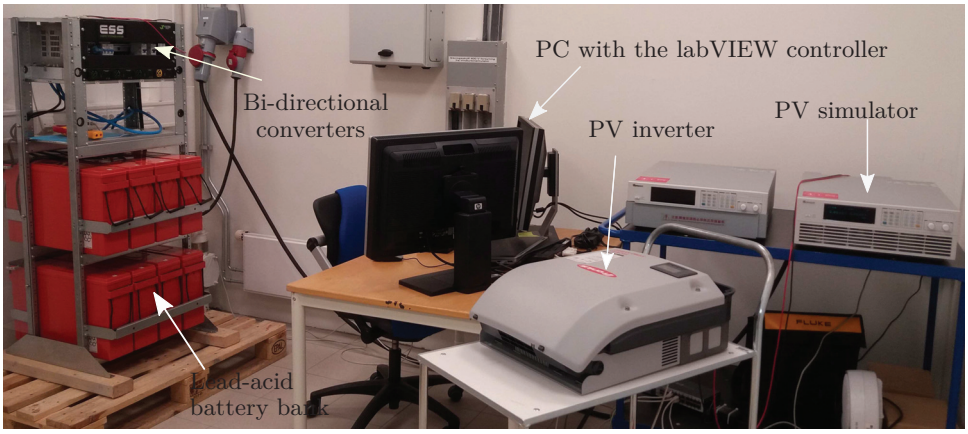

Figure 3.22: Experimental set-up.

3.7 Experimental Set-up

An experimental set up of the residential energy system with a PV system, BES unit and an inelastic load was built to test the performance of the HEMS. Fig. 3.22 shows a picture of the experimental set up being built. The system is AC-coupled. A PV simulator was used to emulate the behaviour of a PV system with a rated capacity of 3.5 kW. This PV emulator is connected to the AC bus via a Fronius symo hybrid inverter. The battery bank consists of 8, valve regulated lead-acid batteries from EnerSys. The nominal voltage and the Ah capacity of each battery is 12 V and 190 Ah respectively. The battery bank is made of connecting two strings in parallel, where each string consists of four series connected batteries. The nominal capacity of the battery bank is 380 Ah/18.24 kWh with a nominal DC link voltage of 48 V. The battery bank is connected to the AC bus via 3 single phase bi-directional converters provided by Eltek. The rated capacity of each single phase converter is 2 kW. The load was simulated inside the controller. The control algorithm of the HEMS was implemented in LabVIEW. The communication between the LabVIEW and the converters (Fronius inverter and the bi-directional converters) were established via Modbus/TCP over Ethernet. The current, voltage and power measurements from the converters were obtained at a sampling rate of 0.1 Hz. The control signals were also sent to the battery converter at the same frequency. An overview of the system can be found in Fig. 3.23.

When using lead-acid batteries with solar in daily cyclic applications, operating the lead-acid battery in a controlled partial state of charge is recommended. In this mode, the battery is charged at a higher voltage threshold, and therefore reaches approximately 95% SoC by the end of the constant(controlled) current charging mode. It is not necessary to fully charge the battery in each cycle. However, it is very important to ensure that the battery is periodically returned to a full

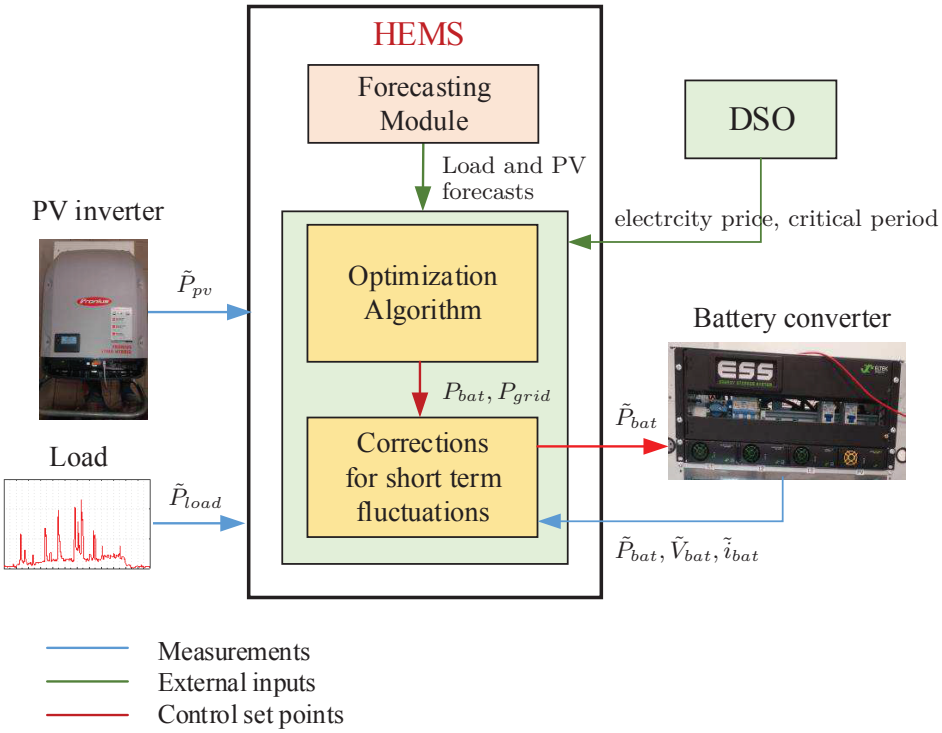

Figure 3.23: Overview of the HEMS.

state of charge to maintain battery state of health. This full charging can be done, for example, every 10 days. According to the data sheet of the EnerSys battery, the recommended charging voltage threshold of the battery in a controlled partial state of charge is 2.4 V per cell at 20 ^{o}C [122]. A battery is made of connecting 6 cells in series and the battery bank is made of connecting 4 such batteries in series. Therefore in this mode, the charging voltage threshold of the battery bank should be 57.6 V. However, the maximum charging voltage threshold of the battery converter used in the experimental set up has been set to 56 V by the converter manufacturer. Therefore, it was not possible to increase the charging voltage threshold to 57.6 V. At 56 V the charging mode changes from a constant current charging mode to a constant voltage charging mode. The constant voltage charging mode has not been modelled in the EMS. Therefore, the following adjustments were made.

- The usable capacity of the battery for charging during the critical period is considered equal to the available capacity of the battery over the operating window from minimum SoC to the SoC at end of the constant charging process.
- Charging is continued when the charging process enters to the constant voltage charging mode, if there is excess energy available from the PV system. Charging of the BES is stopped either when the BES reaches maximum SoC or the discharging time of the BES starts.

Discharging of the battery is stopped when the on-load battery voltage drops to the level equivalent to the configured depth of discharge (DoD) in the duty cycle. According to the data sheet, a 48 V system could be set up for 60% DoD in normal operation, with an end of discharge voltage trigger of 47.8 V (1.99 Vpc) or 70% DoD in abnormal situations with an end of discharge voltage trigger of 47 V (1.96 Vpc). In our set-up, the end of discharge voltage trigger was set to 47.8 V (1.99 Vpc). Consequently, the BES system operates within an SoC window of approximately 40%-100%. The open circuit voltages of the battery bank at 40% and 100% SoC are 48.6 V and 52 V, respectively.

We have made the following two approximations of the BES model used in the optimization algorithm.

Approximation 1: Battery charging/discharging efficiency

The effect of charging/discharging current on the battery efficiency was neglected. Instead, it is assumed that the battery efficiency is constant. In order to calculate an average round-trip efficiency of the battery, we cycled the battery at different currents over the SoC operating window of 40%-100%. At each current, the energy in and out of the battery over one cycle were measured. The round-trip efficiencies of the battery bank at different currents were then calculated. The battery bank's round-trip efficiency was assumed equal to the average of the above calculated

Table 3.2: Battery bank's round-trip efficiency measurement test results.

Current	In		Out		Round trip efficiency	
(A)	Q_{in}(Ah)	E_{in}(kWh)	Q_{out}(Ah)	E_{out}(kWh)	Coulomb eff.	Energy eff.
30	200	10650	192	9450	0.96	0.89
40	205	10890	189	9360	0.92	0.86
50	209	11200	181	9260	0.86	0.83
60	210	11400	180	9150	0.85	0.80

efficiencies. The charging and discharging efficiencies of the battery bank were then calculated using

$$\eta_{chrg} = \eta_{dischrg} = \sqrt{\eta_{rt}} \tag{3.28}$$

where η_{rt} is the average round-trip efficiency of the battery bank. Table 3.2 lists the results of the round-trip efficiency measurement test of the battery bank. The calculated average round-trip coulomb and energy efficiencies of the battery bank are 90% and 85%, respectively.

Approximation 2: Battery voltage

The voltage characteristic of the battery bank was represented by the simplest battery model. This model consists of a voltage source connected in series with a resistance. In this model, the terminal voltage of the battery is given by

$$V_{bat} = V_{ocv} - i_{bat}R_{bat} \tag{3.29}$$

where R_{bat} is the internal resistance of the battery. The battery current, i_{bat} is considered positive when discharging while negative when charging. V_{ocv} is the open circuit voltage of the battery and it is assumed constant. The effect of SoC on the open circuit voltage of the battery bank was neglected. From the measurements, it was found that the open circuit voltage of the battery bank over the SoC window 40% -100% varies from 48.6 V to 52 V. Therefore, V_{ocv} was set at 50.3 V, which is the average of the two voltages 48.6 V and 52 V. The internal resistance of the battery bank was calculated using

$$R_{bat} = \frac{\Delta V_{bat}}{i_{bat}} \tag{3.30}$$

where ΔV_{bat} is the rapid drop in battery terminal voltage when a load is connected. The effect of SoC on the internal resistance of the battery was neglected.

At time t, the stored energy in the battery bank was estimated using the coulomb counting method. Since the battery bank is operated in the SoC range of 40%-100%, the usable capacity of the battery is about 60% from the maximum capacity. The battery is considered empty when the open circuit voltage is equal to or below 48.6 V. The battery is also considered empty when the on-load voltage of the

battery drops to the end of the discharge voltage trigger. The usable capacity of the battery bank over this operating window was estimated as follows. The battery bank was charged at constant current I, until it reaches 100% SoC. The charging process enters from a constant current charging stage to a constant voltage charging stage when the battery voltage reaches 56 V. When it enters the constant voltage charging stage, the current starts to drop. The battery bank was assumed fully charged when the charging current drops below 2 A. The energy and the Ah input to the battery during this period were recorded. This test was performed at different currents. Then the average of the recorded capacities is calculated. This calculated average capacity is considered as the usable capacity of the battery bank over the considered operating window. The average usable capacity of the battery over the operating window from minimum SoC to the SoC at the end of the constant current charging process is also found from the same test.

3.7.1 Experimental results of the HEMS

The set up was run over a 48-hour period to evaluate the performance of the system. The electricity tariff shown in Fig. 3.11 was considered with the battery degradation cost 0.2 \$/kWh. The charging period of the BES unit, which is decided by the DSO, was set to 1100h-1600h. The planning horizon of the optimization algorithm was set to 24 hours. It was assumed that the accurate hourly forecasts of the load and the PV generation are available over the planning horizon. As in the simulation study, the hourly averages of the 1-minute data of the load and PV generation were used as the forecasted load and PV inputs to the optimization problem. The power output profile of a PV system with a rated capacity of 3.5 kW was generated using the irradiance and temperature measurements obtained from a test station at the University of Agder located in the town of Grimstad in southern Norway [3]. The load profile was derived from the residential electrical load profiles obtained from IEA/ECBCS Annex 42 [123].

Due to time limitations, I was not able to embed the optimization algorithm in the LabVIEW program. Instead, the optimization algorithm was run in Matlab. The results obtained from the Matlab model, i.e. the scheduled set points P_{bat} and P_{grid} were then input to the LabVIEW program. Every 6 hours, the optimization was run manually in Matlab with the updated initial conditions, load forecasts and the PV forecasts. The set points calculated from the optimization were then input to the LabVIEW program.

Fig. 3.24(a) shows the load profile and the PV production profile over 2 days. The corresponding battery power and the power flow into/from the grid are shown in Fig. 3.24(b). As can be observed from the figure, the BES starts to charge at 1100h, which is the start of the critical period set by the DSO. In this test, it is considered that the available capacity of the battery for charging during the critical period is equal to the capacity of the battery over the operating window from minimum SoC to the SoC at the end of the constant charging process ($E_{bat,CC}$). The excess energy available during the critical period is higher than $E_{bat,CC}$, therefore some power is

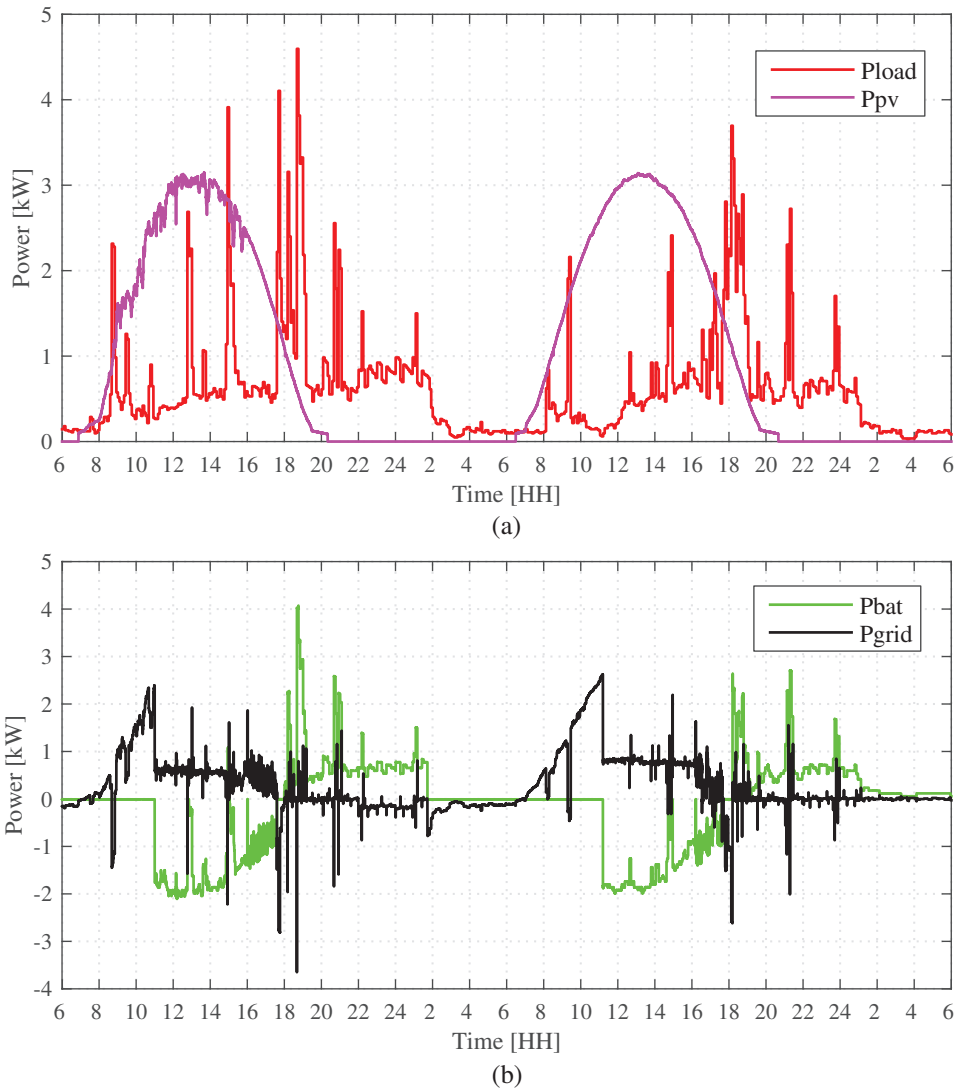

Figure 3.24: Load profile, PV profile, BES power set points and the grid power set points.

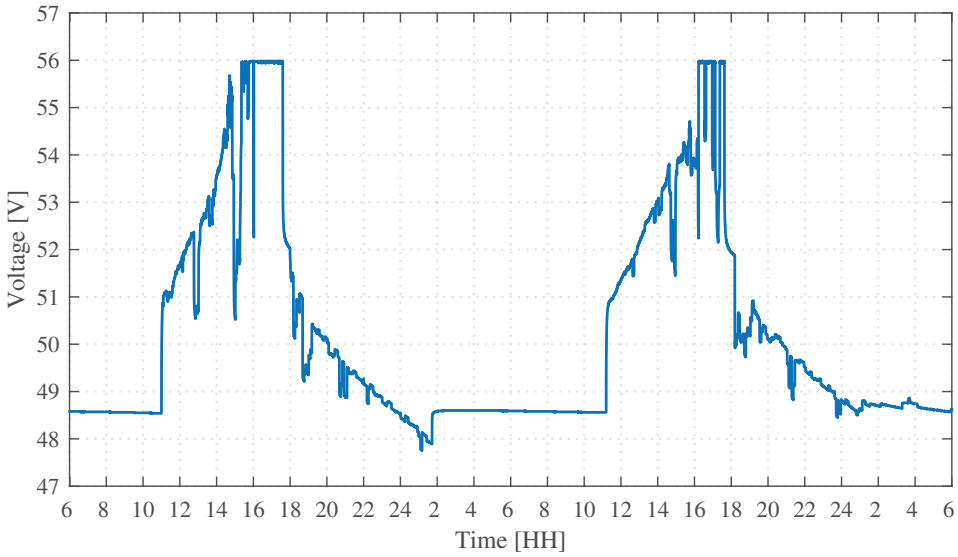

Figure 3.25: Voltage of the battery bank.

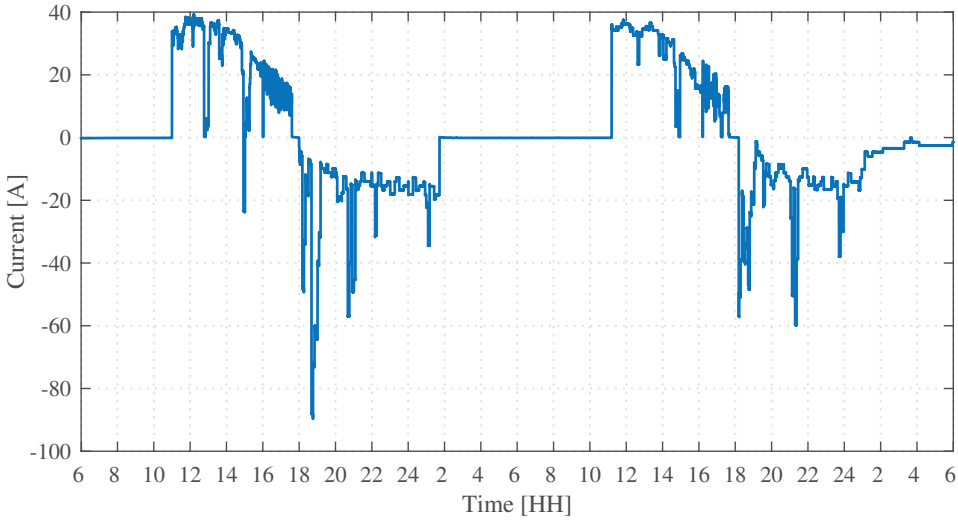

Figure 3.26: Battery current.

injected to the grid so that the battery will not reach the constant voltage charging stage earlier than expected. Fig. 3.25 shows the variation of battery voltage over the time. The voltage reaches 56 V somewhere between 1500h-1600h. Once the battery voltage is 56 V, the charging process enters the constant voltage charging stage. After the end of the critical period, charging is continued if there is excess power available from the PV system. Otherwise, the instantaneous control set points are calculated based on the results from the optimization. Fig. 3.26 shows the variation of battery current over the time. The battery current starts to drop when the charging process enters the constant voltage charging stage. During this stage, the charging current keeps fluctuating. Consequently, the power injection into the grid also fluctuates. Even though the current is fluctuating, the average current gradually drops. Charging of BES stops around 1730h because after this time there is no excess energy available. The battery starts to discharge at 1800h. The stored energy is higher than the load during the high tariff period (1800h-2100h). Therefore, in day-1, part of the load outside the high tariff period is also supplied from the battery. In day-2, the night-time load is fully supplied by the BES.

In Fig. 3.24(b), it can be seen that whenever there is a sudden fluctuation of load or PV production, it is balanced by the grid for a short time. That is because the BES takes some time to respond to changes. The response time of the BES depends on several things. The main reason is the communication delay. The controller needs measurements from the PV inverter, load and the BES converter to calculate the new BES set points. It takes some time to acquire this information from the devices. In our set-up, we have also added a function to write measurements to a text file at each time step. It took about 7 s to complete all these tasks. Therefore, the time between two measurements were set to 10 s. Consequently, the response time of the BES becomes 10 s.

Chapter 4

Distributed Control Strategy for Residential BES Systems

This chapter focuses on a distributed control strategy for controlling the active power set points of the BES systems. With distributed control, we attempt to maximally utilize the active power capability of BES units for over-voltage mitigation. It also presents a centralized reactive power control scheme for voltage regulation. This is the secondary solution that is used if active power control of BES units are not sufficient to maintain the voltage profile within the statutory limits. The chapter starts by introducing the concept of voltage sensitivities in unbalanced three-phase grids. It then provides details of the methodology of the control strategies. A case study is then presented followed by the results from a simulation study.

4.1 Introduction

One of the aspects of the Smart Grid is the extension of intelligent control of electrical power grid functions to the distribution grid. This requires deployment of information and communication technologies (ICT) in distribution grids. Recently, there has been a significant progress towards realization of these concepts. Automatic metering infrastructure, HEMSs, and power electronic converters of distributed energy resources (DER) that include communication interfaces are some of the examples of smart grid-enabled technologies that can be already found in the distribution grid. Management of DERs via real-time monitoring and control become possible with the integration of ICT.

With the assumption of the availability of necessary ICT infrastructure, several authors have presented different real-time control methods for distributed energy storage units that are used for providing voltage support to the grid. Ref. [91]

presents a coordinated control method of distributed energy storage to manage node voltages and thermal constraints. The active power of the storage is controlled to manage network loading, whereas reactive power is used for voltage regulation. The method uses the energy storage system closest to the voltage violated node for the voltage regulation. Ref. [87] presents a coordinated voltage control scheme with the use of energy storage units and the transformer OLTC. In the proposed method, the selection of voltage control device(s) is based on the voltage cost sensitivity factor, which is defined as the ratio of the required voltage change at a selected node to the operating cost of a voltage control device. The device having the highest voltage cost sensitivity is selected first, and the required active and reactive power settings are calculated using voltage sensitivity coefficients with respect to active and reactive power. In the case where sufficient capacity is not available, a second device is chosen. This selection continues until the node voltage reaches the desired level. Ref. [94] presents a similar approach, but the selection is based on both voltage sensitivities and the remaining cycle life of the battery. A centralized controller selects the storage unit(s) to be used and notifies that to the local controller. Having received the command from the centralized controller, the local controller determines the active and reactive power set points based on local voltage measurement. The local controller then communicates this result back to the centralized controller for subsequent decision making. Ref. [124] proposes a real-time voltage control scheme using active and reactive power support from super capacitor bank(s). The active and reactive power set points of the capacitor bank(s) are found by solving an optimization problem with the objectives of minimizing: i) the total active and reactive power adjustments from the scheduled values, and ii) the difference between expected and nominal voltages at the critical nodes.

In this chapter, we propose a distributed control strategy for residential BES units, which is intended to support the grid to solve over-voltage issues. We call this method a distributed control strategy because the local controllers decide the BES set points. A central controller adjusts these set points only when needed. In this method, however, the residential energy systems do not communicate with each other. The local controller optimizes the operation of the local system while the central controller optimize the operation of the overall distribution grid. In that way, two objectives are distributed among the central controller and the local controllers. Unlike the methods mentioned above, in this method, most of the decisions related to the residential BES unit are taken locally with the use of local information. If the locally decided storage set points are not able to maintain the voltage profile of the network within the statutory limits, a central controller adjusts the BES active power set points. If the adjustment of the BES active power set points is still not sufficient to solve the over-voltage problem, then the reactive power support from the PV inverters is utilized. In this case, the central controller attempts to find the optimal reactive power set points of each PV inverter that can minimize the total reactive power support provided by the converters. Compared to the reactive power support method presented in Section. 3.4, with this method, the amount of reactive power support required can be reduced. Therefore, the over-voltage problem can be solved with reduced reactive power support.

4.2 Voltage Sensitivities in Unbalanced Distribution Systems

European LV distribution systems are often three phase four-wire systems, and they accommodate both three- and single-phase loads and DERs. Therefore, the system is usually unbalanced, to some extent. Moreover, distribution grids are characterized by high R/X ratios. Connecting a single phase load or a generator to a three phase four-wire balanced system results in a neutral point shift due to return current through the neutral conductor [42]. A single-phase generator injecting active power into the line results in an increase in the voltage at the phase where it is connected. Because of the neutral point shift, the voltages in the other two phases decrease. Reactive power injection by a single phase generator also has a similar effect on the three phase voltages. The change in voltage due to a change in active or reactive power can be estimated via voltage sensitivity analysis. Using the voltage sensitivities, the changes in voltage for changes in active and/or reactive power can be written as follows.

$$\left[\Delta V\right] = \begin{bmatrix} \frac{\partial V}{\partial P} & \frac{\partial V}{\partial Q} \end{bmatrix} \begin{bmatrix} \Delta P \\ \Delta Q \end{bmatrix}, \tag{4.1}$$

where $\frac{\partial V}{\partial P}$ is the sensitivity of voltage to active power and $\frac{\partial V}{\partial Q}$ is the sensitivity of voltage to reactive power. ΔP and ΔQ are the changes in active and reactive power respectively. The three-phase representations of the first elements of each of the variables are as follows.

$$\left[\Delta V_1\right] = \begin{bmatrix} \Delta V_{a1} \\ \Delta V_{b1} \\ \Delta V_{c1} \end{bmatrix}, \quad \left[\Delta P_1\right] = \begin{bmatrix} \Delta P_{a1} \\ \Delta P_{b1} \\ \Delta P_{c1} \end{bmatrix}, \quad \left[\Delta Q_1\right] = \begin{bmatrix} \Delta Q_{a1} \\ \Delta Q_{b1} \\ \Delta Q_{c1} \end{bmatrix}$$

$$\left[\frac{\partial V_1}{\partial P_1}\right] = \begin{bmatrix} \frac{\partial V_{a1}}{\partial P_{a1}} & \frac{\partial V_{a1}}{\partial P_{b1}} & \frac{\partial V_{a1}}{\partial P_{c1}} \\ \frac{\partial V_{b1}}{\partial P_{a1}} & \frac{\partial V_{b1}}{\partial P_{b1}} & \frac{\partial V_{b1}}{\partial P_{c1}} \\ \frac{\partial V_{c1}}{\partial P_{a1}} & \frac{\partial V_{c1}}{\partial P_{b1}} & \frac{\partial V_{c1}}{\partial P_{c1}} \end{bmatrix}, \left[\frac{\partial V_1}{\partial Q_1}\right] = \begin{bmatrix} \frac{\partial V_{a1}}{\partial Q_{a1}} & \frac{\partial V_{a1}}{\partial Q_{b1}} & \frac{\partial V_{a1}}{\partial Q_{c1}} \\ \frac{\partial V_{b1}}{\partial Q_{a1}} & \frac{\partial V_{b1}}{\partial Q_{b1}} & \frac{\partial V_{b1}}{\partial Q_{c1}} \\ \frac{\partial V_{c1}}{\partial Q_{a1}} & \frac{\partial V_{c1}}{\partial Q_{b1}} & \frac{\partial V_{c1}}{\partial Q_{c1}} \end{bmatrix}$$

The voltage sensitivities in a three-phase balanced grid can be derived using the Jacobian matrix. The Jacobian matrix is calculated when solving the power flow problem using the Newton-Raphson method [125–128]. Unlike a transmission system, a distribution system usually has a radial topological structure. This radial structure, along with the higher R/X ratio of the lines, makes the Newton-Raphson method unsuitable for solving the power flow of the distribution systems. This is because the Newton-Raphson method sometimes fails to converge [129–131]. Therefore, the Jacobian matrix-based method is not suitable for calculating the voltage sensitivities in distribution grids either.

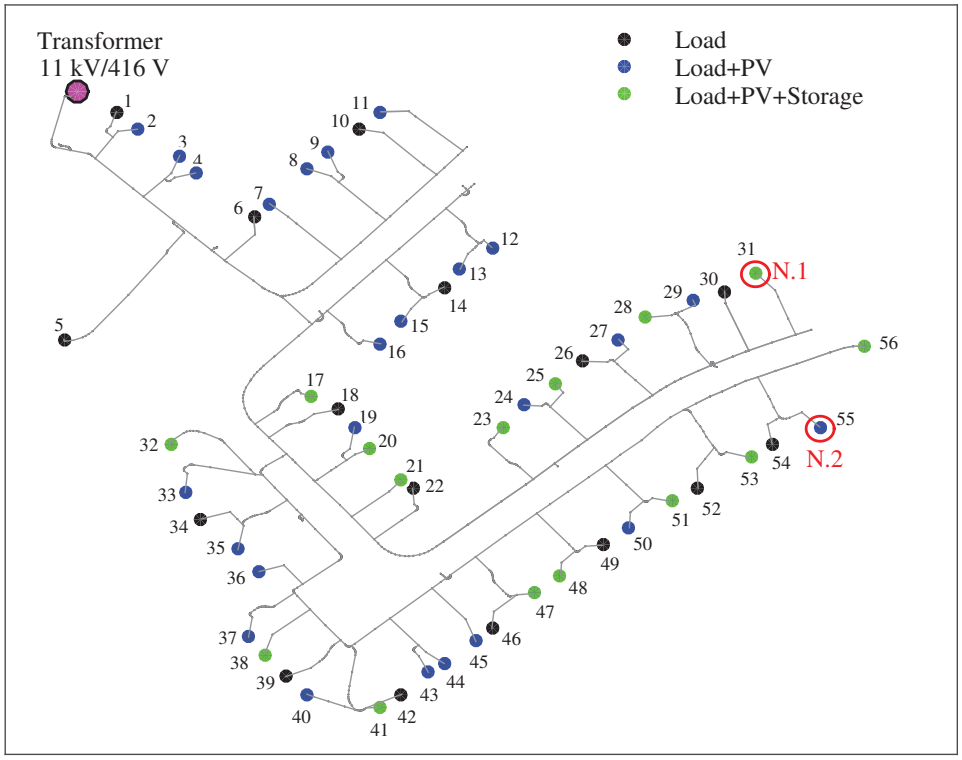

Figure 4.1: Single line diagram of the modified IEEE low voltage test feeder.

Ref. [132] presents an efficient method to calculate the voltage sensitivity coefficients with respect to the active (P) and the reactive power (Q) in unbalanced radial electrical distribution networks. The method is based on taking the partial derivatives of the power flow equations with respect to P and Q, and solving the resulting system of linear equations. The Gauss-Seidel method can be used to solve the system of linear equations. In order to calculate voltage sensitivities with this method, it requires the network admittance matrix [$\mathbf{Y}$], and the voltage measurements at each node of the network (both angle and the magnitude). The node voltages (both the magnitude and the phase) can be estimated using the P, Q measurements obtained from the smart meters via the state estimation process [133, 134]. Using these voltage estimations and the network admittance matrix, one can compute the voltage sensitivities.

Fig. 4.2 and Fig. 4.3 show the calculated voltage sensitivities of the modified IEEE LV test feeder when the system is not balanced. The adopted sign convention is: P is positive when P is injected to the grid, Q is positive when Q is injected to the grid and P, Q are negative when absorbed from the grid. The results shown in the figures are the voltage sensitivity coefficients of phase-a at node 56 with respect to the P and Q injections at nodes 1-56 (see Fig. 4.1 for node indexes). As can

be observed in the figure, the voltage sensitivity increases as the electrical distance between the two nodes decreases. The voltage sensitivities w.r.t P and Q injection from the same phase are shown in Fig. 4.2a and Fig. 4.3a, respectively. Because of the high R/X ratio of the studied network, voltage sensitivities w.r.t P injection are much higher than those of Q. The voltage sensitivity coefficients of phase-a w.r.t. P injection in phase-a are positive while the sensitivities are negative w.r.t. P injections in phases b and c. The voltage sensitivities w.r.t. P injection from another phase are relatively small when compared to the voltage sensitivities w.r.t. P injection in the same phase.

Regarding the Q sensitivities, an interesting behaviour was observed for the studied network. That is the sensitivity coefficients of phase-a w.r.t Q injection in phase-b are negative and they are positive w.r.t. Q injection in phase-c. Moreover, the voltage sensitivities w.r.t. Q injection from another phase are higher than the voltage sensitivities w.r.t. Q injection from the same phase. This may be due to the high R/X ratio of the studied network. From these results it is evident that the mutual couplings between the phases are significant. Hence this cannot be ignored when estimating the voltage changes using the voltage sensitivity coefficients when the network is not balanced.

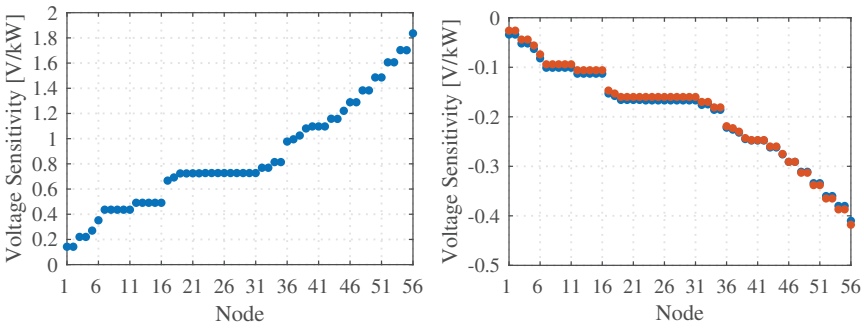

(a) $\frac{\partial V_{a,56}}{\partial P_{a,j}}$ where $j = 1, 2, \ldots, 56$. **(b)** $\frac{\partial V_{a,56}}{\partial P_{b,j}}$ and $\frac{\partial V_{a,56}}{\partial P_{c,j}}$.

Figure 4.2: Voltage sensitivity coefficients of phase-a at node-56, with respect to P injection at nodes 1-56.

Voltage sensitivity coefficients depend on the operating point, because they are calculated based on the linearisation of the power flow equation about an operating point. Fig. 4.4 illustrates the effect of the operating point on the voltage sensitivity coefficients. The effect can be significant when the operating point deviates further away from the reference point. Therefore, it is recommended to calculate the sensitivities at different operating points, for example every hour. In the above analysis it is assumed that the impedance of the grid behind the transformer remains unchanged. Inclusion of an algorithm to calculate the Thevenin equivalent of the grid at discrete time intervals is recommended in order to improve the accuracy of the sensitivity calculation.

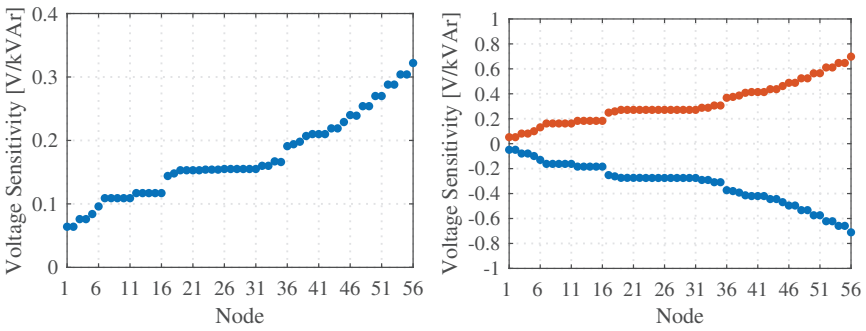

(a) $\frac{\partial V_{a,56}}{\partial Q_{a,j}}$ where $j = 1, 2, \ldots, 56$. **(b)** $\frac{\partial V_{a,56}}{\partial Q_{b,j}}$ and $\frac{\partial V_{a,56}}{\partial Q_{c,j}}$.

Figure 4.3: Voltage sensitivity coefficients of phase-a at node-56, with respect to Q injection at nodes 1-56.

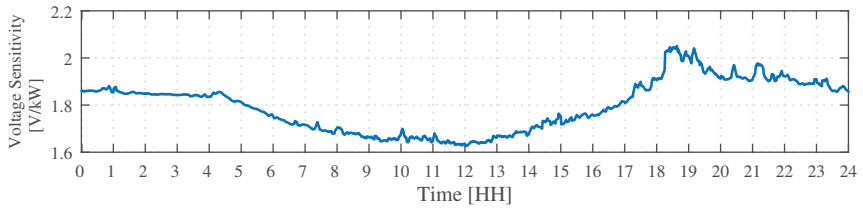

(a) Voltage sensitivities of phase-a at node-56 w.r.t. P injection of phase-a at node-56 $\left(\frac{\partial V_{a,56}}{\partial P_{a,56}}\right)$.

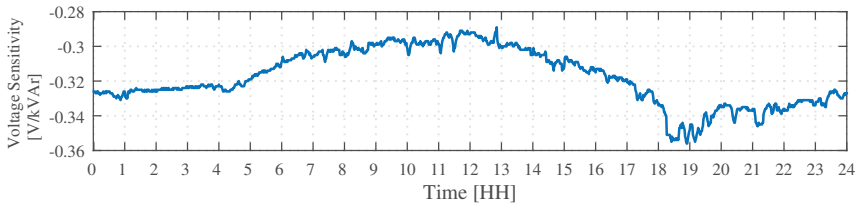

(b) Voltage sensitivities of phase-a at node-56 w.r.t. Q injection of phase-a at node-56 $\left(\frac{\partial V_{a,56}}{\partial Q_{a,56}}\right)$.

Figure 4.4: Variation of the voltage sensitivities with respect to the changes in the operating point.

4.3 Method

Deployment of ICT infrastructure in the electrical distribution network enables real-time monitoring and control of DERs. With the assumption of availability of such infrastructure, in this chapter we propose a distributed control scheme, which involves real-time control of DERs by a central entity when needed. The primary objective of this control strategy is to solve over-voltage issues caused by reverse power flow due to high PV penetration. Residential BES units and PV systems are the DERs being considered. Residential BES units are coupled with PV systems. In this study, we consider BES units that are connected to the grid via three-phase inverters. Moreover, it is considered that power in each phase can be independently controlled. Such BES units can be more supportive to the grid compared to single-phase units or three-phase units with balanced power control.

In this distributed control scheme, the active power set points of the BES units are decided by the HEMS. The algorithm used to compute the active power set points of the BES units is the same as the method described in Sec. 3.3 in Chapter 3. The main purpose of coupling a BES unit with PV at the residential level may not be to support the grid but rather to fulfil the requirements of the BES owner. These requirements could be increasing the consumption of self-generated energy or increase economic benefits. These objectives are local to each residential energy system. Therefore, it important to let the HEMS decide the scheduling of the battery. The grid feed-in limitation over the critical period can easily be introduced in the BES scheduling algorithm. If there is a significant number of BES units in the system, over-voltage issues will be effectively mitigated. This is because the reverse power flow in the grid will be significantly reduced over the critical period due to charging of these BES units. However, when the number of BES units in the system is not sufficient, the over-voltage issue may not be completely solved. In that case, a secondary solution is needed.

In the following sections, we propose a secondary solution that is based on the real-time control of active and reactive power set points of the DERs. Here we assume the existence of a central controller which can monitor the power quality of the network, and also can monitor and control the DERs. This real-time solution is activated when locally decided set points are not sufficient to solve the over-voltage problem completely. Active power adjustments among the phases of the three-phase converters of the BES units and the reactive power support from the converters are the solutions used by the central controller for solving the over-voltage problem.

4.3.1 Centralized control of distributed energy resources

The central controller monitors the quality of the supply voltage in real-time by means of monitoring the voltages at critical nodes in the distribution network. The central control algorithm is triggered whenever the voltage of any critical node violates the statutory limits (event based triggering). When the central controller

is triggered, it obtains the following information from the network: three phase voltage measurements at the critical nodes, the current active power set point of the BES units and the scheduled active power set points at the next time step, and the current P, Q set points of the PV inverters. Having received this information, the central controller computes the new set points of the BES converters and the PV inverters. These new set points are able to maintain the three phase voltages at the critical nodes within the statutory limits and improve the voltage unbalance among the phases. The central controller then transmits these set points to corresponding PV inverters and HEMSs.

4.3.1.1 Active power adjustment of BES systems

In this study, as we mentioned earlier, we consider BES units connected to the grid via three phase converters. The residential energy system is AC-coupled. In their normal operation, i.e. without receiving any command from the central controller, the BES units share the charging power equally among the three phases. Whenever the central controller is triggered, it first tries to adjust the power among the three phases of each BES converter. Power adjustment among the three phases improves the voltage unbalance of unbalanced distribution grids. Because of the improvement of voltage unbalance, the amount of reactive power needed from the converters for solving the over-voltage issue is reduced. In some cases, the over-voltage issue may be solved without any reactive power support as well.

The central controller computes the new set points of the BES converters by solving an optimization problem. The objective of the optimization problem is to minimize the difference between the three phase voltage magnitudes at each critical node.

$$min \sum_{j=1}^{n_{critical}} \left((V_{a,j} - V_{b,j})^2 + (V_{b,j} - V_{c,j})^2 + (V_{c,j} - V_{a,j})^2 \right), \tag{4.2}$$

where $V_{a,j}, V_{b,j}, V_{c,j}$ are the expected voltage magnitudes in phases-a, b, c at the j^{th} critical node. $n_{critical}$ is the number of critical nodes in the network.

The central controller attempts to adjust the active power set points of the three phases of each BES converter without changing the three phase sum. The three phase power is kept at the set point decided by the optimization module in the HEMS. This introduces the constraint

$$P_{bat,i} = \eta_{batC,i}(P_{a,i} + P_{b,i} + P_{c,i}) \tag{4.3}$$

where $P_{bat,i}$ is the scheduled active power set point of the i^{th} BES unit and $\eta_{batC,i}$ is the efficiency of the i^{th} BES converter.

The capacity constraint of the converters

$$\begin{aligned} -P_{batC,rated} \leq P_{a,i} \leq P_{batC,rated} \\ -P_{batC,rated} \leq P_{b,i} \leq P_{batC,rated} \\ -P_{batC,rated} \leq P_{c,i} \leq P_{batC,rated} \end{aligned} \tag{4.4}$$

where $P_{batC,rated}$ is the per-phase rated capacity of the battery converter.

As mentioned earlier, in certain cases improvement of voltage unbalance may solve the over-voltage problem as well. For example, at the time the central controller is triggered, the voltage of only one phase has reached the limit while the voltages of the other phases have not. Therefore, the following voltage constraint is added in the optimization problem. With this constraint, we seek a solution to the optimization problem, which minimizes the difference between the three phase voltage amplitudes while solving the over-voltage issues. However, a solution may be feasible only for certain cases. Therefore, relaxation of this voltage constraint is needed whenever the solution is not feasible.

$$\begin{aligned} V_{min} \leq V_{a,j} \leq V_{max} \\ V_{min} \leq V_{b,j} \leq V_{max} \\ V_{min} \leq V_{c,j} \leq V_{max} \end{aligned} \tag{4.5}$$

where V_{min} and V_{max} are the minimum and maximum limits of the acceptable voltage range.

Using the voltage sensitivity coefficients we can calculate the expected change in voltages at the critical nodes for change in active and reactive power at the buses where the DERs are connected. The expected voltage change in phase-a at j^{th} critical node is

$$\begin{aligned} \Delta V_{a,j} = \sum_k \frac{\partial V_{a,j}}{\partial P_{a,k}} \Delta P_{a,k} + \sum_k \frac{\partial V_{a,j}}{\partial P_{b,k}} \Delta P_{b,k} + \sum_k \frac{\partial V_{a,j}}{\partial P_{c,k}} \Delta P_{c,k} \\ + \sum_k \frac{\partial V_{a,j}}{\partial Q_{a,k}} \Delta Q_{a,k} + \sum_k \frac{\partial V_{a,j}}{\partial Q_{b,k}} \Delta Q_{b,k} + \sum_k \frac{\partial V_{a,j}}{\partial Q_{c,k}} \Delta Q_{c,k} \end{aligned} \tag{4.6}$$

where

$$\Delta V_{a,j} = V_{a,j} - V_{a,j}^{msrd}, \tag{4.7}$$

and the active and reactive power changes at the k^{th} bus are

$$\begin{aligned} \Delta P_{a,k} = P_{a,k} - P_{a,k}^{msrd} \\ \Delta Q_{a,k} = Q_{a,k} - Q_{a,k}^{msrd} \end{aligned} \tag{4.8}$$

$V_{a,j}^{msrd}, P_{a,k}^{msrd}, Q_{a,k}^{msrd}$ are the measured values of the corresponding variables and $Q_{a,k}$ is the new reactive power set point of the k^{th} converter connected to phase-a. Similar equations hold for phases b and c as well. At this step, the new reactive power set points of the converters are set to zero, i.e.

$$\begin{aligned} Q_{a,k} = 0 \quad \text{for all } k \\ \Rightarrow \Delta Q_{a,k} = -Q_{a,k}^{msrd} \end{aligned} \tag{4.9}$$

This is done because, if possible, it is required to solve the over-voltage problem without any reactive power support. If the optimization problem is feasible without

relaxation of the voltage constraints, then the over-voltage problem can be solved without any reactive power support from the converters. If it is not possible, V_{max} is increased gradually until the optimization solver is able to find a solution to the problem.

The optimization problem is non-linear because the objective function is quadratic. This can be solved with any non-linear solver. We used Matlab non-linear solver "*fmincon*" to solve the problem. By solving the optimization problem, the new ac-side active power set points of the converters can be found. The central controller then calculates the power sharing ratio among the phases of each converter.

$$\text{power sharing ratio} = P_{a,i} : P_{b,i} : P_{c,i} \tag{4.10}$$

Instead of the calculated ac-side set points, the central controller sends the power sharing ratios among the three phases to the local controllers of the BES units. This is because the actual BES set points can be different from the scheduled set points due to the adjustments for short-term fluctuations. The local controller then shares the instantaneous battery power set point according to this ratio.

Once the new active power set points of the converters are found, the expected voltages at the critical nodes $(V_{a,j}, V_{b,j}, V_{c,j})$ after P adjustments of the BES units can be calculated using the Eqs.4.6-4.8.

4.3.1.2 Reactive power control of converters

If the expected critical nodes' voltages calculated from the previous step are outside the statutory limits, the reactive support from the converters is needed to solve the over-voltage problem completely. Reactive power support from the converters can solve the over-voltage problem, however the reactive power demand of the distribution grid will increase due to reactive power support from the converters. Consequently, the losses in the network will also increase. Therefore, we need to minimize the reactive power support required from the converters. The optimal reactive power set points of the converters, which results in minimum total reactive power are found by solving an optimization problem with the objective function

$$min\left(\sum_{k} Q_{a,k}^2 + \sum_{k} Q_{b,k}^2 + \sum_{k} Q_{c,k}^2\right) \tag{4.11}$$

With the reactive power support from the converters, the critical nodes' voltages should be maintained within the limits.

$$\begin{aligned} V_{min} \leq V'_{a,j} \leq V_{max} \\ V_{min} \leq V'_{b,j} \leq V_{max} \\ V_{min} \leq V'_{c,j} \leq V_{max} \end{aligned} \tag{4.12}$$

where $V'_{a,j}, V'_{b,j}, V'_{c,j}$ are the expected voltages in phases-a, b and c at the j^{th} critical node with P adjustments and Q support from the converters.

The voltage change at critical nodes due to Q support from the converters can be estimated using the voltage sensitivities w.r.t. reactive power.

$$\Delta V_{a,j} = \sum_k \frac{\partial V_{a,j}}{\partial Q_{a,k}} \Delta Q_{a,k} + \sum_k \frac{\partial V_{a,j}}{\partial Q_{b,k}} \Delta Q_{b,k} + \sum_k \frac{\partial V_{a,j}}{\partial Q_{c,k}} \Delta Q_{c,k} \tag{4.13}$$

where

$$\Delta V_{a,j} = V'_{a,j} - V_{a,j}, \tag{4.14}$$

$$\Delta Q_{a,k} = Q_{a,k} \tag{4.15}$$

The power factors of the converters may be constrained.

$$pf_{a,k} \geq pf_{k,min} \tag{4.16}$$

where $pf_{a,k}$ is the k^{th} converter's power factor in phase-a and $pf_{k,min}$ is the minimum allowable power factor. The same power factor is maintained in each phases of the three phase PV inverters.

$$pf_{a,k} = pf_{b,k} = pf_{c,k} \tag{4.17}$$

The reactive power support from the converters regulates the voltage amplitudes, but also affects the voltage angles. From the above optimization, we seek a solution with the objective of minimizing the total reactive power involved in the system. However, when the voltage magnitudes of the critical nodes are significantly unbalanced, the optimum solution would be unequal reactive power support from the three phases (the sum of the reactive power support provided by the converters connected to each phase will be different). This happens when there is a significant number of DERs connected to the grid via single-phase converters. Even though this corrects the voltage amplitudes, it can worsen the voltage unbalance due to the unequal effects on the voltage angles in the three phases. In step 1, the central controller attempts to minimize the voltage unbalance via adjusting active power among the phases. However, in case that attempt is not successful, it is important not to worsen the voltage unbalance. Therefore, we set a maximum limit for the difference of the total reactive power support between the phases. Total reactive power refers to the sum of the reactive power support provided by the converters in each phase.

$$|\%\Delta Q_{total,ab}| < \varepsilon \ , \quad |\%\Delta Q_{total,bc}| < \varepsilon \ , \quad |\%\Delta Q_{total,ca}| < \varepsilon \tag{4.18}$$

where

$$\begin{aligned} \%\Delta Q_{total,ab} &= \frac{Q_{total,a} - Q_{total,b}}{Q_{total,avg}} \times 100 \\ \%\Delta Q_{total,bc} &= \frac{Q_{total,b} - Q_{total,c}}{Q_{total,avg}} \times 100 \\ \%\Delta Q_{total,ca} &= \frac{Q_{total,c} - Q_{total,a}}{Q_{total,avg}} \times 100 \end{aligned} \tag{4.19}$$

$$Q_{total,avg} = \frac{Q_{total,a} + Q_{total,b} + Q_{total,c}}{3} \tag{4.20}$$

$$\begin{aligned} Q_{total,a} &= \sum_k Q_{a,k} \\ Q_{total,b} &= \sum_k Q_{b,k} \\ Q_{total,c} &= \sum_k Q_{c,k} \end{aligned} \tag{4.21}$$

When the distribution grid supplies several long laterals, constraints given by Eq. 4.18 are applied to each lateral individually. Consequently, the reactive power unbalance among the phases due to reactive power support from the converters can be maintained within the required limit in each long lateral.

The above optimization problem is also non-linear, therefore it was solved using Matlab non-linear solver "*fmincon*". By solving the optimization problem, the reactive power set points of the converters can be found. The corresponding power factor of the converter then can be calculated based on the new active power set points calculated from the previous step. If the active power set points of the converter are not modified by the central controller, for example in PV inverters, the power factor can be calculated based on the measured active power output of the PV inverter. The calculated active power sharing ratios and the power factor set points are then sent to the respective local controllers of the DERs.

4.3.1.3 The functions of the central controller

The main characteristics and the functions of the central controller can be summarized as follows.

- The central controller is triggered by an over-voltage event.
- In addition to event-based triggering, the central controller is also triggered by an internal signal. If the central controller has not been triggered over the last $\Delta t_{trigger}$ time interval, it is triggered by an internal signal. This is because one of the objectives of the central controller is to minimize the reactive power utilized for solving the over-voltage issues. The load and the PV generation changes with the time. In order to find the optimal active and reactive power set points with respect to the changes in the operating point, time-based triggering is also included. Otherwise, the converters will continue to operate at the last power factor set points received by the central converter, even though the voltages are within the acceptable limits. Here we define a voltage dead-band, $V_{db,min} - V_{db,max}$. The central controller is triggered either by an over-voltage event or an internal signal only when the critical node voltages are outside this band.
- Real-time monitoring of the critical nodes' voltages.

- Calculate the voltage sensitivities at discrete time intervals.
- Find the optimal active power adjustments in each phases of the BES converters. The new set point of the converter should not change the scheduled set points of the BES.
- Find the reactive power support required from the converters for solving over-voltage issues.

4.3.1.4 The functions of the local DER controllers

The main functionalities of the DER's local controller are as follows.

PV system

- Send necessary information to the central controller whenever the PV inverter receives a request from the central controller. The information that needs to be sent includes: i) the active power output of the PV inverter (in each phase if the PV inverter is three phase), and ii) the power factor of the inverter. The controller should send the moving averages of these variables instead of instantaneous measurements, because there can be short-term fluctuation of these variables.
- Continue to operate at the last power factor set point received by the central controller until it receives a new power factor set point.
- Locally adjusts the power factor of the inverter, if the kVA rating of the inverter is exceeded because of the changes in the active power output over time.

BES system

- Find the optimal charging/discharging schedule of the BES over a specific planning horizon.
- Correct the instantaneous BES set points in response to the short-term fluctuations of the load and the PV generation.
- Send necessary information to the central controller whenever the local controller receives a request from the central controller. The information that needs to be sent includes: i) current ac-side active power set points of the BES converter (in each phase), ii) scheduled active power set points at the next time step, and iii) power factor of the BES converter.
- Share the instantaneous active power set point among the phases according to the last sharing ratio received by the central controller. Resetting the

sharing ratio once in a while is also required. This is because it may not be necessary to operate at the ratio received by the central controller all the time, for example when the critical node voltages are within the dead band. Since the central controller is not triggered when the voltages are within the dead band, the sharing ratio can be reset locally. The condition for resetting the sharing ratio was set to, $P_{bat} = 0$. That means whenever the scheduled BES set point is zero, the power sharing ratio is reset to default. The default ratio is 1/3.

- Make necessary adjustment of the sharing ratio and the power factor to ensure the per phase apparent power does not exceed the per phase kVA rating of the converter when the BES set point changes.

4.4 Case Study

A simulation study was performed to evaluate the performance of the distributed control scheme. The control scheme was implemented in Matlab and applied to the modified IEEE low voltage test feeder shown in Fig. 4.1. The network was modelled in openDSS. The IEEE low voltage test feeder supplies 56 customers located in the nodes indicated in Fig. 4.1. The loads were modelled as constant PQ loads and represented by the load profiles obtained from an Italian distribution grid located in the city of Brescia. The load data were available with 1 minute time resolution. 56 customers were represented by 56 distinct load profiles. Both single-phase and three-phase customers were considered. The power factor of the load was set to 0.99. Out of the 56 customers, 40 were considered to have roof-top photovoltaic systems. The locations of the customers having PV systems are shown in Fig. 4.1. The rated capacity of each PV system is 4.0 kW. Both single-phase and three-phase PV systems were considered. Measurements recorded from residential PV systems connected to an Italian low voltage network located in the city Brescia were used as the basis of the PV generation profiles. The PV generation data were available with a 1-minute time resolution. Hourly averages of the load and PV generation were derived from these load and PV data sets. These hourly averages were used as the forecasted load and the PV generation profiles in the optimization strategy. Out of the 40 PV system owners, 15 were considered to have lithium-ion based BES systems. The locations of the PV systems coupled with BES are indicted in Fig. 4.1. All the considered BES units are connected to the grid via three-phase bi-directional converters. The nominal capacity of each BES unit is 10 kWh/208 Ah. All the BES units are constrained to operate within the SoC range of 20%-95%. The rated capacity of the three-phase BES converter is 4.5 kW. The rest of the parameters of the residential BES system are the same as those in the case study presented in Chapter 3. The same electricity tariff as in Fig. 3.11 was considered with battery degradation cost of 0.2 \$/kWh. The limit of the unbalance among the sum of reactive power support provided by the inverters in each phase (ε) was set to 10%. The minimum allowed power factor of the converters was set to 0.9. The secondary side manual tap setting of the distribution transformer

was set to 1.04375 pu for preventing under-voltage problems. The time setting of the internal triggering of the central controller was set to $\Delta t_{trigger}$= 30 min with voltage deadband of 0.95 pu-1.05 pu.

It is assumed that the forecasting module in the HEMS is able to predict 24 hours ahead, hourly averages of the load and the PV generation. Two nodes, N.1 and N.2 indicated in Fig. 4.1, were identified as the critical nodes from the off-line load flow. The period from 08:00-14:00h was identified as the critical period. As in the case study presented in Section 3.5, the BES units in the system were divided into two groups, where each group consisted of about half of the BES units. The grouping of the BES units was done in the same way as in the case study in Section 3.5. The grid feed-in limit is active from 0800h-1300h for the residential energy systems within the group-1, while for the other group the grid feed-in limit is active from 0900-1400h.

In this study, we have considered that only PV inverters are supposed to provide reactive power support to the grid when requested. It is possible to provide reactive power support from the battery converter as well. In that case, the residential energy systems that have both PV and BES units will provide more reactive power support to the grid compared to the customers with only PV systems. Therefore, we assumed that it is not compulsory to provide reactive power support from the both converters.

4.5 Simulation Results

We have performed simulations for two different cases: (1) Clear sky day, (2) Cloudy day. In the clear sky day case, the power production profile of the PV system varies smoothly as shown in Fig. 3.4 on page 48. Hence, there is no significant fluctuations of the reverse power flow in the distribution grid and the voltage profile. In the cloudy day case, the power outputs from the PV systems fluctuate due to shadowing caused by moving clouds. Therefore, significant fluctuations of the power flow in the distribution grid and voltage fluctuations can be observed.

4.5.1 Clear sky day

The simulation was run for a 24-hour period with time steps of 1 minute. Fig. 4.5a shows the voltage profiles of the two critical nodes when there are no BES units in the system and no reactive power support is provided by the converters. As can be seen from the figure, the voltages in phase-a at node-N.1 exceed the upper limit during the period around 0900h-1300h, while the voltages in phases-a and c at node-N.2 exceed the upper limit during the period around 0900h-1400h. Moreover, the voltage amplitudes are relatively unbalanced even though the VURs are below the maximum limit of 2%. The nature of voltage unbalance at the two nodes is also different. At node-N.1, the voltage in phase-a is the highest among the three phases, while at node-N.2 voltage in phase-c is the highest. In order to illustrate the benefit of power adjustment among the phases of the three-phase converters when the voltage amplitudes are unbalanced, we have simulated two scenarios: (i) the central controller does not modify the active power set points of the BES converters, but modifies the reactive power set points of the DERs, (ii) the central controller modifies both active and reactive power set points.

Fig. 4.6 and Fig. 4.7 show the voltage profiles and the VURs of two critical nodes for scenario (i) and (ii), respectively. In both scenarios, the grid supportive charging strategy along with the real-time centralized control of active and/or reactive power control method is able to maintain the three phase voltage profiles within the statutory limits. Fig. 4.8 compares the active and reactive power flow through the transformer for the base case and the two simulated scenarios. We can see an increase in reactive power flow through the transformer around the time 1120h-1300h for scenario (ii). This is because, at this time the PV inverters provide reactive power support to the grid to maintain the voltage profile within the statutory limits. Charging set points calculated by the local HEMSs are sufficient to maintain the voltage profile within the limits during rest of the time. From Fig. 4.6a we can see that the voltage profile of phase-c in node-N.2 hits the upper limit at about 1120h. Consequently, the central controller is triggered and calculates the required operating power factor of the PV inverters by solving the optimization problem detailed in Section 4.3.1.2. Those power factor set points are then sent to the corresponding PV inverters. Once the PV inverters start to operate at the power factor received by the central controller, the voltage of phase-c drops below the up-

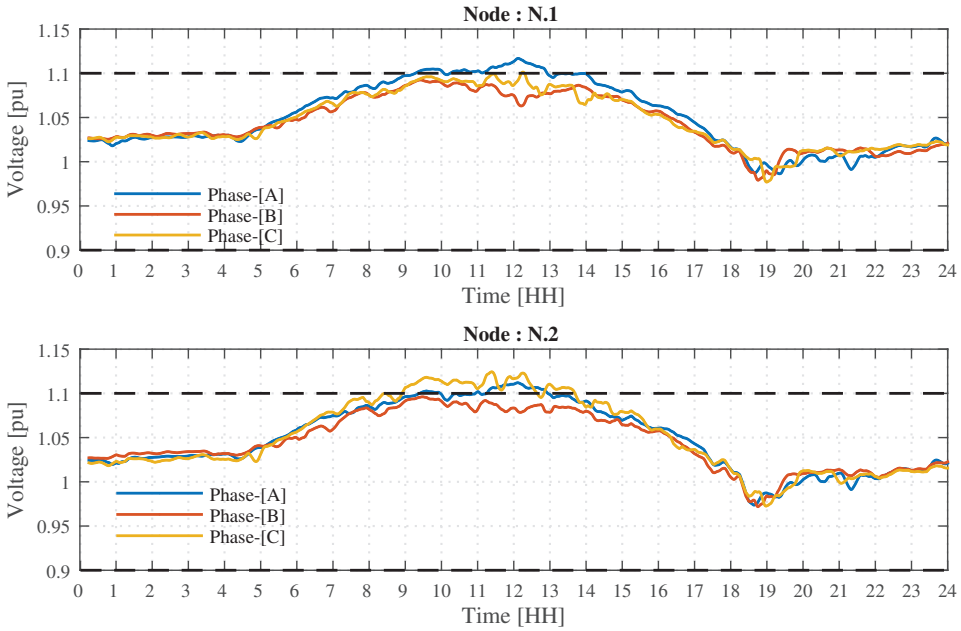

(a) Supply voltage variations.

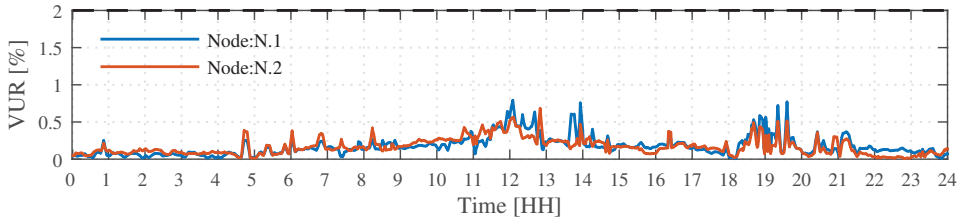

(b) Voltage unbalance rates.

Figure 4.5: Quality of the voltage at the critical nodes when there are no BES units in the system and reactive power support from the converters is not available (Base case).

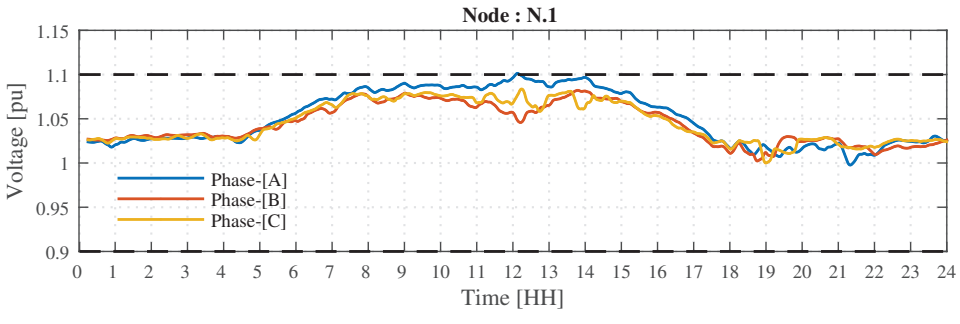

(a) Supply voltage variations.

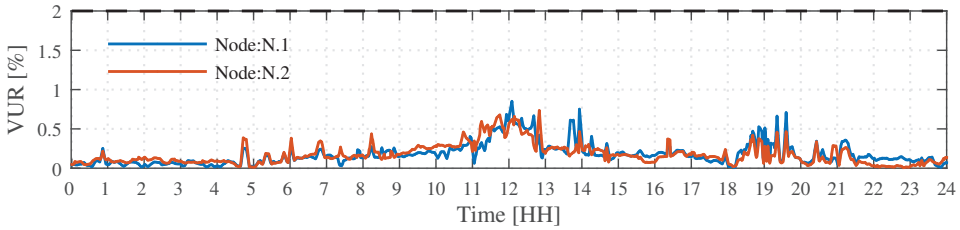

(b) Voltage unbalance rates.

Figure 4.6: Quality of the voltage at the critical nodes with proposed control scheme of DERs without active power set point adjustment among the three phases of the BES converters.

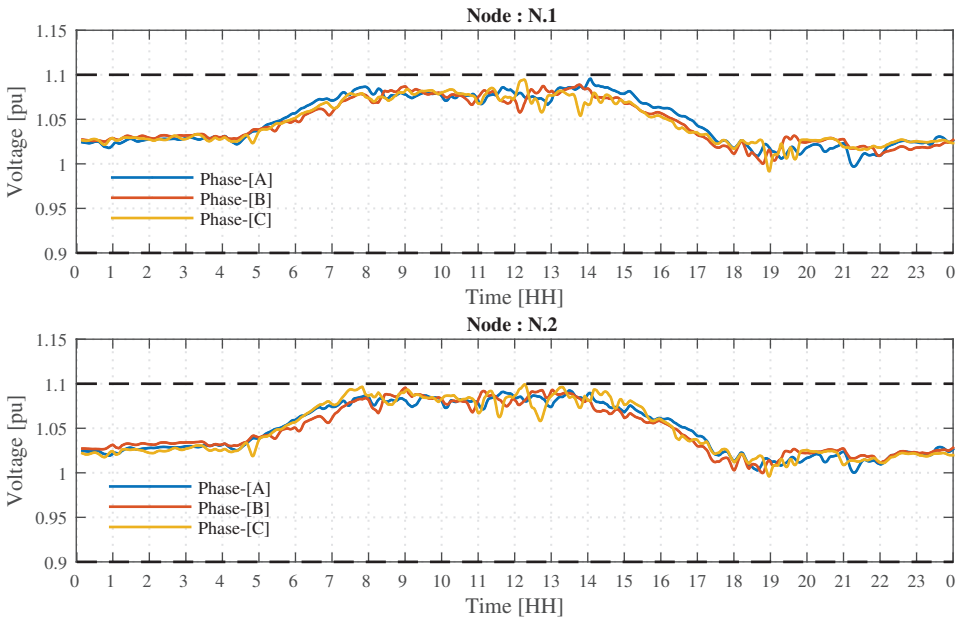

(a) Supply voltage variations.

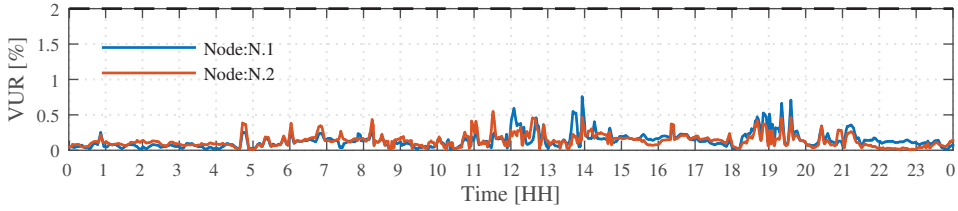

(b) Voltage unbalance rates.

Figure 4.7: Quality of the voltage at the critical nodes with proposed control scheme of DERs with active power set point adjustment among the three phases of the BES converters.

per limit. The PV inverters continue to operate at this power factor for 30 minutes. Within this 30 minutes no voltage violation is detected, therefore the central controller is not triggered. Since the central controller has not been triggered over the last 30 minutes and the critical node voltages are outside the voltage dead-band of 0.95pu-1.05pu, the central controller is triggered by an internal signal. At this time, the central controller finds that reactive power support from the converters is no longer needed for maintaining the voltage profiles at the critical nodes within the limits. Therefore, it sets the power factor of the converters to 1. Consequently, the reactive power flow through the transformer drops. However, in about 10 minutes, the voltage in phase-a at node-N.1 hits the upper limit. Therefore, the central controller is activated again and the power factors of the converters are adjusted. In this scenario, we can observe that a significant amount of reactive power support is needed for maintaining the voltage profiles within the acceptable limits. This is because of the high R/X ratio of the studied distribution grid.

There is no significant difference in the reactive power flow trough the transformer between the base case and scenario (ii). That means in scenario (ii) no reactive power support is required to maintain the critical node voltage profiles within the statutory range. In this case, the active power adjustment among the phases is sufficient to maintain the voltage profile below the upper limit. As can be seen from Fig. 4.7, the voltage unbalance has improved compared to the base case and scenario (i). Consequently, the voltages of all three phases at both critical nodes have also dropped below the upper limit. As a result, no reactive support from the converters are needed. From these results, we can see that power balancing among the phases can not only improve the voltage unbalance, but also reduces the need of reactive power support for voltage regulation. This is an effective solution for distribution grids that are usually unbalanced. When the grid is balanced, the central controller will only control the reactive power set points of the converters to maintain the voltage profile within the acceptable limits.

Fig. 4.9 shows the sum of the active power transferred to/from the BES units in each phase for two scenarios. In scenario (i), each BES converter shares the charging/discharging power equally among the phases, therefore the total power transferred to/from the BES units in the system via three phases are equal. However, in scenario (ii), as the BES units start charging at 0800h, the central controller adjusts the active power among the phases without changing the three phase sum of each BES unit. At this time, the three phase voltages at both critical nodes are below the upper limit, however they are outside the voltage dead-band (0.95pu-1.05pu). Therefore, the central controller is triggered by an internal signal. The condition for resetting the power sharing ratio to default was set to $P_{bat,i} = 0$, hence the power sharing ratios of each BES units have been reset to 1/3 before the BES units start discharging. Consequently, during discharging, power is shared equally among the phases.

The highest demand in the network is observed in the period from 1800h-2000h. During this period, the utility electricity price is relatively high (Fig. 3.11). From the simulation results, it was observed that the local loads are fully supplied by

the BES units during this high tariff period. During this period, power is drawn from the grid only when the load exceeds the rated capacity of the BES converter. In this case, because of the time-of-use tariff scheme, the evening peak demand on the transformer has decreased from about 105 kW to 75 kW (three phase load).

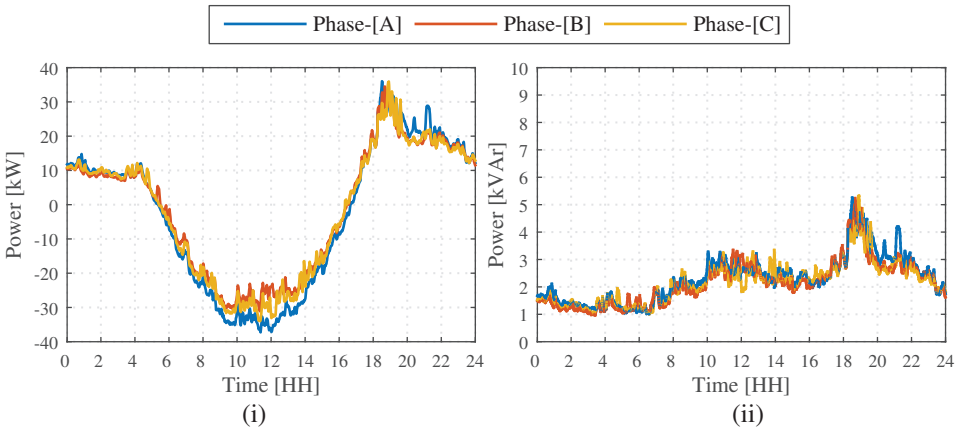

(a) Base case.

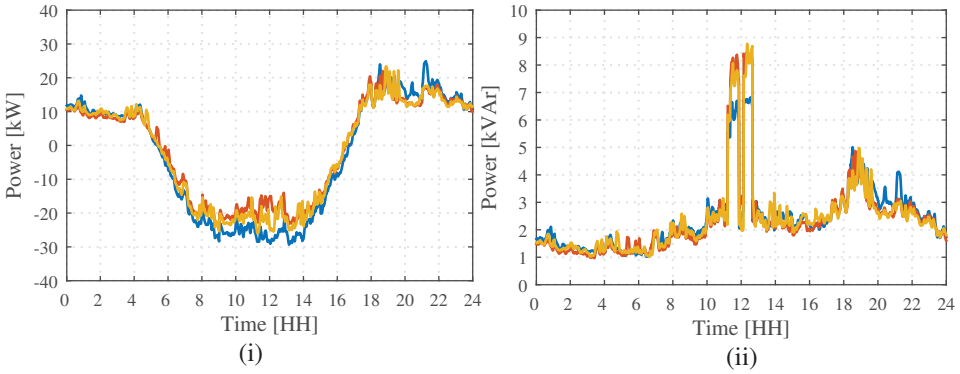

(b) With proposed control scheme of DERs without active power set point adjustment among the three phases of BES converters.

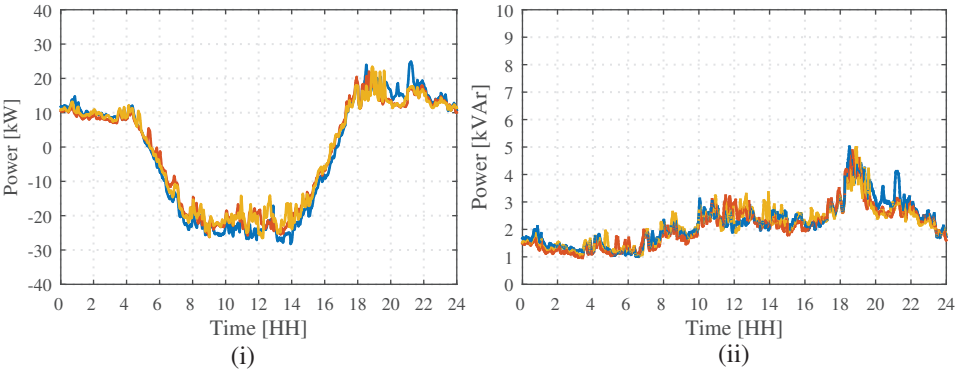

(c) With proposed control scheme of DERs with active power set point adjustment among the three phases of BES converters.

Figure 4.8: The load on the distribution transformer, (i) Active power (ii) Reactive power.

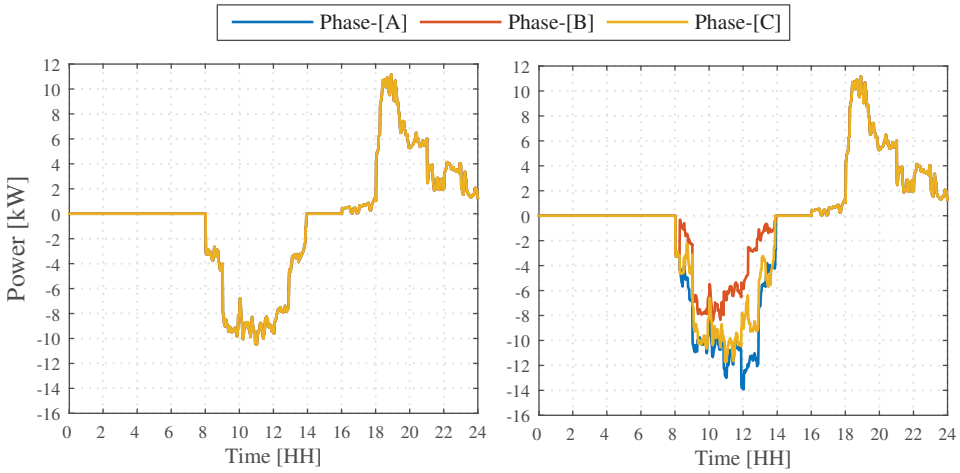

(a) (b)

Figure 4.9: Total sum of active power supplied to/from the BES units via three phases, (a) without active power set point adjustment among the three phases (b) with active power set point adjustment among the three phases.

4.5.2 Cloudy day

The PV production of two exemplary households on a cloudy day along with the load, battery power, and the power supplied by/to the grid are shown in Fig. 4.10. As can be observed, there are sudden fluctuations of the PV system's power output on this day. The power flow through the distribution transformer and the voltage profiles of the two critical nodes on this day when there are no BES units in the system are shown in Fig. 4.11a and Fig. 4.12a respectively. As can be observed from the figure, in addition to over-voltage issues, there are significant fluctuations of the voltages due to power fluctuations in the distribution grid. The voltage profiles of the two critical nodes with the proposed control strategy are shown in Fig. 4.12b. The over-voltage problem has been effectively mitigated with the proposed DER control strategy. From these results, it is shown that the proposed control algorithm works effectively in days with significant voltage fluctuations due to fluctuations of power production from PV systems.

From Fig. 4.11b, one can observe that the amplitudes of power fluctuations in the grid have reduced to some extent due to the charging of the BES units. Consequently, the amplitudes of voltage fluctuations have also relatively reduced when compared to the base case. In the local control algorithm of the BES units, $\tilde{P}_{grid}$ is kept at the set point decided by the optimization based scheduling algorithm. Consequently, during the time when the BES is charging and discharging, the fluctuations of both PV and load are compensated by the BES unit. Therefore, as shown in Fig. 4.10, there are no significant fluctuations of the power supplied to/by the grid when the BES unit is charging or discharging. As the main objective of the BES in this application is not to smooth out the power fluctuations at PCC, there is no improvement of power fluctuations at PCC during the time when the BES is idle.

From the DSO's perspective, the primary concern has been to force charging of BES units to the critical period. From the customer's perspective, besides maximizing the economic benefits, prolong battery lifetime is also of primary concern. Therefore, the HEMS prevents BES from performing short charging/discharging cycles. However, if the DSO imposes constraints on the power ramp rate at PCC, a power smoothing function also needs to be included in the HEMS. In that case, the battery will go through multiple short charging/discharging cycles over a day.

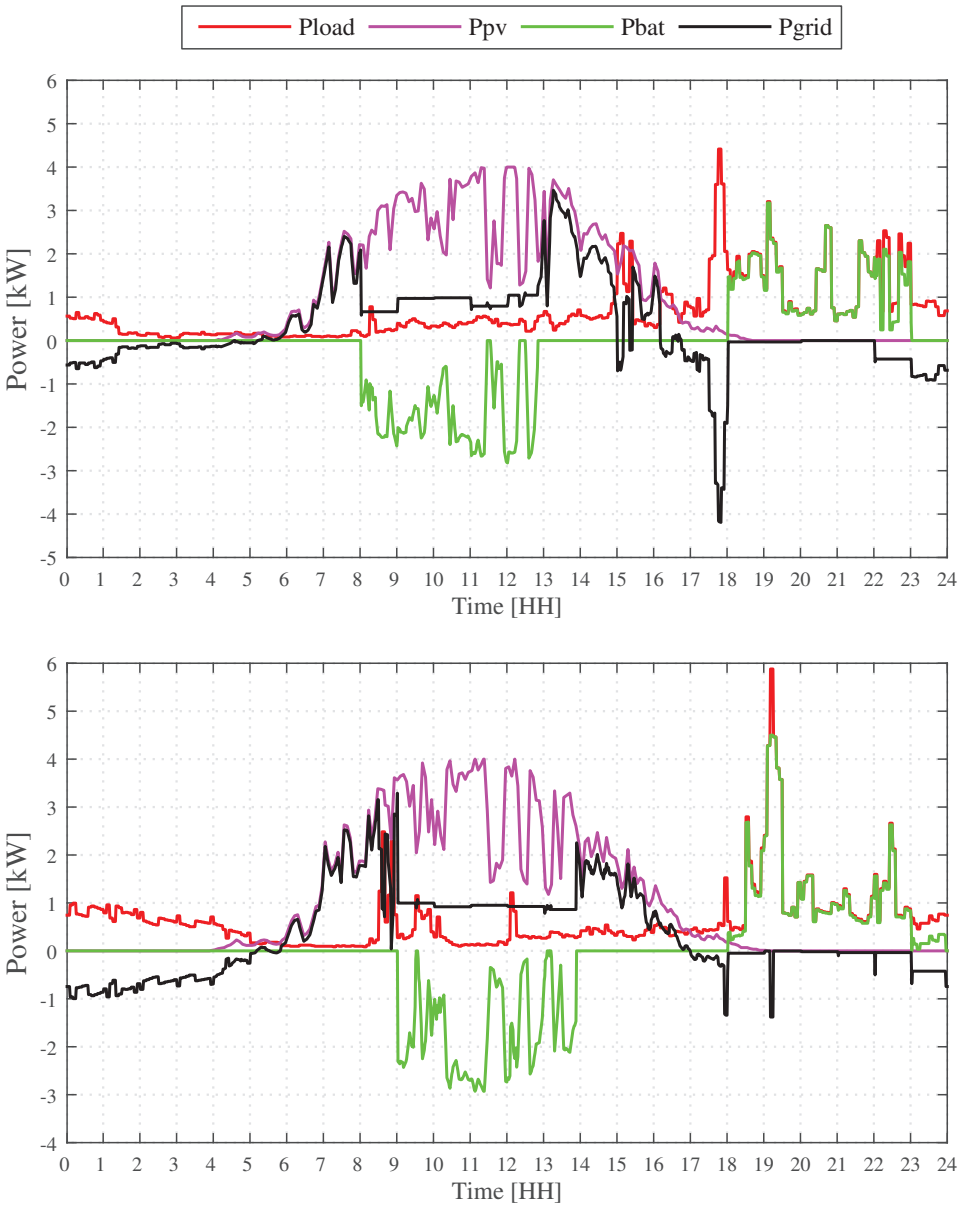

Figure 4.10: Load, PV production, battery power and the power supplied to/by the grid for two exemplary households. The PV production profiles correspond to a cloudy day.

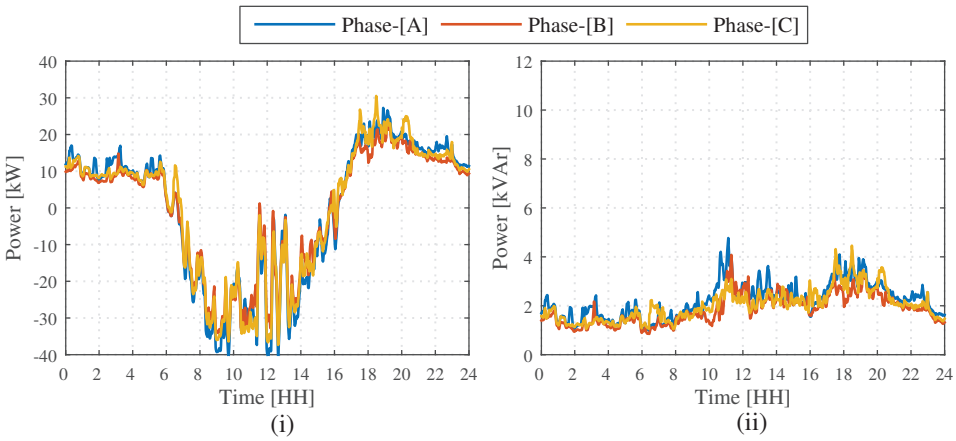

(a) Base case.

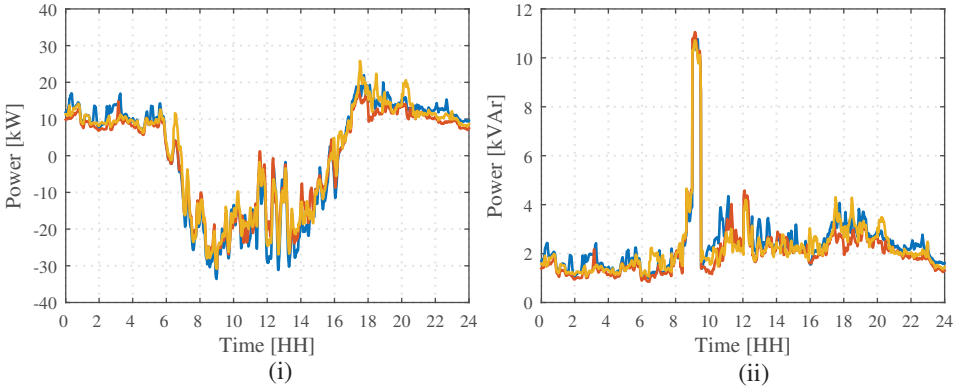

(b) With proposed control scheme of DERs with active power set point adjustment among the three phases of BES converters.

Figure 4.11: The load on the distribution transformer, (i) Active power (ii) Reactive power.

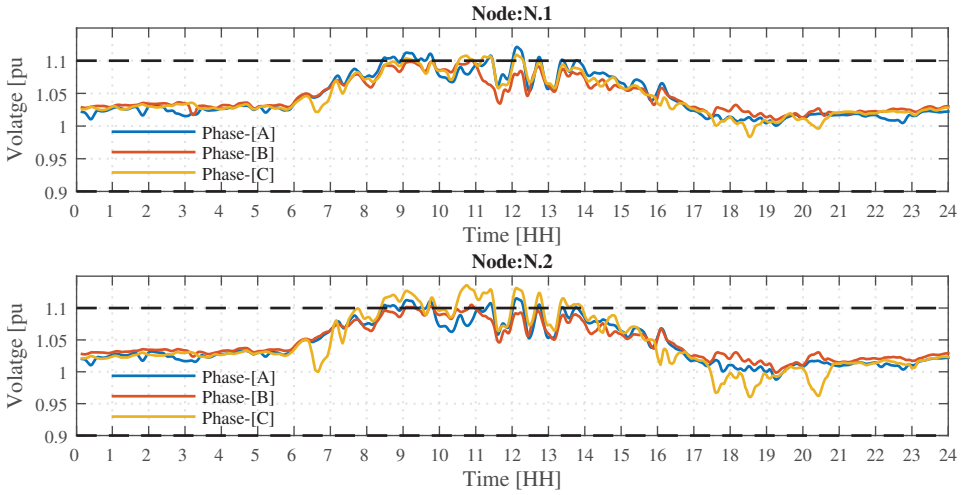

(a) Base Case.

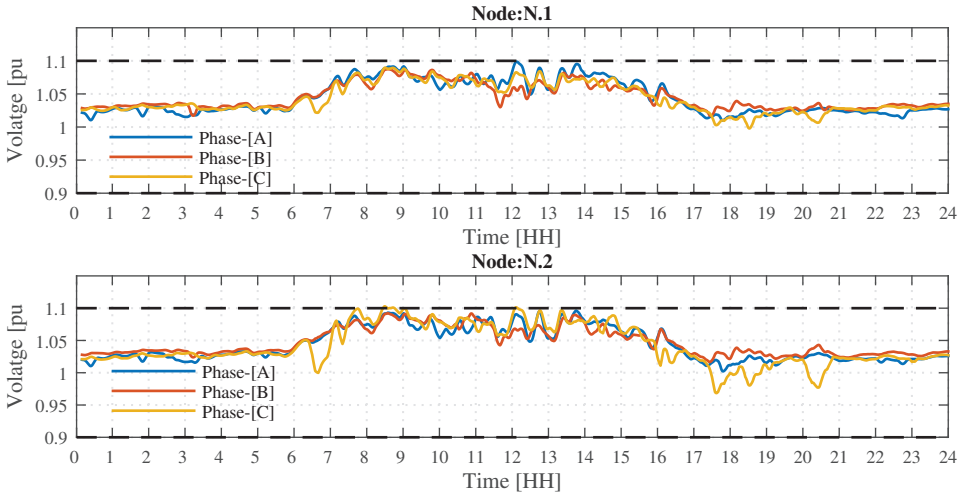

(b) With proposed control scheme of DERs with active power set point adjustment among the three phases of BES converters.

Figure 4.12: Supply voltage variations at the critical nodes.

Chapter 5

Performance Comparison of Proposed Control Strategies

This chapter compares the performance of the two proposed control strategies presented in the earlier chapters. The effects of the control strategies on the customer's electricity bill, the self-consumption rate, and the self-sufficiency rate are investigated. Also, the grid-side benefits such as the impact on the reactive power flow and the power losses are investigated. The chapter first describes the rule-based control strategy that is used as the base case for this comparison. Then, it presents the details of the evaluation criteria. Results from a simulation study are then presented followed by a discussion of the findings.

5.1 Introduction

In the previous two chapters, we have proposed two grid-supportive charging strategies for residential BES units. The first method presented is a local control strategy. In this method, the local controller determines the BES charging/ discharging set points by solving a finite time horizon optimization problem. The objective function of the optimization problem is locally decided according to the requirement of the BES owner. The BES units were forced to charge during a particular period by introducing a grid feed-in limit during this period. This period was called the critical period and it is defined by the DSO. The DSO can control the charging time of the residential BES units via this parameter. The DSO sends information about the critical period to the local controllers. This information can be updated at any time depending on the PV forecasts, if the DSO so wants to. The BES scheduling algorithm is based on receding horizon control, therefore the local controller runs an optimization problem every ΔT hour. The updated grid feed-in limit can therefore be included in the algorithm at any time of the

day. Other than this control input, there is no other involvement of the DSO in controlling the operation of the BES units.

In the second method, the charging/discharging set points of the BES units are decided by the local controller in the same way. But, in order to optimize the operation of the overall distribution grid, the DSO may adjust these set points. In this case, a central controller computes the necessary adjustment at each BES unit to achieve the desired objective, i.e. solving over-voltage issues. Although, here it is called "the central controller", when considering the whole distribution grid including the MV section, this controller is simply a decentralized controller. It is responsible for monitoring and controlling only a small section of the distribution grid, for example an LV network supplied by a distribution transformer. The central controller adjusts the set points in real-time and therefore needs the necessary ICT infrastructure to enable bi-directional information transfer between the central controller and the local controllers.

The number of BES units in the network may be limited. In that case, the support provided by the BES units may not be sufficient to solve the over-voltage issues completely. Therefore, we have also presented two reactive power control strategies, which work in coordination with the operation of the BES units. The local control method of BES relies little on the communication and the information about the rest of the network. Therefore, a reactive power support method, which does not need any information about the rest of the network or involvement of a central controller, is proposed to work in coordination with the local control method of the BES units. This method, however, relies on real-time communication. But, it only requires a one-way communication channel in which smart meters can broadcast a message to all corresponding converters. By contrast, in the second method, the reactive power set points of the converters are decided by a central controller. This method requires full information about the distribution grid, the BES units and the PV inverters. Also, it relies on bi-directional information transfer between the central controller and the DERs. The central controller updates the power sharing ratios among the three phases of the BES converters and the reactive power set points of the converters whenever it is triggered. The central controller can be triggered either by an event or an internal signal (time-based triggering).

The advantage of the second method over the first method is that the second method optimizes the operation of the overall network. This is because the central controller has information about the whole network and has access to the real-time information from the devices in the network. In the central control algorithm, the DSO could define the desired objective. In this case, the objective of the DSO is to solve the over-voltage issues with minimum reactive power support from the converters.

The two methods presented have two different control architectures and involve different levels of information. Therefore, it is worth comparing the benefits of these two methods. Moreover, it is important to see whether the DSO's involvement of scheduling the residential BES units adversely affects the local objective of the BES

owner. Therefore, this chapter compares 1) the impacts of DSO's involvement on the control of residential BES units on the BES owner's local objectives, 2) the benefits of incorporating residential BES units for solving over-voltage issues, and 3) the benefits of local versus centralized control methods.

5.2 Method

In the previous two chapters, we have made simulations for one or two days to validate the proposed control strategies. In this chapter, we extended the simulation period to about a month period to evaluate the benefits of these control strategies for the DSO, and to investigate the impacts of these grid-supportive operational strategies on the local objectives of the BES owner. In this chapter, we call the two methods presented in chapters 3 and 4, I) Local RHC with time-based power feed-in control, II) Distributed control, respectively. In addition to these methods, we also simulated a rule based control strategy. This strategy is primarily concerned with the local objectives, and does not intentionally contribute to over-voltage support.

Rule-based control

In rule-based control, a set of rules is defined to control the operation of the BES units. Here, the primary objective has been set to store the excess energy available from the PV system for later use. The stored energy is used for supplying the local load only. In this strategy, for each day, we define a time to start charging ($T_{chrg,start}$) and a time to start discharging ($T_{dischrg,start}$) the BES unit where $T_{chrg,start} < T_{dischrg,start}$. During the period from $T_{chrg,start}$ to $T_{dischrg,start}$, the BES is charged if there is excess power available from the PV system. Excess power refers to the remaining power from the PV system after supplying the local load. The charging continues until the BES reaches the maximum SoC level. The excess power that cannot be diverted to the BES is fed into the grid. The reasons for not being able to divert the excess power from the PV system to the BES are that the battery has either reached maximum SoC level or the excess power exceeds the power/current ratings of the BES and the converters. The stored energy is then used for supplying the evening load. The BES starts to discharge in the evening at $T_{dischrg,start}$ and continues supplying the local load until the BES reaches minimum SoC level. During the time when the BES is discharging, the power is drawn from the grid only when the load exceeds the power ratings of the BES converter. When the BES reaches the minimum SoC level, discharging of the BES is stopped. Charging of the BES starts again the next day at $T_{chrg,start}$.

The BES neither charges during the period from $T_{dischrg,start}$ to $T_{chrg,start}$ nor discharges in the period from $T_{chrg,start}$ to $T_{dischrg,start}$. In this way, we prevent the BES performing multiple short charging/discharging cycles within one planning horizon, which is normally 24 hours. Self-consumption may increase when the battery performs multiple short cycles during the day. However, this will shorten

the battery cycle life. Therefore, the number of cycles per planning horizon was constrained to one. This cycle could be a complete cycle or a partial cycle depending on the load and the PV generation. For example, the BES will perform one full cycle, if excess energy available from the PV system during the charging period and the load during the discharging period are larger than the usable capacity of the BES. If either the excess energy available during the charging period or the load during the discharging period is lower than the usable capacity of the BES, it will perform a partial cycle over a 24-hour planning horizon.

In this method, the charging period of the BES units are not constrained. Therefore, there is no coordination of the charging periods of the BES units in the system.

5.2.1 Reactive power support strategy

Reactive power support from the converters is utilized when the reduction of reverse power flow due to charging of BES units is not sufficient to maintain the voltage profile within the acceptable limits. Reactive power support strategies for local RHC with time-based power feed-in control and the distributed control strategies of BES units are presented in chapters 3 and 4, respectively. Rule-based control method is a local control method, which does not involve a central controller. Therefore, the reactive power support strategy from the converters presented in chapter 3 was implemented in coordination with the rule-based control method.

5.2.2 Evaluation criteria

The presence of customer-owned BES units in the distribution grid is beneficial for the DSO in many ways. In this thesis, we are particularly interested in the application of BES units for over-voltage support. The benefits of grid-supportive operational strategies for the DSO related to this application are:

- Ability to solve over-voltage issues without or with reduced reactive power support from the converters.
- Reduction in reactive power demand of distribution grids with high PV penetration.
- Reduction of distribution losses due to charging of BES units during high PV penetration hours and reduction of reactive power flow in the distribution grid.
- Prevent over-loading of distribution transformers both during high PV penetration hours and peak demand hours.
- Ability to increase the PV penetration capacity of distribution networks without upgrading the network.

In order to evaluate the benefits of the proposed grid-supportive operational strategies for the DSO, we simulated the three control strategies over a month period. For each control strategy, we calculated the losses in the distribution system and the reactive power demand of the converters.

The local characteristics of residential energy systems that are important for BES owners are:

- Electricity bill,
- Self-consumption rate,
- Self-sufficiency rate,
- Battery ageing.

We calculated the cost of the energy component in the electricity bill of each customer over the simulated period using the equations given in Section 3.3.2.1 in Chapter 3.

The self-consumption rate (SCR) is the share of the total generation that is consumed within the household. It is calculated using

$$\mathrm{SCR} = 1 - \frac{\int_{t_o}^{t_1} P^{+}_{grid}(t)\, dt}{\int_{t_o}^{t_1} P_{pv}(t)\, dt} \tag{5.1}$$

where

$$P^{+}_{grid}(t) = \begin{cases} P_{grid}(t), & \text{if } P_{grid}(t) > 0 \\ 0, & \text{otherwise} \end{cases}$$

The self-sufficiency rate (SSR) is the share of the energy demand that can be covered by the local production. It is calculated using

$$\mathrm{SSR} = 1 - \frac{\int_{t_o}^{t_1} P^{-}_{grid}(t)\, dt}{\int_{t_o}^{t_1} P_{load}(t)\, dt} \tag{5.2}$$

where

$$P^{-}_{grid}(t) = \begin{cases} -P_{grid}(t), & \text{if } P_{grid}(t) < 0 \\ 0, & \text{otherwise} \end{cases}$$

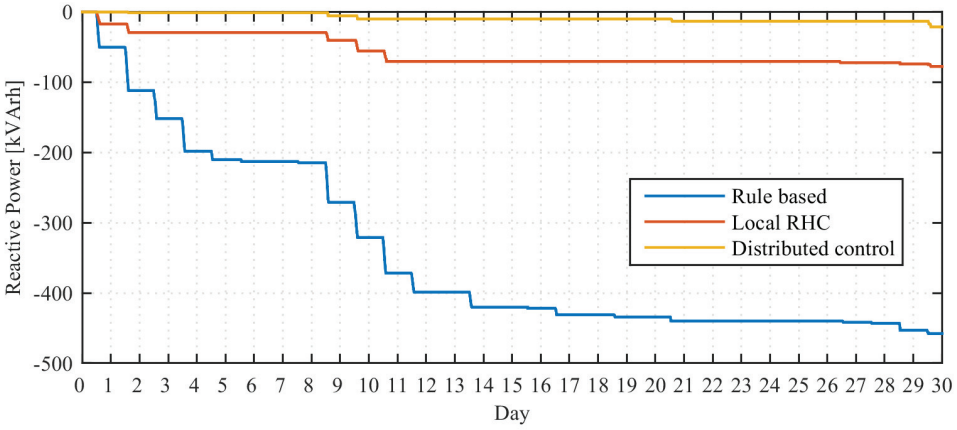

Figure 5.1: Cumulative sum of reactive power support provided by the converters over the month.

5.3 Simulation Results

The three control strategies were implemented in Matlab and applied to the modified IEEE low voltage test feeder shown in Fig. 4.1 on page 88. The number of customers supplied by this network is 56. Out of this 56, we assumed 40 customers are equipped with roof-top PV systems with a rated capacity of 4 kW. Out of these 40 PV systems, 15 PV systems were coupled with BES units. The nominal capacities of all the BES unit were 10 kWh/208 Ah. The BES units were connected to the grid via three phase converter with rated capacity of 4.5 kW. The operating window of the BES units were constrained to 20%-95% SoC. The loads were modelled as constant PQ loads and represented by the load profiles obtained from an Italian distribution grid located in the city of Brescia. Power production profiles of the PV systems were derived from the PV power measurements data obtained from the same network. The time resolution of both data sets was 1 minute. Hourly averages of the load and PV generation were derived from these load and PV data sets. These hourly averages were used as the forecasted load and the PV generation profiles in the optimization strategy. All other parameters and the conditions remains the same as in the case studies presented in Sections 3.5 and 4.4. In the rule-based charging strategy, the charging start time and the discharging start time were set to 0800h and 1700h, respectively.

Simulations were run over the period from 1st July to 30th July. This month was chosen because of high PV production. Fig. 5.1 shows a comparison of the cumulative sum of the total reactive power support provided by the converters over the month. As can be seen, the highest reactive power support is observed when the BES units are operated with the rule-based strategy. In this strategy, the charging operation of the BES units is uncoordinated and not subjected to any constraints. Starting from 0800h, the excess power available in the system is diverted to the BES

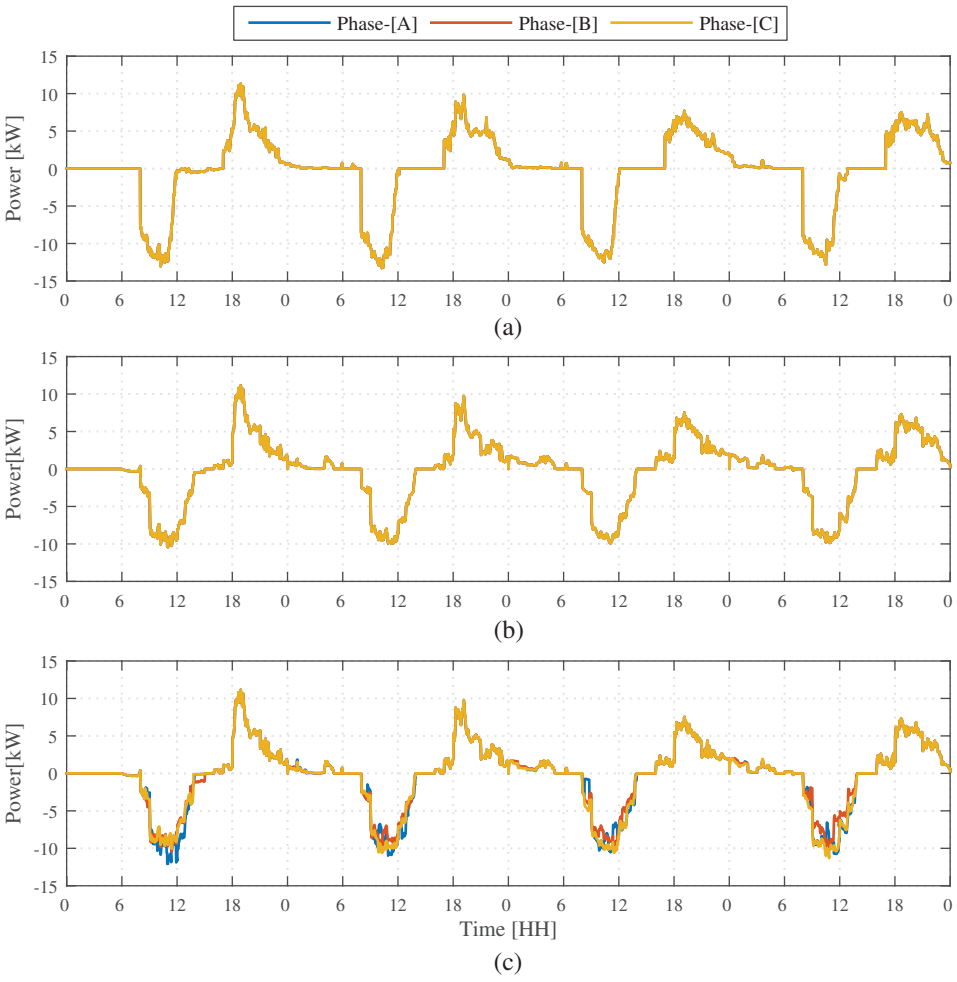

Figure 5.2: The aggregate sum of the power transferred to/by the BES units. Results are shown for the period from 1st July to 4th July. (a) Rule-based strategy, (b) Local RHC based strategy, and (c) Distributed control strategy.

unit. Therefore, the BES units reach maximum SoC limit before the critical period ends. Fig. 5.2 shows the aggregate sum of the power transferred to/by the BES units over four exemplary days. As can be seen, in rule-based strategy, charging of BES units starts at 0800h and stops around 1200h on all four days. Charging stops because by that time the BES units are fully charged. When the BES units are fully charged, they are no longer able to support the grid to lower the reverse power flow in the grid. Therefore, possible over voltage issues that may occur after the BES units are fully charged have to be solved using reactive power support from the converters. In the local RHC strategy, the RHC-based controller schedules the charging power of the BES unit, such that the BES does not reach maximum SoC level before the charging period defined by the DSO ends. As shown in Fig. 5.2(b), BES units maintain charging over the period from 0800h-1400h. Consequently, the reverse power flow in the grid over the whole critical period is reduced, therefore, the over-voltage problem is solved with reduced reactive power support. The distributed control method further reduces the reactive power support requirement. Table 5.1 lists the total reactive power support required over the simulated period. For the studied case, compared to the rule-based operational strategy, 83% and 95% reductions of reactive power requirement are achieved with the local RHC-based operational strategy and the distributed control strategy, respectively. The percentage reduction of reactive power requirement with the distributed control method when compared to the local RHC-based method is 73%. Compared to the rule-based method, a significant reduction of reactive power is achieved with the two proposed methods. The distribution control method gives the best results in terms of reduction in reactive power.

Table 5.1: Performance comparison of different control strategies.

Method	Required reactive power from the converters [kVArh]	Network power loss: daytime [kWh]	Network power loss: night-time [kWh]
Rule-based control	457	361	250
Local RHC with time-based power feed-in control	78	343	256
Distributed control	21	341	256

The total losses in the distribution system over the simulated period for various control strategies are listed in Table 5.1. We have stated the total losses during the daytime (0800h-1500h) and the night-time (1500h-0800h) separately. The time period where the aggregate BES power is negative (charging) is considered daytime and the time period where the aggregate BES power is positive (charging) is considered night-time. This is in order to distinguish the effect of charging and discharging on the distribution system losses. The line power loss is proportional to the square of the line current. Therefore, the greater the current the greater the losses. Use of reactive power for voltage regulation increases the line current,

consequently the losses also increase. Besides line currents, the network loading condition when the BES units are charging and discharging also has a significant impact on the cumulative losses. Consider a line with impedance $R + jX$. The active power loss of the line for current I is I^2R. If the line current is reduced by ΔI due to charging of BES units, the line loss reduces to $(I - \Delta I)^2R$. Then the reduction of power loss is

$$\begin{aligned}\Delta P_{lineLoss} &= I^2R - (I - \Delta I)^2R \\ &= \Delta I(2I - \Delta I)R\end{aligned}$$

From the above expression it can be observed that, for a given ΔI the higher the I, the higher the $\Delta P_{lineLoss}$. Therefore, more reduction in losses can be achieved when BES units are charged and discharged during the times of high currents in the lines. Similarly, the load on the network when reactive power is utilized also has an effect on the losses. The losses are higher when reactive power is utilized during the times the network is heavily loaded compared to the times when the load is less. According to the results shown in the table, the highest day-time power loss occurs when the BES units are operated with rule-based strategy. Both the reasons mentioned above are the causes for this higher power loss. In the local RHC strategy and the distributed control strategy, the charging of the BES units mostly occurs in the period of high currents in the network. Therefore, the daytime losses are lower compared to the rule-based strategy. The BES power set points are the same in two grid-supportive charging strategies. The reduction of loss by 2 kWh with distributed control strategy compared to the Local RHC method is therefore solely due to reduction of reactive power support. This reduction of loss over a month period is insignificant when compared to the reduction of reactive power flow in the network. However, here, this reactive power is coming from the medium voltage grid. The loss in the MV grid due to increase of reactive power demand in the distribution grid is not included here. Therefore, the effective loss reduction would be much higher than 2 kWh. During night-time, lower losses are observed when the BES units are operated with the rule-based strategy. In the rule-based strategy, BES units start discharging at 1700h everyday. However, in the other two strategies, BES units start discharging at 1800h on most of the days. That is because the high tariff period starts at 1800h, therefore the HEMS schedules discharging from 1800h onwards. Since discharging is delayed about an hour compared to the rule-based strategy, the BES units are able to supply the late-night load too. However, at this period the network is lightly loaded compared to the period from 1700h-1800h. Consequently, the reduction in losses is lower compared to the losses that would have occurred if they had discharged during the period from 1700-1800h.

Fig. 5.3 shows the ratio of local generation to the local load of the customers who possess BES units. The results shown are for the month of July. In this month, the local generation exceeds the local load of customers 2, 5, 6, 10, 11, 13, and 15. The local generation of the rest of the customers is lower than the local load, however it is still higher than 80%. The self-sufficiency and the self-consumption rates of these customers without BES units and with various BES control strategies

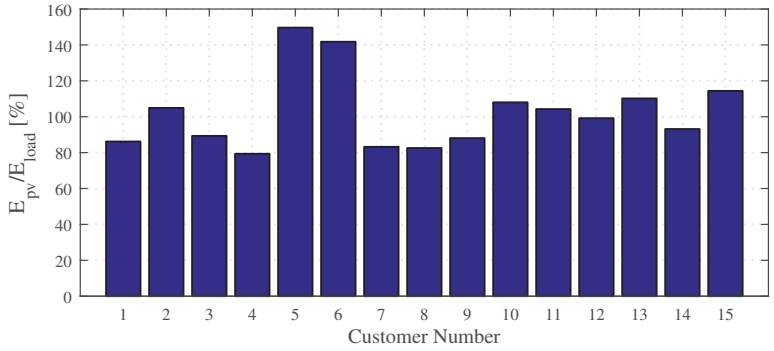

Figure 5.3: The ratio of local generation to the local load in July.

are shown in Fig. 5.4. As can be seen, the BES increases the SCR and the SSR significantly. Both rates are slightly higher when the BES units are operated with the rule-based strategy than the local RHC and the distributed control methods. Another noticeable fact from these results is that the SCRs when the BES units are operated with the local RHC method and the distributed control method are equal. The same holds for the SSR as well. This is because, in both methods the BES set points are equal. In the distributed control method, the central controller only adjusts the power sharing ratio among the three phases of the BES converter. From these results, we can observe that the two grid-supportive operational strategies have not adversely affected the SCR and the SSR.

The total amount of energy discharged from the battery during the simulated period is shown in Fig. 5.5. According to the results, the energy discharged from the BES units in the rule-based strategy is slightly higher than that of the other two strategies. This explains the cause of the slightly higher SSR and SCR for the rule-based operational strategy. The discharged energy in other two operational strategies are equal. Again, there is no significant difference in the total energy discharged from the BES unit for different control strategies. Total discharged energy from the battery is a rough indicator of battery ageing due to cycling. As the discharged energy from the BES units in different control strategies is similar, the effect of cyclical ageing of batteries is also roughly similar.

The costs of the energy component in the electricity bill without BES units and with different BES control strategies are shown in Fig. 5.6. In the studied case, the electricity selling rate is lower than the buying rate. Therefore, the electricity bill can be reduced by storing the excess energy in the BES unit and using that energy later to supply the local load. From the figure, we can observe that the month-end electricity costs are almost the same for all three different control strategies. The savings of a few customers increases slightly when the BES units are operated with the rule-based strategy. However, this increase is so small that is negligible.

According to these results, the two grid-supportive BES operational strategies have not adversely affected any of the local characteristics. Therefore, in this case the

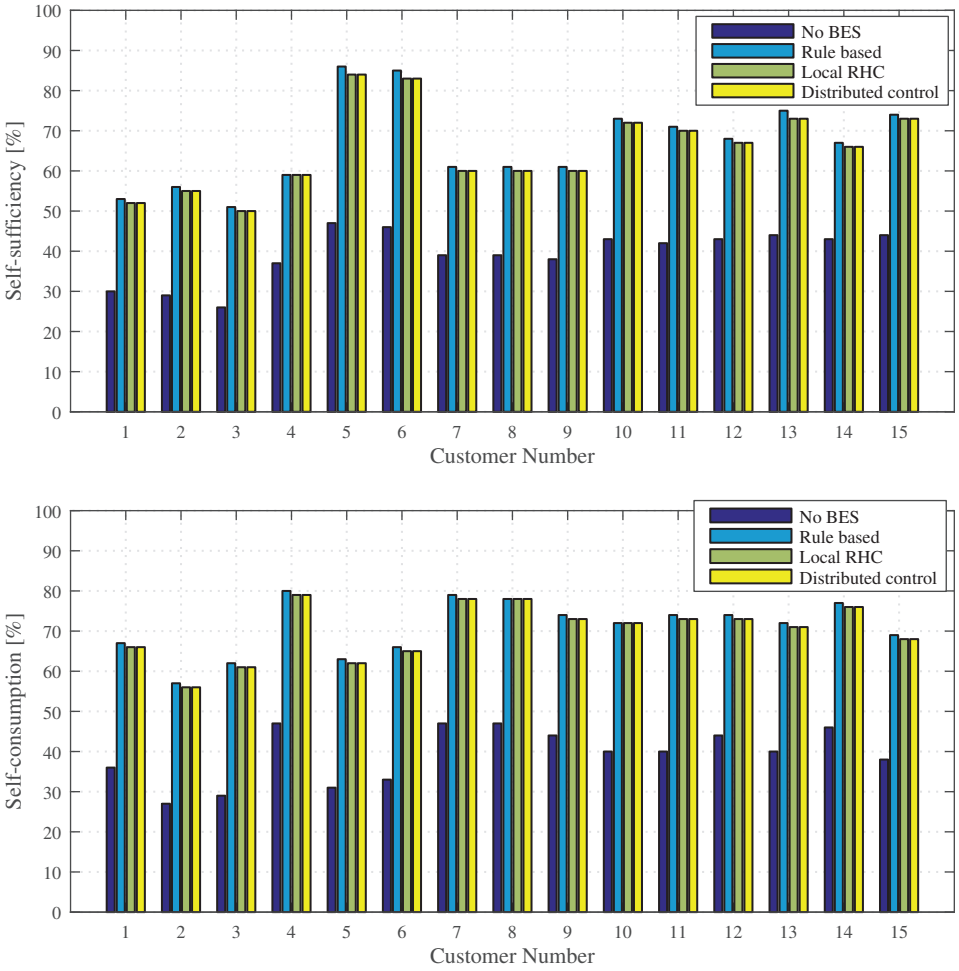

Figure 5.4: Self-sufficiency rates and self-consumptions rate in July.

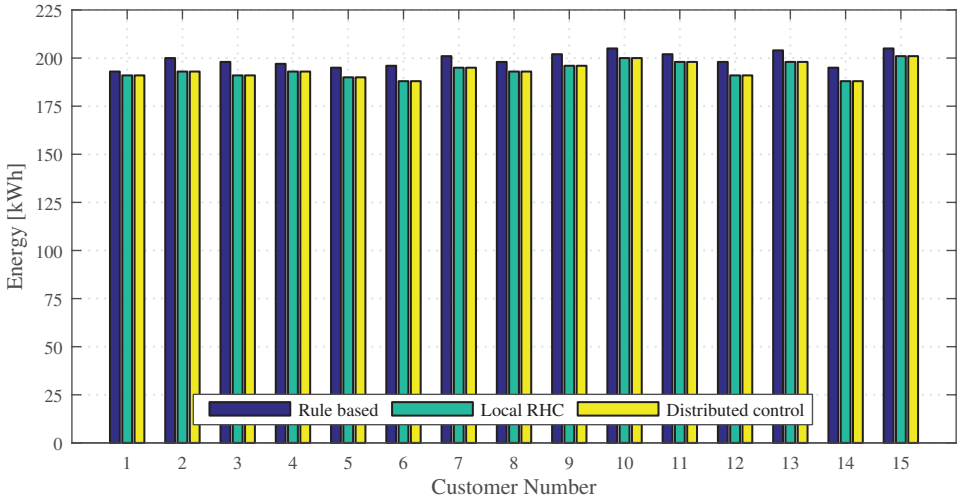

Figure 5.5: Total discharged energy from the BES units.

DSO's involvement in controlling the BES units does not have a negative effect for the customer. The two grid-supportive control strategies are able to fulfil the objective of the BES owner while supporting the grid in maintaining the voltage profile within the acceptable level with reduced reactive power support.

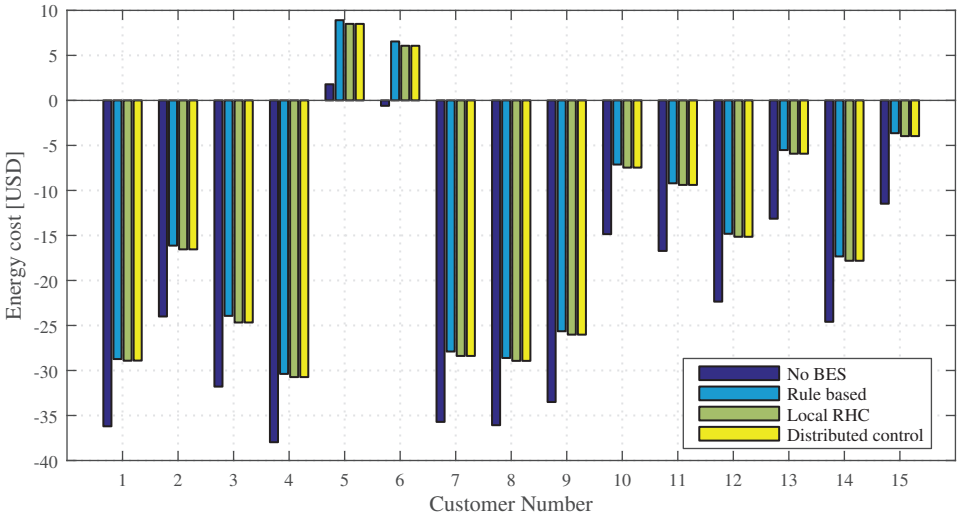

Figure 5.6: Energy cost for July. Negative values correspond to the cost paid for the utility and positive values corresponds to earnings made by the customer.

5.4 Discussion

In this chapter, we have compared the effect of two proposed grid-supportive BES control strategies on the local characteristics of a residential energy system. Moreover, we have compared the benefits for the utility. A rule-based strategy, which is not intentionally supportive for the gird, is used as the base scenario for this comparison. In this study, we have considered a tariff structure, where the selling rate is lower than the buying rate. A lower selling rate is the main motivation for a residential customer to consider installing a BES unit. If the selling rate is higher than or equal to the buying rate, and there is no limitation on the power feed-in to the grid, then it makes no sense for a customer to install a BES unit. Among different retail electricity rates, we have chosen the time-of-use tariff. The time-of-use tariff has been chosen such that there are two peak-tariff periods in the day. One is in the early morning while the other is in the evening. These are the periods during which the distribution grids, which mostly supply residential customers, are typically heavily loaded. Such a time-of-use tariff would push BES units to discharge during these periods. Consequently, the load on the grid will decrease. Moreover, this will alleviate possible under-voltage issues too. Under such a tariff scheme, the BES owner's primary concern would be maximizing the savings in his electricity bill.

In some countries, financial incentives are available to support the purchase of batteries for solar systems. In such cases, this incentive could be accompanied by a requirement to control the charging operation according to the DSO's guidelines. According to the analysis presented in this chapter, the customer can fulfil his local objective while supporting the grid when the BES is operated with the two proposed control strategies. The involvement of the DSO in controlling the operation of the BES units has no adverse impact on the local objectives. In the proposed control strategies, there is no direct monetary compensation for the customer for charging according to the DSO's requirement and allowing real-time adjustment of the set point. Yet, maximum support from the BES units can be achieved to alleviate over-voltage issues without adverse effect on the customer's requirements. Therefore, in this case, compensation for grid-supportive operation of residential BES units is not needed.

From this analysis we have seen that one of the main benefits of incorporating BES for voltage support is the reduction of the reactive power demand of the distribution grid. Since the over-voltage issue is associated with the reverse power flow, alleviation of the over-voltage issue via charging of BES units will reduce the reverse power flow too. Consequently, potential distribution grid overloading issues due to excessive reverse power flow will also be mitigated. The reactive power demand of the grid is expected to increase significantly in the future as the amount of DGs in the grid increases. The reason for this is reactive power control of DGs for mitigating local over-voltage issues. This will increase the need for reactive power compensators in distribution grids [135]. The local RHC-based control strategy is able to reduce the reactive power demand of the grid significantly

when compared to the rule-based method. Further reduction is achieved with the distributed control strategy because the distributed control strategy attempts to optimize the operation of the overall distribution grid. The main purpose of installing a BES unit in a residential household may not be supporting the grid but to increase savings by increasing self-consumption. Yet, these small systems are capable of supporting the grid while providing other local services to the BES owner. Therefore, it is important to incorporate distributed storage units into local voltage control methods if such resources are already available in the system.

In this thesis we have proposed two grid-supportive control strategies for customer-owned BES units. The first control strategy is based on a local control architecture while the second is based on a distributed control architecture. The local control strategy of BES units relies little on communication with an external party. The only input it needs from the DSO is the information about the charging period. The reactive power control strategy of the converters, however, relies on one-way communication between the meter and the PV inverter. By contrast, the distributed control strategy relies on two-way communication, real-time measurements and knowledge about the distribution grid. The second control strategy is distributed in the sense that the local controllers decide the BES set points while a central controller is involved in controlling the operation of BES units to a certain extent. The local controllers optimize the operation of the local system while the central controller optimizes the operation of the overall distribution grid. In that way, the two objectives are distributed across the central controller and the local controllers. Therefore, the operation of the BES units is not completely dependent on the central controller. In the distributed control scheme, if the central controller is not involved in the operation of the BES units, the BES control strategy becomes the same as the local RHC-based control strategy. The local control strategy also includes a grid-supportive function. Therefore, the BES units are able to operate in a grid-supportive manner even when communication between the central controller and the local controller fails. However, this may not be the optimal operation with respect to the operation of the overall distribution grid. In the distributed control strategy, if a BES unit stops responding to the central controller, that unit can be discarded from the central control algorithm. Consequently, the central controller will update the power sharing ratios of those units which have responded to the central controller. A unit that loses the connection with the central controller will continue to operate at the last power sharing ratio received by the central controller. As for the PV inverters, the reactive power set points are completely decided by the central controller. The reactive power is utilized only when the active power reduction due to charging of BES units is not sufficient to solve the over-voltage issue completely. If any inverter loses the connection with the central controller, that unit can be discarded from the central control algorithm. The inverter that loses the connection will continue to operate at the last power factor set point received by the central controller. The reactive power consumption of this inverter will eventually drop to zero as the power output of the inverter decreases. Communication failure of one unit has no adverse impact on the reactive power control algorithm. The only consequence is that the inverter that lost the connection may

not operate at the optimal set point.

Chapter 6

Summary and Conclusions

This chapter presents a summary of this PhD thesis and the conclusions drawn from the main findings. The chapter ends with several ideas for future work.

6.1 Summary and Conclusions

Solar PV systems are becoming cheaper every year. Consequently, an increasing number of customers are becoming interested in installing a PV system on their houses. Along with this flourishing of the residential PV market, the residential storage market is also gradually growing. Recently, there has been an increasing interest in energy storage systems among residential customers. Increasing the self-consumption rate of locally produced energy has been the main concern of customers who are interested in storage. Besides customer requirements, these storage systems can be useful for the DSO in many ways. Nevertheless, it is important to identify the most appropriate application(s) considering the size of the BES systems, location of the system, and the characteristics of the local grid. For example, in distribution grids with high PV penetration, voltage support would be a useful application. Proper control of BES systems can reduce the reverse power flow in the grid, consequently over-voltage issues and over-loading issues can be alleviated. In this thesis, we have investigated control strategies for customer-owned BES systems that can not only fulfil the customer's requirement, but also help the DSO to alleviate the problems caused by high PV penetration. The problems considered in this thesis are over-voltage issues and over-loading issues.

In the first part of the thesis, we have proposed a local control strategy for customer-owned BES systems. The proposed control strategy is based on receding horizon control, which involves solving an optimization problem repeatedly over a moving time horizon to determine the set points of the BES system. The objective of this optimization has been set to maximize the economic benefits for the customer.

Grid supportive operation was achieved by constraining the charging operation of the BES systems over the critical period specified by the DSO. The period of the day that the grid is under risk of over-voltage issues has been selected as the critical period. By constraining the charging operation to this period, the maximum contribution from all the BES systems to reducing the reverse power flow is achieved. This is important especially when the number of BES systems in the network is relatively low compared to the number of PV systems, which is typically the case today, as while BES system adoption is growing it still lags behind the pace set by PV uptake. The algorithm schedules charging operation such that the BES system does not reach a fully charged state before the critical period ends. This ensures the availability of storage capacity for charging at any time within the critical period. The algorithm also allows charging outside the critical period, if the excess energy available during the critical period is not sufficient to fully charge the BES. Therefore, the BES is optimally utilized under any operating conditions. In some cases, when the available BES capacity is insufficient, the over-voltage problem may not be completely solved only by charging the BES units. A secondary solution is needed when that happens. We have proposed a solution for this using the reactive power support from the PV systems. This secondary solution operates only if the charging of BES units is not sufficient to mitigate over-voltage issues. This solution is based on a gradual increment of reactive power support from the PV inverters until the problem is solved. The PV inverters respond to a broadcast signal received by a monitoring device located at a selected node in the network. The improvement of the voltage profile of the grid with the proposed local control strategy is shown via a simulation study. Via the simulation results we have shown that the control strategy works as expected and effectively solves the over-voltage issues.

Secondly, we have proposed a distributed control strategy for controlling the active power set points of the BES systems and the reactive power set points of the PV inverters. In this method, the local controller decides the control set points of the BES systems using the same algorithm adopted in the local control strategy. Therefore, the control objective can be locally decided by the customer. A central controller is involved only if the locally decided set points are not able to solve the over-voltage problem completely. In this method, we have proposed the use of BES systems that are connected to the grid via three-phase converters. The power set point of each phase of this converter can be independently controlled (a three-phase unbalanced operation). The local controller determines the DC side power set points of the converter. The function of the central controller is to set the power sharing ratio among the three phases of the converter. At the beginning of the day, the power is shared equally among the three phases. This behaviour continues until a voltage violation is detected. When a voltage violation is detected, the power is shared among the three phases according to the ratio received from the central controller. There is no need to change the power sharing ratio among the phases by the central controller if no voltage violations are detected. That is because, sometimes, the three-phase balanced operation with the locally decided set points may be sufficient to solve the over-voltage problem. Some times the

over-voltage problem may not be completely solved by active power control of the BES systems only. When this occurs, reactive power support from the PV inverters is also utilized. In such cases, the power factor set point of the inverter is controlled by the central controller. Using a simulation study, we have shown that the proposed control strategy is able to effectively improve the voltage quality in distribution grids with high PV penetration. Active power control of BES units lowers the voltage magnitudes while three-phase unbalanced active power control improves the voltage unbalance. Consequently, over-voltage issues are completely solved either only with active power control of BES systems or active power control plus reduced reactive power support from the converters.

Finally, we have made an evaluation of the two proposed control strategies. The objective of this thesis was to investigate the control strategies of customer-owned BES systems that can improve the voltage profile of the distribution grid. The main concern was that the grid supportive control strategies should not adversely affect the storage owner's local objective. To investigate the impacts of the proposed control strategies on the local objectives, we calculated the electricity bill, the self-consumption ratio, and the self-sufficiency ratio for several customers. This calculation was made for a period of 30 days. Then we compared the results with those for the rule-based control strategy. In the rule-based strategy, the rules have been carefully defined to increase the savings for the customer. In this method, we limited the maximum number of full discharge cycles of the battery bank over a 24-hour period to one. According to the results, there were no noticeable differences of the self-consumption ratio, the self-sufficiency ratio, or the electricity bills of the majority of the customers considered. Several studies have mentioned the need for monetary compensation for the use of customer-owned BES systems for voltage support. Unless the main function of the BES is providing voltage support, there is no need to provide direct monitory compensation to BES owners. This is because the voltage support function can be combined with the local functions without significant adverse impact on the local objective.

In this study, we have also compared the benefits of the proposed control strategies for the utility with the rule-based control strategy. In the rule-based control strategy, the rules have been particularly defined so that they are favourable to the customer, and have not intentionally been designed to support the grid. A reactive power support strategy was also implemented in coordination with the rule-based control strategy. The reactive power support strategy is the same as that implemented with the local control strategy of BES systems. We then compared the required reactive power support from the converters for maintaining the voltage profile of the network within the standard limits. From this study, we have shown that a significant reduction of reactive power support required from the converters can be achieved with the two proposed control strategies. Among the two proposed control strategies, the distributed control scheme is able to solve the over-voltage problem with the least reactive power utilization from the converters. This is clearly because of the central coordination of the operation of the BES systems. The active power capability of the BES units can be maximally utilized to improve the voltage profile via central coordination.

We have also compared the power loss in the network. We calculated the cumulative loss over the simulated period for different operational strategies. The highest daytime cumulative loss is observed for the rule-based control strategy while the lowest is observed for the distributed control strategy. The cumulative loss profile of the network is determined by several factors. One cause is the increase of line currents due to reactive power support from the converters. The other is the load on the network at the times the reactive power is utilized. The higher the load on the network the higher the increase of losses due to reactive power flow. In addition, the load on the network during the times the BES units are charging and discharging also affects the cumulative loss. The reduction of power loss will be higher when the BES units are charged at the times of higher reverse power flow in the grid. Therefore, charging the BES units during the critical period will not only reduce the risk of over voltages but also reduce the power loss in the network. Nevertheless, the proposed control strategies may not result in the minimum cumulative power loss in the network. This is because the proposed control strategies are not optimized to minimize the cumulative loss.

6.2 Recommendations for Future Works

The focus of this thesis was to investigate grid-supportive operational strategies for customer-owned BES systems. In this thesis, we have mainly investigated solutions to the over-voltage problem using customer-owned BES systems. Because over-voltage has been the most common problem that has been experienced with increased penetration of PV systems in LV distribution grids. The cause of the over-voltage problem is high reverse power flow. BES-based solutions reduce reverse power flow by charging batteries. Besides the over-voltage problem, the use of distributed BES systems for dealing with other voltage quality problems such as flickers, voltage dips and voltage swells can be investigated. The improvement of the overall voltage quality of the distribution grid due to the aggregate contribution from multiple distributed BES systems can be investigated.

In the proposed distributed control strategy, a central controller is involved in making certain decisions. When this approach is used, there is a significant time delay between the time the monitoring device detects the voltage deviation and the time measures are taken to mitigate it. This is due to the central controller requiring real-time measurements from the network to calculate the set points. Then, those set points need to be sent to the corresponding systems. In this thesis, all the simulations were carried out with a 1-minute time delay. The load as well as the PV generation can change rapidly. The control scheme can be unstable if these changes are faster than the response time of the control strategy. We have checked the performance of the control scheme both for a clear sky day and a cloudy day. On the clear sky day, the power production of the PV systems change smoothly over the course of the day while the residential load profiles fluctuate significantly. On the cloudy day, the power production of the PV systems also fluctuate significantly. In both of these cases, the performance of the control scheme

was stable for the 1-minute time delay. Further work could therefore be done to understand the interactions between power and communication networks via co-simulation of communication networks and power networks.

During this Ph.D work, we were able to implement only a part of the local control system in the laboratory; that is, the home energy management system. The aggregate effect of multiple BES systems on the grid voltage was not tested. This part can therefore be implemented in the laboratory to observe the impact on the grid voltage profile. Moreover, the distributed control scheme may also be implemented in the laboratory. Practical implementation of this control scheme will aid the understanding of realistic values for the aforementioned time delay.

Bibliography

[1] "2018 Snapshot of Global Photovoltaic Markets," tech. rep., International Energy Agency, 2018.

[2] "Global market outlook for solar power /2018-2022," tech. rep., SolarPower Europe - European Photovoltaic Industry Association, 2018.

[3] A. G. Imenes, G. H. Yordanov, O.-M. Midtgård, and T. O. Sætre, "Development of a test station for accurate in situ I-V curve measurements of photovoltaic modules in Southern Norway," in *Photovoltaic Specialists Conference (PVSC), 2011 37th IEEE*, pp. 003153–003158, June 2011.

[4] J. V. Appen, M. Braun, T. Stetz, K. Diwold, and D. Geibel, "Time in the sun: The challenge of high PV penetration in the german electric grid," *IEEE Power and Energy Magazine*, vol. 11, pp. 55–64, Mar 2013.

[5] J. Eyer and G. Corey, "Energy Storage for the Electricity Grid: Benefits and Market Potential Assessment Guide," tech. rep., Sandia National Laboratories, 2010.

[6] R. Bussar, M. Lippert, G. Bonduelle, R. Linke, G. Crugnola, J. Cilia, K.-D. Merz, C. Heron, and E. Marckx, "Battery Eerngy Storage for Smart Grid Applications," tech. rep., Association of European Automotive and Industrial Battery Manufacturers, 2013.

[7] K. Divya and J. Østergaard, "Battery energy storage technology for power systems-An overview," *Electric Power Systems Research*, vol. 79, no. 4, pp. 511 – 520, 2009.

[8] S. Wilkinson, "Energy Storage in PV Report - 2014," tech. rep., IHS Technology, 2014.

[9] "Global residential solar energy storage market 2015-2019," tech. rep., Technavio, 2015.

[10] "Distributed energy storage systems for energy cost management and grid management: Global market analysis and forecasts," tech. rep., Navigant Research, 2014.

[11] M. del P. Pablo-Romero, "Solar energy: Incentives to promote PV in EU27," *AIMS Energy*, vol. 1, no. 1, pp. 28–47, 2013.

[12] H. Wirth, "Recent Facts about Photovoltaics in Germany," tech. rep., Fraunhofer Institute for Solar Energy, 2017.

[13] "2016 Snapshot of Global Photovoltaic Markets," tech. rep., International Energy Agency, 2017.

[14] "Global market outlook for solar power /2016-2020," tech. rep., SolarPower Europe - European Photovoltaic Industry Association, 2016.

[15] T. Stetz, M. Kraiczy, K. Diwold, B. Noone, A. Bruce, and et el, "Transition from Uni-directional to Bi-directional Distribution Grids," tech. rep., International Energy Agency, 2014.

[16] H. Laukamp, E. Caamano, S. Cobben, T. Erge, and J. Thornycroft, "Recommendations for utilities: PV UPSCALE WP4," tech. rep., Intelligent Energy-Europe, 2008.

[17] E. Demirok, D. Sera, R. Teodorescu, P. Rodriguez, and U. Borup, "Evaluation of the voltage support strategies for the low voltage grid connected PV generators," in *2010 IEEE Energy Conversion Congress and Exposition*, pp. 710–717, Sept 2010.

[18] R. A. Shayani and M. A. G. de Oliveira, "Photovoltaic Generation Penetration Limits in Radial Distribution Systems," *IEEE Transactions on Power Systems*, vol. 26, pp. 1625–1631, Aug 2011.

[19] R. Tonkoski, D. Turcotte, and T. H. M. EL-Fouly, "Impact of high PV penetration on voltage profiles in residential neighborhoods," *IEEE Transactions on Sustainable Energy*, vol. 3, pp. 518–527, July 2012.

[20] M. A. Eltawil and Z. Zhao, "Grid-connected photovoltaic power systems: Technical and potential problems - A review," *Renewable and Sustainable Energy Reviews*, vol. 14, no. 1, pp. 112 – 129, 2010.

[21] M. M. Haque and P. Wolfs, "A review of high PV penetrations in LV distribution networks: Present status, impacts and mitigation measures," *Renewable and Sustainable Energy Reviews*, vol. 62, pp. 1195 – 1208, 2016.

[22] M. Karimi, H. Mokhlis, K. Naidu, S. Uddin, and A. Bakar, "Photovoltaic penetration issues and impacts in distribution network - A review," *Renewable and Sustainable Energy Reviews*, vol. 53, pp. 594 – 605, 2016.

[23] E. Caamano, J. Thornycroft, H. D. Moor, S. Cobben, M. Jantsch, T. Erge, H. Laukamp, D. Suna, and B. Gaiddon, "State of the art on dispersed PV power generation: Publication review on the impacts of PV distributed generation and electricity networks," tech. rep., Intelligent Energy-Europe, 2007.

[24] C. Gonzalez, J. Geuns, S. Weckx, T. Wijnhoven, P. Vingerhoets, T. D. Rybel, and J. Driesen, "LV distribution network feeders in Belgium and power quality issues due to increasing PV penetration levels," in *2012 3rd IEEE PES Innovative Smart Grid Technologies Europe (ISGT Europe)*, pp. 1–8, Oct 2012.

[25] F. Katiraei and J. R. Aguero, "Solar PV Integration Challenges," *IEEE Power and Energy Magazine*, vol. 9, pp. 62–71, May 2011.

[26] J. von Appen, M. Braun, T. Stetz, K. Diwold, and D. Geibel, "Time in the Sun: The Challenge of High PV Penetration in the German Electric Grid," *IEEE Power and Energy Magazine*, vol. 11, pp. 55–64, March 2013.

[27] S. J. Lewis, "Analysis and management of the impacts of a high penetration of photovoltaic systems in an electricity distribution network," in *2011 IEEE PES Innovative Smart Grid Technologies*, pp. 1–7, Nov 2011.

[28] R. A. Walling, R. Saint, R. C. Dugan, J. Burke, and L. A. Kojovic, "Summary of distributed resources impact on power delivery systems," *IEEE Transactions on Power Delivery*, vol. 23, pp. 1636–1644, July 2008.

[29] J. Wong, Y. S. Lim, J. H. Tang, and E. Morris, "Grid-connected photovoltaic system in Malaysia: A review on voltage issues," *Renewable and Sustainable Energy Reviews*, vol. 29, pp. 535 – 545, 2014.

[30] T. Stetz, F. Marten, and M. Braun, "Improved low voltage grid-integration of photovoltaic systems in germany," *IEEE Transactions on Sustainable Energy*, vol. 4, pp. 534–542, April 2013.

[31] B. Seal, "Common Functions for Smart Inverters, version 3," tech. rep., Electric Power Research Institute (EPRI), 2014.

[32] B. I. Craciun, T. Kerekes, D. Séra, and R. Teodorescu, "Overview of recent grid codes for PV power integration," in *2012 13th International Conference on Optimization of Electrical and Electronic Equipment (OPTIM)*, pp. 959–965, May 2012.

[33] L. Schwartfeger and D. Santos-Martin, "Review of distributed Generation Interconnection Standards," in *EEA Conference and Exhibition 2014*, pp. 1–13, June 2014.

[34] T. Fawzy, D. Premm, B. Bletterie, and A. Goršek, "Active contribution of PV inverters to voltage control from a smart grid vision to full-scale implementation," *e & i Elektrotechnik und Informationstechnik*, vol. 128, no. 4, pp. 110–115, 2011.

[35] R. Seguin, J. Woyak, D. Costyk, J. Hambrick, and B. Mather, "High-penetration PV integration handbook for distribution engineers," tech. rep., National Renewable Energy Laboratory, 2016.

[36] J. R. Agüero and S. J. Steffel, "Integration challenges of photovoltaic distributed generation on power distribution systems," in *Power and Energy Society General Meeting, 2011 IEEE*, July 2011.

[37] G. K. Ari and Y. Baghzouz, "Impact of high PV penetration on voltage regulation in electrical distribution systems," in *Clean Electrical Power (ICCEP), 2011 International Conference on*, October 2011.

[38] W. H. Kersting, *Distribution System Modeling and Analysis*. CRC Press, 2002.

[39] "Voltage Characteristics of Electricity Supplied by Public Distribution Systems," tech. rep., European Committee for Electrotechnical Standardization, 2005.

[40] T. Gönen, *Electric Power Distribution System Engineering*. McGraw-Hill Inc., 1986.

[41] R. Tonkoski, L. A. C. Lopes, and T. H. M. El-Fouly, "Coordinated active power curtailment of grid connected PV inverters for overvoltage prevention," *IEEE Transactions on Sustainable Energy*, vol. 2, pp. 139–147, April 2011.

[42] S. Weckx, C. Gonzalez, and J. Driesen, "Combined central and local active and reactive power control of PV inverters," *IEEE Transactions on Sustainable Energy*, vol. 5, pp. 776–784, July 2014.

[43] E. Dall'Anese, S. V. Dhople, B. B. Johnson, and G. B. Giannakis, "Decentralized optimal dispatch of photovoltaic inverters in residential distribution systems," *IEEE Transactions on Energy Conversion*, vol. 29, pp. 957–967, Dec 2014.

[44] X. Su, M. A. S. Masoum, and P. J. Wolfs, "Optimal PV inverter reactive power control and real power curtailment to improve performance of unbalanced four-wire LV distribution networks," *IEEE Transactions on Sustainable Energy*, vol. 5, pp. 967–977, July 2014.

[45] S. Weckx and J. Driesen, "Optimal local reactive power control by PV inverters," *IEEE Transactions on Sustainable Energy*, vol. 7, pp. 1624–1633, Oct 2016.

[46] A. Samadi, R. Eriksson, L. Soder, B. G. Rawn, and J. C. Boemer, "Coordinated active power-dependent voltage regulation in distribution grids with PV systems," *IEEE Transactions on Power Delivery*, vol. 29, pp. 1454–1464, June 2014.

[47] A. Samadi, E. Shayesteh, R. Eriksson, B. Rawn, and L. Soder, "Multi-objective coordinated droop-based voltage regulation in distribution grids with PV systems," *Renewable Energy*, vol. 71, pp. 315 – 323, 2014.

[48] P. Jahangiri and D. C. Aliprantis, "Distributed Volt/VAr Control by PV Inverters," *IEEE Transactions on Power Systems*, vol. 28, pp. 3429–3439, Aug 2013.

[49] E. Demirok, P. C. González, K. H. B. Frederiksen, D. Sera, P. Rodriguez, and R. Teodorescu, "Local reactive power control methods for overvoltage prevention of distributed solar inverters in low-voltage grids," *IEEE Journal of Photovoltaics*, vol. 1, pp. 174–182, Oct 2011.

[50] L. Collins and J. Ward, "Real and reactive power control of distributed PV inverters for overvoltage prevention and increased renewable generation hosting capacity," *Renewable Energy*, vol. 81, pp. 464 – 471, 2015.

[51] S. Alyami, Y. Wang, C. Wang, J. Zhao, and B. Zhao, "Adaptive real power capping method for fair overvoltage regulation of distribution networks with high penetration of PV systems," *IEEE Transactions on Smart Grid*, vol. 5, pp. 2729–2738, Nov 2014.

[52] H. Huang, J. Xu, Z. Peng, S. Yoo, D. Yu, D. Huang, and H. Qin, "Cloud motion estimation for short term solar irradiation prediction," in *Smart Grid Communications (SmartGridComm), 2013 IEEE International Conference on*, December 2013.

[53] S. Sayeef, S. Heslop, D. Cornforth, T. Moore, S. Percy, J. K. Ward, A. Berry, and D. Rowe, "Solar intermittency : Australia's clean energy challenge," tech. rep., Commonwealth Scientific and Industrial Research Organisation, 2012.

[54] P. Munshi, J. Pichel, and E. Kwe, "Energy storage: Game-changing component of the future grid," tech. rep., Piper Jaffray Investment Research, 2009.

[55] B. P. Roberts and C. Sandberg, "The role of energy storage in development of smart grids," *Proceedings of the IEEE*, vol. 99, pp. 1139–1144, Jun 2011.

[56] "The future role and challenges of energy storage." DG ENER Working Paper. European Commission.

[57] A. F. Zobaa, "Electrical energy storage - The future roles and challenges," in *2016 International Middle East Power Systems Conference (MEPCON)*, Dec 2016.

[58] C. A. Hill, M. C. Such, D. Chen, J. Gonzalez, and W. M. Grady, "Battery energy storage for enabling integration of distributed solar power generation," *IEEE Transactions on Smart Grid*, vol. 3, pp. 850–857, June 2012.

[59] J. Eyer and G. Corey, "Energy storage for the electricity grid: Benefits and market potential assessment guide," tech. rep., Sandia National Laboratories, 201.

[60] A. A. Akhil, G. Huff, A. B. Currier, B. C. Kaun, D. M. Rastler, S. B. Chen, A. L. Cotter, D. T. Bradshaw, and W. D. Gauntlett, "DOE/EPRI 2013 Electricity storage handbook in collaboration with NRECA," tech. rep., Sandia National Laboratories, 2013.

[61] T. Kousksou, P. Bruel, A. Jamil, T. E. Rhafiki, and Y. Zeraouli, "Energy storage: Applications and challenges," *Solar Energy Materials and Solar Cells*, vol. 120, pp. 59 – 80, 2014.

[62] "EPRI-DOE handbook of energy storage for transmission and distribution applications," tech. rep., Technology Insights, EPRI PEAC Corporation, 2003.

[63] "Electrical energy storage," tech. rep., International Electrotechnical Commission (IEC), 2011.

[64] "Grid energy storage," tech. rep., U.S. Department of Energy, 2013.

[65] H. Ibrahima, A. Ilinca, and J. Perron, "Energy storage systems - Characteristics and comparisons," *Renewable and Sustainable Energy Reviews*, vol. 12, pp. 1221–1250, 2008.

[66] A. Oberhofer and P. Meisen, "Energy storage technologies and their role in renewable integration," tech. rep., Global Energy Network Institute (GENI), 2012.

[67] C. McKerracher, "EV market trends and outlook." Presentation slides, September 2017.

[68] X. Li, D. Hui, and X. Lai, "Battery energy storage station (BESS)-based smoothing control of photovoltaic (PV) and wind power generation fluctuations," *IEEE Transactions on Sustainable Energy*, vol. 4, pp. 464–473, April 2013.

[69] M. S. Lu, C. L. Chang, W. J. Lee, and L. Wang, "Combining the wind power generation system with energy storage equipments," in *2008 IEEE Industry Applications Society Annual Meeting*, pp. 1–6, Oct 2008.

[70] C. Coe, A. Hurst, M. Hardin, M. Such, and R. Jennings, "Managing renewable power generation," Nov. 10 2011. US Patent App. 12/773,504.

[71] J. von Appen, T. Stetz, M. Braun, and A. Schmiegel, "Local voltage control strategies for pv storage systems in distribution grids," *IEEE Transactions on Smart Grid*, vol. 5, pp. 1002–1009, March 2014.

[72] M. N. Kabir, Y. Mishra, G. Ledwich, Z. Y. Dong, and K. P. Wong, "Coordinated control of grid-connected photovoltaic reactive power and battery energy storage systems to improve the voltage profile of a residential distribution feeder," *IEEE Transactions on Industrial Informatics*, vol. 10, pp. 967–977, May 2014.

[73] D. Torres, J. Crichigno, G. Padilla, and R. Rivera, "Scheduling coupled photovoltaic, battery and conventional energy sources to maximize profit using linear programming," *Renewable Energy*, vol. 72, pp. 284 – 290, 2014.

[74] T. Hubert and S. Grijalva, "Modeling for residential electricity optimization in dynamic pricing environments," *IEEE Transactions on Smart Grid*, vol. 3, pp. 2224–2231, Dec 2012.

[75] M. Urbina and Z. Li, "A fuzzy optimization approach to PV/battery scheduling with uncertainty in PV generation," in *2006 38th North American Power Symposium*, pp. 561–566, Sept 2006.

[76] J. Li and M. A. Danzer, "Optimal charge control strategies for stationary photovoltaic battery systems," *Journal of Power Sources*, vol. 258, pp. 365–373, Jul 2014.

[77] Y. Riffonneau, S. Bacha, F. Barruel, and S. Ploix, "Optimal power flow management for grid connected PV systems with batteries," *IEEE Transactions on Sustainable Energy*, vol. 2, pp. 309–320, July 2011.

[78] C. Changsong, D. Shanxu, C. Tao, L. Bangyin, and Y. Jinjun, "Energy trading model for optimal microgrid scheduling based on genetic algorithm," in *2009 IEEE 6th International Power Electronics and Motion Control Conference*, pp. 2136–2139, May 2009.

[79] A. Nottrott, J. Kleissl, and B. Washom, "Energy dispatch schedule optimization and cost benefit analysis for grid-connected, photovoltaic-battery storage systems," *Renewable Energy*, vol. 55, pp. 230–240, Jul 2013.

[80] E. L. Ratnam, S. R. Weller, and C. M. Kellett, "An optimization-based approach to scheduling residential battery storage with solar PV: Assessing customer benefit," *Renewable Energy*, vol. 75, pp. 123–134, Mar 2015.

[81] M. Schreiber and P. Hochloff, "Capacity-dependent tariffs and residential energy management for photovoltaic storage systems," in *2013 IEEE Power Energy Society General Meeting*, pp. 1–5, July 2013.

[82] M. Liu, P. K. Phanivong, Y. Shi, and D. S. Callaway, "Decentralized charging control of electric vehicles in residential distribution networks," *IEEE Transactions on Control Systems Technology*, vol. PP, no. 99, pp. 1–16, 2017.

[83] K. Worthmann, C. M. Kellett, P. Braun, L. Grüne, and S. R. Weller, "Distributed and decentralized control of residential energy systems incorporating battery storage," *IEEE Transactions on Smart Grid*, vol. 6, pp. 1914–1923, July 2015.

[84] N. Jayasekara, P. Wolfs, and M. A. Masoum, "An optimal management strategy for distributed storages in distribution networks with high penetrations of PV," *Electric Power Systems Research*, vol. 116, pp. 147 – 157, 2014.

[85] B. Olek and M. Wierzbowski, "Local energy balancing and ancillary services in low-voltage networks with distributed generation, energy storage, and active loads," *IEEE Transactions on Industrial Electronics*, vol. 62, pp. 2499–2508, April 2015.

[86] X. Liu, A. Aichhorn, L. Liu, and H. Li, "Coordinated control of distributed energy storage system with tap changer transformers for voltage rise mitigation under high photovoltaic penetration," *IEEE Transactions on Smart Grid*, vol. 3, pp. 897–906, June 2012.

[87] P. Wang, D. Liang, J. Yi, P. Lyons, P. Davison, and P. Taylor, "Integrating electrical energy storage into coordinated voltage control schemes for distribution networks," *Smart Grid, IEEE Transactions on*, vol. 5, pp. 1018–1032, March 2014.

[88] R. Carli and M. Dotoli, "A decentralized control strategy for optimal charging of electric vehicle fleets with congestion management," in *2017 IEEE International Conference on Service Operations and Logistics, and Informatics (SOLI)*, pp. 63–67, Sept 2017.

[89] Y. Wang, B. F. Wang, and P. L. So, "A voltage regulation method using distributed energy storage systems in LV distribution networks," in *2016 IEEE International Energy Conference (ENERGYCON)*, pp. 1–6, April 2016.

[90] Y. Wang, K. T. Tan, X. Y. Peng, and P. L. So, "Coordinated control of distributed energy-storage systems for voltage regulation in distribution networks," *IEEE Transactions on Power Delivery*, vol. 31, pp. 1132–1141, June 2016.

[91] G. Mokhtari, G. Nourbakhsh, and A. Ghosh, "Smart coordination of energy storage units (ESUs) for voltage and loading management in distribution networks," *Power Systems, IEEE Transactions on*, vol. 28, pp. 4812–4820, Nov 2013.

[92] Y. Xu, W. Zhang, G. Hug, S. Kar, and Z. Li, "Cooperative control of distributed energy storage systems in a microgrid," *IEEE Transactions on Smart Grid*, vol. 6, pp. 238–248, Jan 2015.

[93] S. J. Lee, J. H. Kim, C. H. Kim, S. K. Kim, E. S. Kim, D. U. Kim, K. K. Mehmood, and S. U. Khan, "Coordinated control algorithm for distributed battery energy storage systems for mitigating voltage and frequency deviations," *IEEE Transactions on Smart Grid*, vol. 7, pp. 1713–1722, May 2016.

[94] L. Wang, D. Liang, A. Crossland, P. Taylor, D. Jones, and N. Wade, "Coordination of multiple energy storage units in a low-voltage distribution network," *Smart Grid, IEEE Transactions on*, vol. 6, pp. 2906–2918, Nov 2015.

[95] Y. Ru, J. Kleissl, and S. Martinez, "Storage size determination for grid-connected photovoltaic systems," *IEEE Transactions on Sustainable Energy*, vol. 4, pp. 68–81, Jan 2013.

[96] D. Wu, M. Kintner-Meyer, T. Yang, and P. Balducci, "Economic analysis and optimal sizing for behind-the-meter battery storage," in *2016 IEEE Power and Energy Society General Meeting (PESGM)*, pp. 1–5, July 2016.

[97] B. S. Borowy and Z. M. Salameh, "Methodology for optimally sizing the combination of a battery bank and PV array in a wind/PV hybrid system," *IEEE Transactions on Energy Conversion*, vol. 11, pp. 367–375, Jun 1996.

[98] T. A. Nguyen, M. L. Crow, and A. C. Elmore, "Optimal sizing of a vanadium redox battery system for microgrid systems," *IEEE Transactions on Sustainable Energy*, vol. 6, pp. 729–737, July 2015.

[99] T. Senjyu, D. Hayashi, N. Urasaki, and T. Funabashi, "Optimum configuration for renewable generating systems in residence using genetic algorithm," *IEEE Transactions on Energy Conversion*, vol. 21, pp. 459–466, June 2006.

[100] M. H. Nehrir, C. Wang, K. Strunz, H. Aki, R. Ramakumar, J. Bing, Z. Miao, and Z. Salameh, "A review of hybrid renewable/alternative energy systems for electric power generation: Configurations, control, and applications," *IEEE Transactions on Sustainable Energy*, vol. 2, pp. 392–403, Oct 2011.

[101] M. Albadi and E. El-Saadany, "A summary of demand response in electricity markets," *Electric Power Systems Research*, vol. 78, no. 11, pp. 1989 – 1996, 2008.

[102] S. Borenstein, M. Jaske, and A. Rosenfeld, "Dynamic pricing, advanced metering and demand response in electricity markets," tech. rep., University of California Energy Institute, 2002.

[103] A. Faruqui and S. Sergici, "Household response to dynamic pricing of electricity: A survey of 15 experiments," *Journal of Regulatory Economics*, vol. 38, no. 2, pp. 193 – 225, 2010.

[104] C. Eid, E. Koliou, M. Valles, J. Reneses, and R. Hakvoort, "Time-based pricing and electricity demand response: Existing barriers and next steps," *Utilities Policy*, vol. 40, pp. 15 – 25, 2016.

[105] K. Sun and Q. Shu, "Overview of the types of battery models," in *Proceedings of the 30th Chinese Control Conference*, pp. 3644–3648, July 2011.

[106] M. Chen and G. A. Rincon-Mora, "Accurate electrical battery model capable of predicting runtime and I-V performance," *IEEE Transactions on Energy Conversion*, vol. 21, pp. 504–511, June 2006.

[107] H. He, R. Xiong, H. Guo, and S. Li, "Comparison study on the battery models used for the energy management of batteries in electric vehicles," *Energy Conversion and Management*, vol. 64, pp. 113 – 121, 2012. IREC 2011, The International Renewable Energy Congress.

[108] S. M. G. and M. Nikdel, "Various battery models for various simulation studies and applications," *Renewable and Sustainable Energy Reviews*, vol. 32, pp. 477 – 485, 2014.

[109] C. M. Shepherd, "Design of primary and secondary cells - An equation describing battery discharge," *Journal of the Electrochemical Society*, vol. 112, no. 7, pp. 657–664, 1965.

[110] O. Tremblay, L. A. Dessaint, and A. I. Dekkiche, "A generic battery model for the dynamic simulation of hybrid electric vehicles," in *2007 IEEE Vehicle Power and Propulsion Conference*, pp. 284–289, Sept 2007.

[111] O. Tremblay and L. A. Dessaint, "Experimental validation of a battery dynamic model for EV applications," *World Electric Vehicle Journal*, vol. 3, pp. 289–298, 2009.

[112] "How to Prolong Lithium-based Batteries." `http://batteryuniversity.com/learn/article/how_to_prolong_lithium_based_batteries`, 2003. [Online; accessed 05-05-2017].

[113] "Dynamic pricing in electricity supply," tech. rep., The Union of the Electricity Industry - EURELECTRIC, 2017.

[114] A. Poullikkas, "A comparative assessment of net metering and feed in tariff schemes for residential PV systems," *Sustainable Energy Technologies and Assessments*, vol. 3, pp. 1–8, Sep 2013.

[115] Y. Yamamoto, "Pricing electricity from residential photovoltaic systems: A comparison of feed-in tariffs, net metering, and net purchase and sale," *Solar Energy*, vol. 86, pp. 2678–2685, Sep 2012.

[116] A. D. E. Lemaire, F. Mattera and P. Malbranche, "Assessment of storage ageing in different types of PV systems: Technical and economical aspects," in *23rd European Photovoltaic Solar Energy Conference and Exhibition (EU PVSEC)*, September 2008.

[117] J. Mattingley, Y. Wang, and S. Boyd, "Code generation for receding horizon control," in *2010 IEEE International Symposium on Computer-Aided Control System Design*, pp. 985–992, Sept 2010.

[118] R. Bellman, *Dynamic Programming*. Dover Publications, 2003.

[119] "IEEE PES distribution systems analysis subcommittee radial test feeders." `https://ewh.ieee.org/soc/pes/dsacom/testfeeders/`. [Online; accessed 26-05-2017].

[120] R. C. Dugan, *The Open Distribution System Simulator - Reference Guide*, 2013.

[121] A. Dedé, D. D. Giustina, S. Rinaldi, P. Ferrari, A. Flammini, and A. Vezzoli, "Smart meters as part of a sensor network for monitoring the low voltage grid," in *2015 IEEE Sensors Applications Symposium (SAS)*, pp. 1–6, April 2015.

[122] *PowerSafe SBS:Operation guide for hybrid applications*.

[123] "Specific European Electrical Profiles." `http://www.ecbcs.org/annexes/annex42.htm`. [Online; accessed 29-07-2017].

[124] K. Christakou, D.-C. Tomozei, M. Bahramipanah, J.-Y. Le Boudec, and M. Paolone, "Primary voltage control in active distribution networks via broadcast signals: The case of distributed storage," *Smart Grid, IEEE Transactions on*, vol. 5, pp. 2314–2325, Sept 2014.

[125] S. Sundhararajan and A. Pahwa, "Optimal selection of capacitors for radial distribution systems using a genetic algorithm," *IEEE Transactions on Power Systems*, vol. 9, pp. 1499–1507, Aug 1994.

[126] M. M. Begovic and A. G. Phadke, "Control of voltage stability using sensitivity analysis," *IEEE Transactions on Power Systems*, vol. 7, pp. 114–123, Feb 1992.

[127] R. Caire, N. Retiere, E. Morin, M. Fontela, and N. Hadjsaid, "Voltage management of distributed generation in distribution networks," in *2003 IEEE Power Engineering Society General Meeting (IEEE Cat. No.03CH37491)*, vol. 1, pp. 282–287 Vol. 1, July 2003.

[128] J. Peschon, D. S. Piercy, W. F. Tinney, and O. J. Tveit, "Sensitivity in power systems," *IEEE Transactions on Power Apparatus and Systems*, vol. PAS-87, pp. 1687–1696, Aug 1968.

[129] M. H. Haque, "Efficient load flow method for distribution systems with radial or mesh configuration," *IEE Proceedings - Generation, Transmission and Distribution*, vol. 143, pp. 33–38, Jan 1996.

[130] M. Haque, "A general load flow method for distribution systems," *Electric Power Systems Research*, vol. 54, no. 1, pp. 47 – 54, 2000.

[131] R. D. Zimmerman, *Comprehensive distribution power flow: Modelling, Formulation, Solution algorithms and Analysis*. PhD thesis, Graduate School of Cornell University.

[132] K. Christakou, J. LeBoudec, M. Paolone, and D.-C. Tomozei, "Efficient computation of sensitivity coefficients of node voltages and line currents in unbalanced radial electrical distribution networks," *Smart Grid, IEEE Transactions on*, vol. 4, pp. 741–750, June 2013.

[133] A. Abdel-Majeed and M. Braun, "Low voltage system state estimation using smart meters," in *2012 47th International Universities Power Engineering Conference (UPEC)*, pp. 1–6, Sept 2012.

[134] D. Waeresch, R. Brandalik, W. H. Wellssow, J. Jordan, R. Bischler, and N. Schneider, "Linear state estimation in low voltage grids based on smart meter data," in *2015 IEEE Eindhoven PowerTech*, pp. 1–6, June 2015.

[135] M. Kraiczy, L. A. Fakhri, T. Stetz, and M. Braun, "Do It Locally: Local voltage support by distributed generation - A management summary," tech. rep., International Energy Agency - Photovoltaic Power Systems Programme, 2017.